

# Berichte

zur Polar-  
und Meeresforschung

596  
2009

Reports  
on Polar and Marine Research



**Crustal evolution of the submarine plateaux of  
New Zealand and their tectonic reconstruction  
based on crustal balancing**

**Entwicklung der Kruste der submarinen Plateaus von  
Neuseeland und deren tektonische Rekonstruktion  
mit Hilfe von Krustenbilanzierungen**

---

**Jan Werner Gerhard Grobys**

---

 **HELMHOLTZ  
| GEMEINSCHAFT**

**ALFRED-WEGENER-INSTITUT FÜR  
POLAR- UND MEERESFORSCHUNG**  
In der Helmholtz-Gemeinschaft  
D-27570 BREMERHAVEN  
Bundesrepublik Deutschland

ISSN 1866-3192

# Hinweis

Die Berichte zur Polar- und Meeresforschung werden vom Alfred-Wegener-Institut für Polar- und Meeresforschung in Bremerhaven\* in unregelmäßiger Abfolge herausgegeben.

Sie enthalten Beschreibungen und Ergebnisse der vom Institut (AWI) oder mit seiner Unterstützung durchgeführten Forschungsarbeiten in den Polargebieten und in den Meeren.

Es werden veröffentlicht:

- Expeditionsberichte (inkl. Stationslisten und Routenkarten)
- Expeditionsergebnisse (inkl. Dissertationen)
- wissenschaftliche Ergebnisse der Antarktis-Stationen und anderer Forschungs-Stationen des AWI
- Berichte wissenschaftlicher Tagungen

Die Beiträge geben nicht notwendigerweise die Auffassung des Instituts wieder.

# Notice

The Reports on Polar and Marine Research are issued by the Alfred Wegener Institute for Polar and Marine Research in Bremerhaven\*, Federal Republic of Germany. They appear in irregular intervals.

They contain descriptions and results of investigations in polar regions and in the seas either conducted by the Institute (AWI) or with its support.

The following items are published:

- expedition reports (incl. station lists and route maps)
- expedition results (incl. Ph.D. theses)
- scientific results of the Antarctic stations and of other AWI research stations
- reports on scientific meetings

The papers contained in the Reports do not necessarily reflect the opinion of the Institute.

The „Berichte zur Polar- und Meeresforschung“  
continue the former „Berichte zur Polarforschung“

## \* Anschrift / Address

Alfred-Wegener-Institut  
Für Polar- und Meeresforschung  
D-27570 Bremerhaven  
Germany  
[www.awi.de](http://www.awi.de)

Editor in charge:  
Dr. Horst Bornemann

Assistant editor:  
Birgit Chiaventone

Die "Berichte zur Polar- und Meeresforschung" (ISSN 1866-3192) werden ab 2008 ausschließlich als Open-Access-Publikation herausgegeben (URL: <http://epic.awi.de>).

Since 2008 the "Reports on Polar and Marine Research" (ISSN 1866-3192) are only available as web based open-access-publications (URL: <http://epic.awi.de>)

**Crustal evolution of the submarine plateaux of New Zealand and their tectonic reconstruction based on crustal balancing**

**Entwicklung der Kruste der submarinen Plateaus von Neuseeland und deren tektonische Rekonstruktion mit Hilfe von Krustenbilanzierungen**

---

**Jan Werner Gerhard Grobys**

**Please cite or link this publication using the identifier  
hdl:10013/epic.33265 or <http://hdl.handle.net/10013/epic.33265>**

**ISSN 1866-3192**

„Tektonik ist die Kunst, Verwickeltes  
einfach, Ruhendes bewegt zu sehen“  
(Hans Cloos, 1939)

Jan Grobys

Alfred-Wegener-Institut für Polar und Meeresforschung  
Geosystem  
Sektion Geophysik  
Postfach 12 01 61  
D-27515 Bremerhaven  
jan.grobys@awi.de

jetzt:

RWE Dea AG  
Überseering 40  
22297 Hamburg  
jan.grobys@rwe.com

Die vorliegende Arbeit ist die inhaltlich unveränderte Fassung einer Dissertation, die 2007 dem Fachbereich Geowissenschaften der Universität Bremen vorgelegt wurde. Sie ist in elektronischer Form erhältlich unter:  
<http://nbn-resolving.de/urn:nbn:de:gbv:46-diss000108692>

# List of Content

List of Content.....	i
Zusammenfassung.....	iii
Abstract.....	v
<b>1 Introduction.....</b>	<b>1</b>
<b>2 Some spotlights on mechanisms driving extension.....</b>	<b>4</b>
<b>3 Overview of the Late Cretaceous Southwest Pacific.....</b>	<b>8</b>
<b>4 Geophysical methods and principles of interpretation applied.....</b>	<b>11</b>
4.1 Seismic methods.....	11
4.2 Gravity methods and crustal thickness grid.....	17
<b>5 Structure of this thesis.....</b>	<b>20</b>
<b>6 Contributions to Publications.....</b>	<b>22</b>
<b>7 Is the Bounty Trough, off eastern New Zealand, an aborted rift?.....</b>	<b>23</b>
7.1 Introduction.....	24
7.2 Geological Setting.....	27
7.3 Data acquisition and processing.....	30
7.4 Data description.....	32
7.5 Seismic travel-time modeling.....	35
7.6 Discussion of seismic models.....	43
7.7 Discussion of gravity data.....	47
7.8 Tectonic implications.....	49
7.9 Comparison with other rift systems.....	53
7.10 Conclusions.....	54
<b>8 Extensional and magmatic nature of the Campbell Plateau and Great South Basin from deep crustal studies.....</b>	<b>56</b>
8.1 Abstract.....	56
8.2 Introduction.....	56
8.3 Geological Setting.....	59
8.4 Data acquisition and processing.....	62
8.5 Data description.....	63
8.6 Seismic travel-time modelling.....	66
8.7 Discussion of seismic and gravity models.....	71
8.8 Interpretation.....	73
8.9 Conclusions.....	77
<b>9 Crustal balancing applied for plate-tectonic reconstruction of Zealandia.....</b>	<b>79</b>
9.1 Abstract.....	79

## LIST OF CONTENT

9.2	Introduction .....	80
9.3	Tectonic introduction.....	82
9.4	Crustal thickness grid .....	84
9.5	Method of fitting plate-kinematic boundaries .....	88
9.6	Assumptions and restrictions.....	91
9.7	Application to Zealandia .....	95
9.8	Discussion.....	98
9.9	Conclusions .....	102
<b>10</b>	<b>Conclusions and Outlook .....</b>	<b>104</b>
10.1	Conclusions .....	104
10.2	Outlook.....	106
<b>11</b>	<b>References .....</b>	<b>108</b>
<b>12</b>	<b>Acknowledgements .....</b>	<b>120</b>

## Zusammenfassung

Der letzte Superkontinent brach mit Gondwana auseinander. In diesem Zusammenhang ist die Separation Zealandias, des Mikrokontinents Neuseeland, von der Antarktis als ein Puzzle mit vielen Teilen zu sehen. Diese Teile lagen an der konvergenten Plattengrenze Ostgondwanas, die sich innerhalb geologisch kurzer Zeit in eine divergente Plattengrenze verwandelte. Deswegen durchlebte Zealandia verschiedene tektonische Regime und Phasen des Wilson-Zyklus. Obwohl es ein hervorragendes Untersuchungsobjekt ist, ist erstaunlich wenig über seine submarinen Teile bekannt. Das Wissen um die magmatisch-tektonische Entwicklung der submarinen Plateaus wie des Campbellplateaus und der Chathamschwelle werden sehr dazu beitragen, die Prozesse zu verstehen, die zum späten Gondwanaaufbruch geführt haben. Gleichzeitig wird dadurch die Rekonstruktion Ostgondwanas verbessert, weil Zealandia eine Schlüsselposition in plattenkinematischen Rekonstruktionen dieses Teils Gondwanas einnimmt.

Der zentrale Teil dieser Arbeit behandelt den Abbruchprozess Zealandias von der Antarktis und führt zu einer verbesserten Rekonstruktion Neuseelands. Dabei liegt der Schwerpunkt auf den submarinen Plateaus. Der Bountytrog, der die Chathamschwelle vom Campbellplateau trennt und das Great South Basin, das das Campbellplateau von der Südinsel Neuseelands trennt, wurden mit refraktions- und reflexionsseismischen Methoden untersucht und gemeinsam mit Magnetik- und Schwerefelddaten interpretiert. Diese Ergebnisse einer Modellierung von Krustenmächtigkeiten basierend auf Satellitenschwerefelddaten wurden überprüft und zusammengeführt mit gemessenen Krustenmächtigkeiten Zealandias. Aus diesem Datensatz ist eine Krustenmächtigkeitskarte berechnet worden, die die Grundlage darstellt für eine neuartige Technik zur plattenkinematischen Rekonstruktion in Gebieten gedehnter kontinentaler Kruste, in denen magnetischen Spreizungsanomalien fehlen. Diese Rekonstruktion arbeitet mit der vertikalen Aufteilung der Kruste und Zuweisung der Teile zu verschiedenen Platten („crustal balancing“). Damit wird die Extension in den Becken und Trögen ausgeglichen.

Die refraktions- und reflexionsseismische Auswertung des Datensatzes über den Bountytrog zeigt eine stark gedehnte Kruste im Trog. Dessen Unterkruste zeigt Gebiete hoher S- und P-Wellengeschwindigkeit. Der Vergleich gemessener P-Wellengeschwindigkeiten und Poissonverhältnisse mit Gesteinstypdiagrammen von Laborwerten führte zu einem Modell der Gesteinszusammensetzung in der Kruste des Bountytrogs. Die gemeinsame Interpretation aller Modelle legte nahe, daß die Extension im Bountytrog gerade bis zum Beginn von Seafloor-Spreading im mittleren Bountytrog fortschritt und abbrach. Die geophysikalischen Daten aus dem Great South Basin zeigen Unterplattungen unter dem zentralen Campbellplateau (Pukakischwelle) und Krustenausdünnung im Becken selbst, allerdings deutlich weniger als im Bountytrog. Ein Vergleich der seismischen Daten mit existierenden Magnetikdaten vom Great South Basin (Stokes Magnetic Anomaly System – SMAS) und vom Campbellplateau (Campbell Magnetic Anomaly System – CMAS) führte zu dem Schluss, daß beide Anomaliesysteme entweder unterschiedliche Herkunft oder Entwicklung besitzen. Im Gegensatz zu den Ergebnissen dieser Arbeit nahmen frühere

## ZUSAMMENFASSUNG

Untersuchungen eine gemeinsame Geschichte von SMAS und CMAS an Plattenkinematische Rekonstruktionen auf der Grundlage von Messungen und Interpretationen in Verbindung mit gemessener und modellierter Krustenmächtigkeit ergaben, dass die Extension in Bountytrog und Great South Basin, genauso wie im Neukaledonabecken, deutlich geringer war als bisher angenommen. Die hier entwickelte neue Technik zur plattentektonischen Rekonstruktion in gedehnter kontinentaler Kruste hat das Potential zur deutlichen weltweiten Verbesserung von Rekonstruktionen von frühen Rifting-Phasen und Aulakogenen, versagten Rifts.

## Abstract

The last supercontinent fell into pieces with the break-up of Gondwana. In this context, the separation of the microcontinent of New Zealand from Antarctica is a jigsaw puzzle of many pieces. Its parts lay at the convergent margin of East Gondwana, which changed into a divergent margin within a geologically short time. That is why the microcontinent of New Zealand experienced different tectonic regimes and phases of the Wilson cycle. Although it is a good object of investigation due to its changing history, remarkably little is known about the submerged parts of the microcontinent. Knowledge of the magmatic-tectonic development of the submarine plateaux such as Campbell Plateau and Chatham Rise will improve the understanding of the processes that led to the late Gondwana break-up, and, in turn, lead to better reconstructions of East Gondwana, as Zealandia is a key piece in plate-kinematic reconstructions of this part of Gondwana.

The central part of this thesis deals with the separation process of Zealandia from Antarctica leading to an improved reconstruction of New Zealand with emphasis on the submarine plateaux. Bounty Trough separating Chatham Rise from Campbell Plateau, and the Great South Basin separating Campbell Plateau from the South Island are investigated with seismic refraction and reflection methods. They are interpreted jointly with magnetic and gravity data. The results of crustal thickness modelling based on satellite gravity data are combined with existing information about crustal thickness of Zealandia. With these data, a crustal thickness grid is calculated which creates the basis for a novel technique for plate-kinematic reconstructions in areas of crustal thinning and in the absence of magnetic seafloor anomalies. This reconstruction consists of crustal balancing to compensate for extension within basins and troughs.

The seismic refraction and reflection survey across the Bounty Trough shows a strongly thinned crust in the trough. Zones of high P- and S-wave velocities were found in the lower crust shows. Comparison of the P-wave model and a Poisson's ratio model with rock type diagrams leads to a compositional model of the crust. The joint interpretation of all models suggests that extension in the Bounty Trough proceeded until seafloor spreading in the Middle Bounty Trough began. Geophysical data from the Great South Basin show underplating beneath the Central Campbell Plateau and crustal thinning in the basin, to a lesser extent than in Bounty Trough. Comparison of the seismic data with existing magnetic data across the Great South Basin (Stokes Magnetic Anomaly System - SMAS) and the Campbell Plateau (Campbell Magnetic Anomaly System - CMAS) resulted in the conclusion that these anomaly systems have different origins or histories. Contrary to the results of this thesis, previous investigations assumed a common origin of SMAS and CMAS. Plate-kinematic reconstruction on the base of observations and interpretations combined with existing and modelled crustal thickness shows that extension in Bounty Trough and Great South Basin as well as in New Caledonia Basin was significantly less than previously assumed. The novel technique for plate tectonic reconstructions in thinned continental crust presented in this thesis has the potential to improve plate-kinematic reconstructions for early break-up settings and failed rift systems with stretched continental crust worldwide.



# 1 Introduction

Rift systems play a key role in the Wilson Cycle and their investigation yields important insights into the processes and driving mechanisms that control the break-up of continents [Woodcock, 2004] and the motion of plates. The ridge push-slab pull model and the mantle plume model have been identified as the main driving mechanisms, but their particular influence is still under discussion. World-wide, the effects of extension in the Wilson Cycle can be seen in different stages. An early rift system is the East African Rift System, where all of the extension of ca. 20 – 100 km is compensated by crustal thinning; in later stages, the subsequent extension is compensated by seafloor spreading, e.g. in the Atlantic Ocean, but again, the early opening of the Atlantic may have happened similarly. Reconstructions of these extensional processes improve our understanding of geodynamic processes and plate-driving mechanisms in global scales and e.g. basin forming processes in regional scales. Therefore, understanding the early stages of continental break-up are crucial, but are the parts in reconstructions that are most error-prone, as classic reconstructions fail.

The margin of East Gondwana experienced the main phases of Wilson Cycles within a few tenths of Ma. At 175 Ma [DiVinere, *et al.*, 1995], and still at 115 Ma [Mortimer, *et al.*, 2006], the Phoenix Plate was subducted beneath the margin of East Gondwana. Already 25 Ma later, East Gondwana broke up into several parts, while other parts were at a destructive plate boundary (Figure 1-1). New Zealand and its adjacent submarine plateaux, in this context referred to as Zealandia (Figure 1-2), were located at this changing plate boundary. Therefore, Zealandia is an exceptional research area for the investigation of break-up processes and the transition from a convergent to a divergent margin. It is important to know the magmatic-tectonic development for a thorough understanding of these processes. An analysis of the first deep-crustal seismic refraction lines ever crossing the Great South Basin and Bounty Trough are part of this thesis.

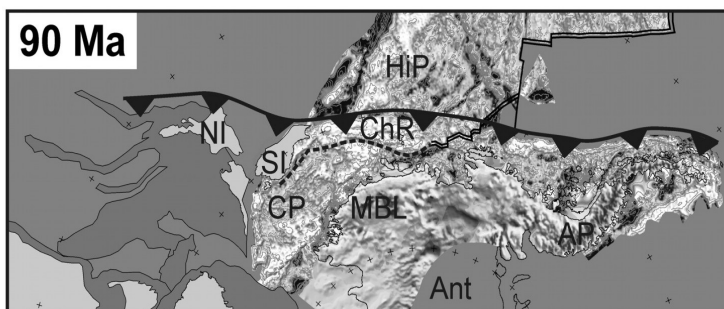


**Figure 1-1: Pre-break-up situation of Zealandia.** For full caption see Figure 1-2. Abbreviations are: Ant – Antarctica, AP – Antarctic Peninsula, ChR – Chatham Rise, CP – Campbell Plateau, HiP – Hikurangi Plateau, MBL – Marie Byrd Land, NI, SI – Islands of New Zealand

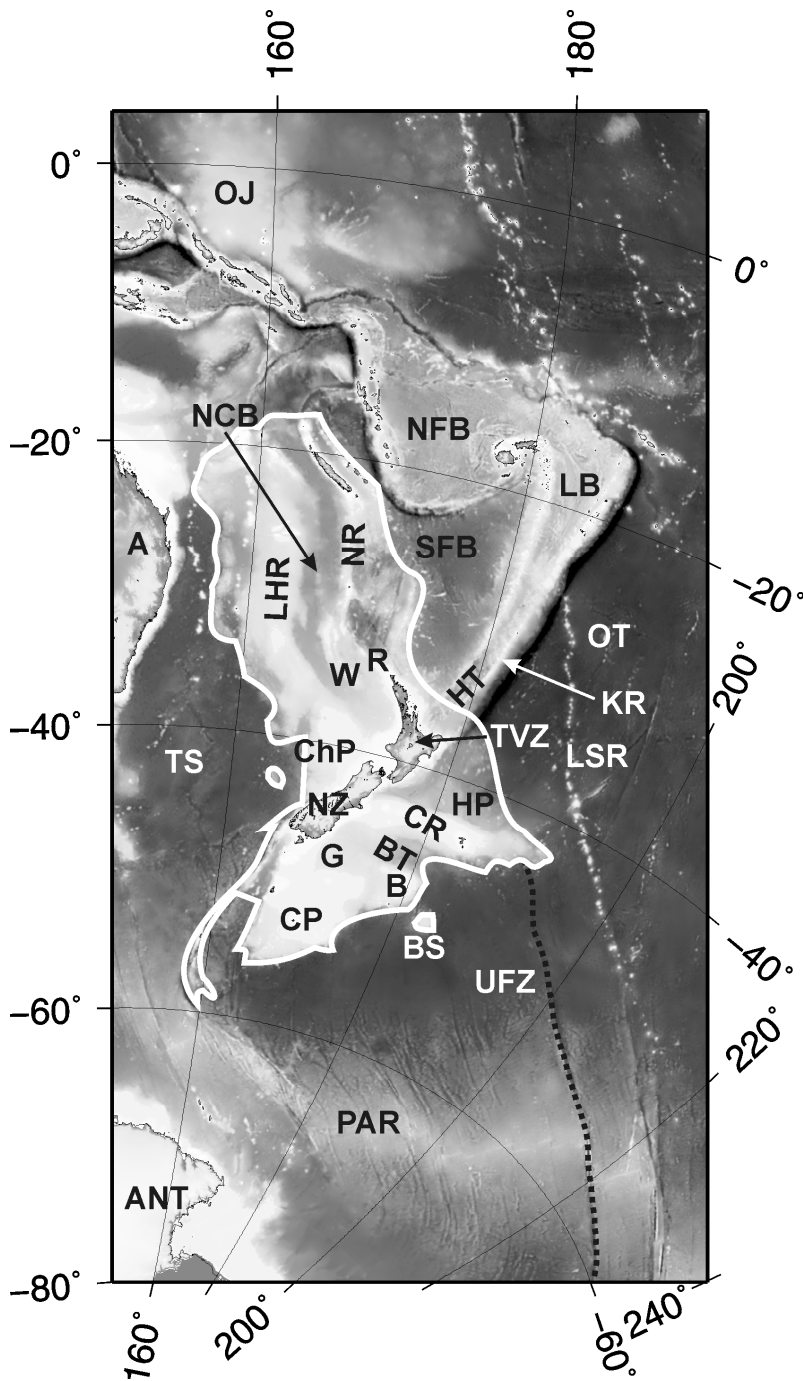


**Figure 1-2: Overview map showing the principal features of the Southwest Pacific.** Topographic data are taken from the SRTM30 PLUS dataset [Sandwell and Smith, 1997]. Fracture zones (dashed line), hotspot chains and mid-ocean ridge help determine plate motions. None of these features can be found in the submarine plateaux of Zealandia. Abbreviations are: A- Australia, ANT – Antarctica, B – Bounty Platform, BT – Bounty Trough, BS – Bollons Seamount, ChP – Challenger Plateau, CP – Campbell Plateau, CR – Chatham Rise, G – Great South Basin, HP – Hikurangi Plateau, HT – Havre Trough, KR – Kermadec Ridge, LB – Lau Basin, LHR – Lord Howe Rise, LSR – Louisville Hotspot Ridge, NCB – New Caledonia Basin, NFB – North Fiji Basin, NR – Norfolk Ridge, NZ – New Zealand, OJ – Ontong Java Plateau, OT – Osborn Trough, PAR – Pacific Antarctic Ridge, R – Reinga Ridge, SFB – South Fiji Basin, TS – Tasman Sea, TVZ – Taupo Volcanic Zone, UFZ – Udintsev Fracture Zone, W – West Norfolk Ridge. White line indicates the extent of Zealandia.

## INTRODUCTION

Chatham Rise and Campbell Plateau separated from Marie Byrd Land of East Gondwana at ca. 90 Ma. respectively 84 Ma. This event is well documented using magnetic seafloor anomalies southeast of the plateaux. Chron 34y is found at the mouth of the Bounty Trough and chron 33o can be identified south of the Campbell Plateau. Two major magnetic anomaly systems occur at the Campbell Plateau [Sutherland, 1999]. The Stokes Magnetic Anomaly System crosses the South Island and the Great South Basin terminating at the Campbell Plateau. Parts of the SMAS are related to mafic and ultramafic rocks of the Maitai Terrane. The Campbell Magnetic Anomaly System runs in a SW-NE direction along the middle of the Campbell Plateau. Although postulated, it has never been proven that the two magnetic anomaly systems are parts of a single anomaly system which was offset by a dextral movement of ca. 300 km [Davey and Christoffel, 1978; Kamp, 1986].

Campbell Plateau shows evidence of widespread magmatism, during and subsequent to rifting and break-up, possibly even in Cenozoic times [Hoernle, *et al.*, 2006]. The occurrence of the magnetic anomaly systems and the low crustal thickness raise questions as to whether the Campbell Plateau is composed of thinned continental or transitional crust.

The morphological step from Campbell Plateau to the oceanic crust of the Pacific Plate is very steep (Figure 1-2). This step suggests a rapid break-up with little or no crustal extension. The gravity field of the Campbell Plateau indicates a rather thin crust of unknown composition. Larter *et al.* [2002] assumed oceanic crust beneath the Great South Basin, while Carter and Carter [1993] suggested thinned continental crust beneath the Bounty Trough. The idea of oceanic crust beneath Bounty Trough and Great South Basin complies with the observation of an abrupt opening of the Pacific Ocean between Zealandia and Marie Byrd Land, but leads to a much larger (ca. 2 times) relative motion between Campbell Plateau and Chatham Rise than the assumption of continental crust. In contrast, the model of continental crust in the troughs implies a longer and more intense phase of continental stretching, but a smaller relative motion between the plateaux.

Summing up the introduction leads to the following questions:

1. "What is the crustal structure and composition of the Campbell Plateau and Bounty Trough?"
2. "How and to which extent did the extensions occur between Campbell Plateau and Chatham Rise and between Campbell Plateau and the South Island?"
3. "What is the origin of the magnetic anomaly systems and the reason for and the timing of the extension of the plateaux of Zealandia?"

Finally, the essence of these questions is:

4. "How can a plate-kinematic reconstruction for this region be improved?"

## 2 Some spotlights on mechanisms driving extension

In this thesis, consequences of back-arc extension and mantle-plumes are discussed. Back-arc extension is discussed in the context of the subduction of the Phoenix Plate beneath the Chatham Rise [Davy, 1993]. Davy [1993] suggested formation of a proto-Bounty Trough, possibly in Permian times caused by back-arc extension. It has been suggested by Weaver et al. [Weaver, et al., 1994] that the location of the subsequent separation of Campbell Plateau from Marie Byrd Land was controlled by a mantle-plume; these arguments are paraphrased in this thesis. For this reason, this chapter emphasises those extensional processes that control extension in addition to the ridge-push-slab-pull-model.

In a global view, the mechanisms of slab pull and ridge push are the main plate-driving forces. The contribution of slab pull to plate motion exceeds ridge push by ca. eight to nine times [Lithgow-Bertelloni and Richards, 1998]. Modelling of slab pulls suggests that the cold oceanic lithosphere has a lower buoyancy than the hot mantle. This leads to subduction of oceanic crust where oceanic crust collides with another plate [Conrad and Lithgow-Bertelloni, 2004]. The slab of subducting oceanic crust is then pulled into the mantle by gravitational forces. Due to the rigidity of the crust, the entire plate is pulled towards the subduction zone. Contrary to this force, the ridge push force is generated at mid-ocean ridges. Where hot mantle rises at mid-ocean ridges, the hot and young oceanic crust is elevated. With increasing time, this crust cools and contracts resulting in a higher density. This forces the cooled crust to slide down from the ridge caused by the rising mantle [Lithgow-Bertelloni and Richards, 1998].

In a divergent setting crustal extension leads to proto-oceanic rifts or to aulacogens (failed rifts). In convergent settings, forearc and backarc basins can be generated. Generally, divergent settings leading to crustal extension are found in continental crust, convergent settings in oceanic or arc crust [Woodcock, 2004]. However, both settings can lead to the formation of oceanic crust (e.g. Gondwana break-up, South China Sea). As the Gondwana margin underwent phases of subduction and rifting in a few tenths of Ma and both processes may be applicable for this margin, the principles of these concepts are briefly discussed here.

Most back-arc basins can be found where both the overriding and the subducting plate consist of oceanic crust (e.g. Lau Basin-Havre Trough, [Parson and Wright, 1996]). In few settings, a back-arc basin is formed when the overriding plate consists of continental crust (e.g. Japan Sea, [Sato, et al., 2006]). Along the subduction zone of the west Pacific Margin, the crustal composition of the overriding plate changes from oceanic crust in the Lau Basin-Havre Trough to continental in the Taupo Volcanic Zone [Harrison and White, 2004]. One of the main differences appears to be the distance of the basin margin from the subduction zone, or alternatively the width of the arc. In oceanic crust, the width of the arc often has widths of ca. 50 – 80 km (e.g. [Christeson, et al., 2003; Lizarralde, et al., 2002; Van Avendonk, et al., 2004b]), while the width of the arc in continental crust can reach a few hundred kilometres (e.g. [Harrison and White, 2004; Sato, et al., 2006]).

The mechanism that drives back-arc extension is still widely under discussion. Most models relate the back-arc formation directly to subduction, some only indirectly. The most frequently used models will be presented briefly in the following paragraphs.

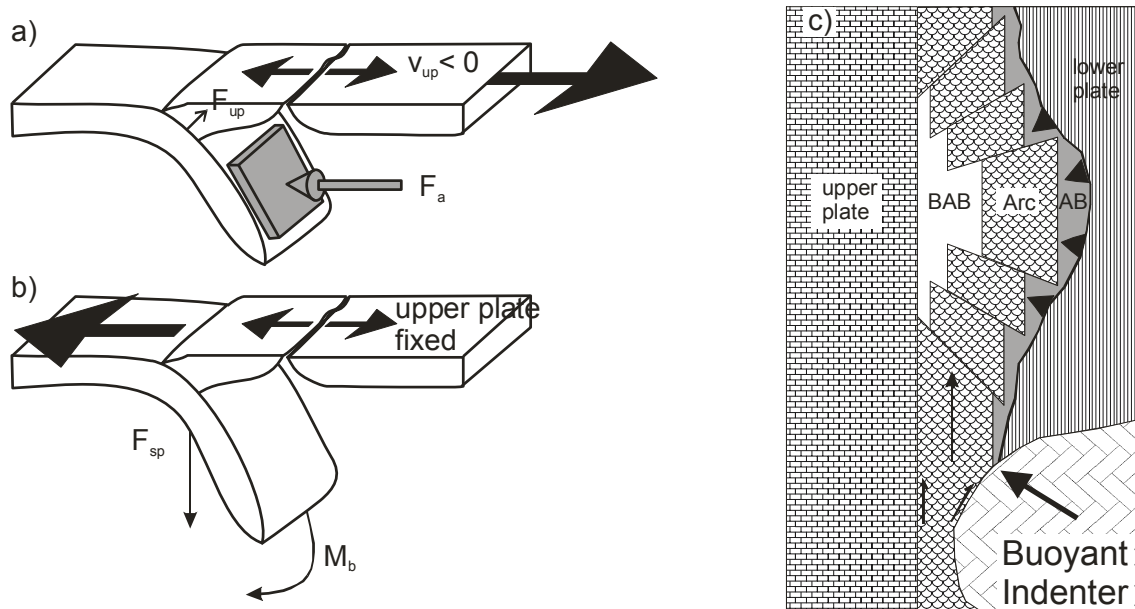


**Figure 2-1: Models of back-arc extension.** a) Sea anchor model: The suction/pushing force,  $F_{up}$ , related to the upper plate absolute motion, tends to move the arc, while the slab anchoring force,  $F_a$ , tends to resist this force. Upper plate retreat relative to the (more or less) fixed slab caused back-arc extension. After Heuret and Lallemand [2005] b) Slab pull model: Negative buoyancy of the subducted crust ( $F_{sp}$  – slab pull force), causes bending ( $M_b$  – bending moment) of the slab and therefore seaward trench migration and opening of a back-arc basin. After Heuret and Lallemand [2005]. c) Extrusion model: Oblique indentation of a buoyant structure induces a compression parallel to the arc. This leads to an outward extrusion and partial separation from the upper plate. The separation is accommodated by back-arc extension and formation of a basin. After Mantovani et al. [2001]. Abbreviations are: AB – Accretionary Belt, BAB – Back-arc basin.

The sea anchor model (Figure 2-1a) suggests that a viscous resistivity force, also called anchoring force, in the upper mantle opposes the lateral motion of the subducted slab [Uyeda and Kanamori, 1979]. Any back-arc deformation is a balance between the anchoring force and an uplift force that produces interaction between the overriding and the subducting plate. While the uplift force moves the trench, the anchoring force tends to resist this force. In this case, the formation of back-arc basins depends on the absolute motion of the upper plate with respect to a more or less fixed trench [Heuret and Lallemand, 2005]. However, this model fails to explain some back-arc basins (e.g. New Hebrides subduction zone [Scholz and Campos, 1995]) and it does not produce enough force to overcome lithospheric strength [Mantovani, et al., 2001].

The slab pull model (Figure 2-1b) postulates that the slab of the subducting plate retreats with respect to the surrounding mantle driven by negative buoyancy of the subducted lithosphere (slab pull). The slab pull force would produce a spontaneous seaward migration of the slab and the trench [Molnar and Atwater, 1978]. The slab pull force is also interpreted to be age dependent, so that this model generates more back-arc

extension in older crust. However, the most probable effect of the negative buoyancy would be a simple slab steepening without trench retreat [Mantovani, et al., 2001]. Also, there is no correlation between the age of the crust and the formation of back-arc basins [Heuret and Lallemand, 2005].

A third model (Figure 2-1c) presented in this context is the extrusion model which relates back-arc extension to subduction only indirectly. It suggests that a buoyant structure on the subducting plate collides with the overriding plate in a direction not perpendicular to the trench. This results in longitudinal shortening which is compensated by lateral bending or extrusion [Tapponnier, et al., 1986]. This model leads to the consequence of strong bending of arcs [Mantovani, et al., 2001]. However, this model fails to explain the low curvature of the Kermadec Arc and extension in the Lau Basin-Havre Trough if used without complicated constraints [Mantovani, et al., 2001].

It has been shown in the above paragraphs that the development of most short-lived back-arc basins [Ziegler and Cloetingh, 2004] occurs in both oceanic and continental crust. However, the driving forces of the back-arc extension remain unclear.

The second part of this chapter deals with mantle-plumes and mantle-drag forces as the forces (Figure 2-2) that controlled the location of continental rifting in Zealandia in the Late Cretaceous.

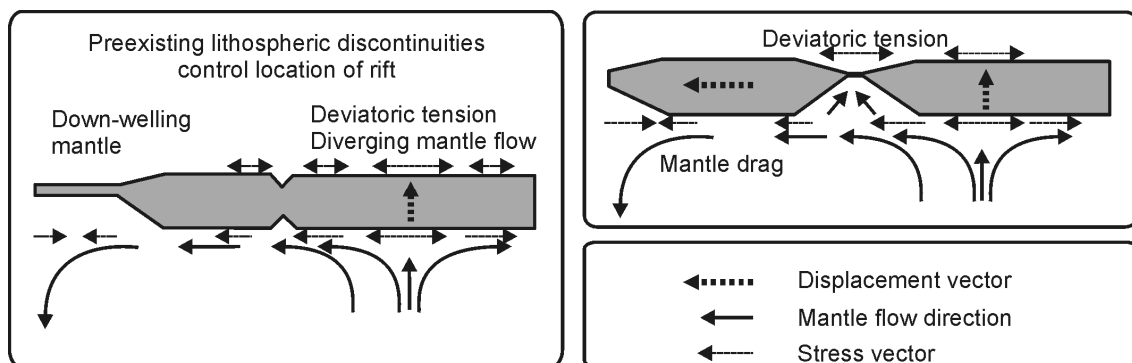


**Figure 2-2: Interaction of shear-traction** exerted on the base of the lithosphere by asthenospheric flow (left), deviatoric tension above upwelling convection cells in the mantle (right). The forces produced by positive interference of mantle convection and plate boundary and/or mantle drag stresses overcomes the strength of the lithosphere and causes rifting and break-up. After [Ziegler and Cloetingh, 2004].

Mantle-plumes seem to be one of the most controversial concepts in geoscience. Observations at volcanic provinces, e.g. Iceland, often require a posteriori adjustment of this concept, which raises doubts about this model [Foulger and Anderson, 2005]. I do not intend to solve this problem, but only to introduce the reader to the main concept. Today, mantle drag forces (Figure 2-2) as the main driving force of crustal extension within the Wilson Cycle are widely accepted [Ziegler and Cloetingh, 2004]. Mantle drag forces occur whenever the vector of motion of a lithospheric plate differs from the vector of motion of the mantle flow beneath it [Ziegler and Cloetingh, 2004]. If the mantle drag force interferes positively with plate boundary forces like slab pull or ridge push forces, it can enhance intraplate stresses and lead to the break-up of continents

[Artemieva and Mooney, 2002]. Mantle plumes and upwelling convection cells in the mantle also appear to be able to contribute to the stress field leading to the break-up of continents, but do not seem to be the only cause for the break-up of continents [Bott, 1993]. In the case of positive interference of these forces, the stress field may exceed the lithospheric strength and induce rifting (Figure 2-2).

It remains unclear whether plumes exist at all. The number of proposed plumes has ranged from 20 to 5200 plumes in the last few decades [Foulger and Natland, 2003]. The concept of mantle plumes suggests that they are formed at the core-mantle boundary rising diapirically through the lower mantle. In a certain depth, they reach a density equilibrium and spread out at the 660- and 410-km discontinuities (Figure 2-3). Plume heads that spread out at these discontinuities appear to be heat sources that can trigger partial melting within the upper mantle. Also, secondary plumes can be initiated. Partial melts elevated by these secondary plumes spread out at the base of the lithosphere where the melts can interact with the lithosphere [Wilson, 1992]. The observation that there are many intraoceanic and intracontinental hotspots, assumed to be equivalent with plumes, which do not lead to major extension (e.g. Hawaii or Hoggar), suggests that plumes are not the major driving mechanism for crustal extension. But if they do cause thermal weakening and regional uplift and if radial outflow of the plume material at the base of the lithosphere interferes positively with mantle drag forces, they would contribute to the break-up of continents and may control the position of break-up [Bott, 1992].

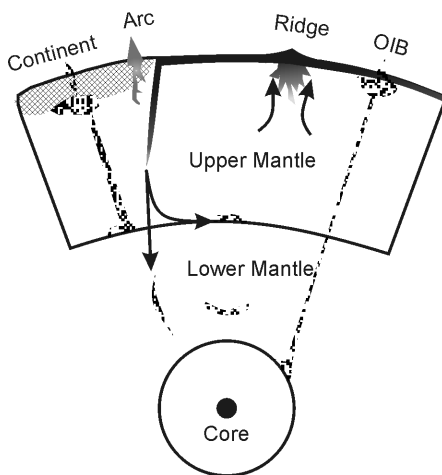


**Figure 2-3: Basic mechanism of mantle-plumes.** Subducted slabs sink into the mantle due to their negative buoyancy. They are recycled at the boundary between upper and lower mantle or the core-mantle boundary. From there, the (altered and reheated) material rises diapirically to the lithosphere, where it interacts with the lithosphere. Abbreviation is: OIB – Ocean Island Basalt.

### 3 Overview of the Late Cretaceous Southwest Pacific

The shape of continents has remained largely unchanged since 50 Ma. Prior to this, until about 160 Ma, the landmasses consisted of the single supercontinent Pangaea with two major regions: Laurentia in the north and Gondwana in the south. All continents from the southern hemisphere evolved from Gondwana: South America, Africa, India, Australia, Antarctica and Zealandia. The break-up of Gondwana took place in three major phases. Beginning at ca. 160 Ma, South America and Africa moved northwards and broke apart from each other. In a second phase, India broke off from Africa and Antarctica, and finally Australia and Zealandia separated from Antarctica in Middle to Late Cretaceous times. Zealandia and its conjugate plate, West Antarctica, consisted of several microplates, including the Campbell Plateau/Chatham Rise, South and North Island of New Zealand, Challenger Plateau and Lord Howe Rise as parts of Zealandia and Marie Byrd Land, Ellsworth Land, Thurston Island Block and the Antarctic Peninsula as parts of West Antarctica. The region of East Gondwana in the vicinity of New Zealand underwent several phases of rifting and extension before it finally began to break up at 90 Ma (Figure 3-1).

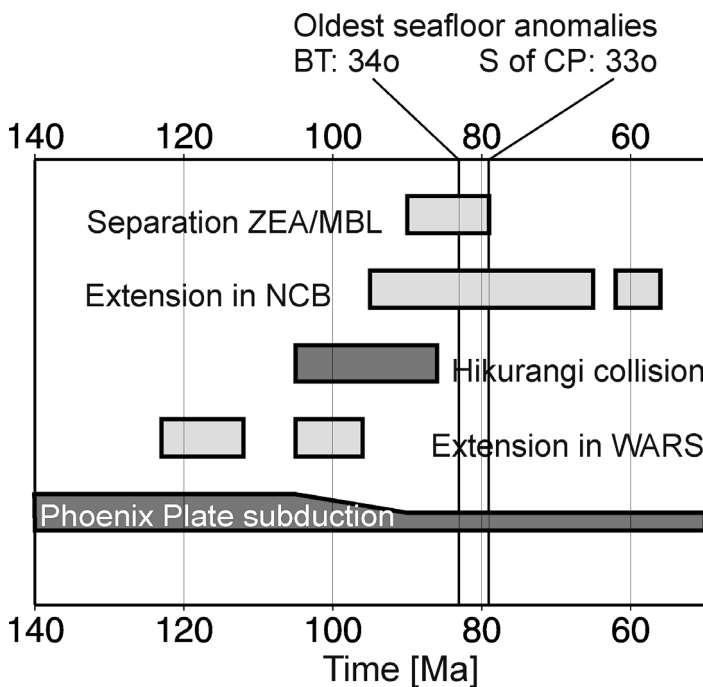


**Figure 3-1: Time scale of major tectonic events at the margin of East Gondwana.** Bars show the duration including the uncertainty of tectonic events that happened at the margin of East Gondwana during the Cretaceous. Dark grey bars indicate compressional events, light grey bars indicate extensional events. Vertical lines indicate the timing of the oldest seafloor anomalies observed at the mouth of the Bounty Trough and at the margin of the Campbell Plateau. Overlapping bars of the Hikurangi Collision and the separation between Marie Byrd Land and Zealandia outline the existing uncertainties of timing of these events. Thinning bar of Phoenix Plate subduction means that subduction of the Phoenix Plate ceased in the western part of the subduction zone. Abbreviations are:

BT – Bounty Trough, CP – Campbell Plateau, MBL – Marie Byrd Land, NCB – New Caledonia Basin, WARS – (Proto-) West Antarctic Rift System, ZEA – Zealandia

At ca. 123 - 112 Ma, extension in a (Proto-) West Antarctic Rift System occurred (Figure 3-1), coinciding with the Australia-East Antarctica break-up [Wandres, et al., 2004]. At this time, the Phoenix Plate subducted beneath East Gondwana [Mortimer, et al., 2006] (Figure 3-2). Marie Byrd Land rifted from East Antarctica in a further extensional episode from 105 Ma until 96 Ma upon being driven by a proposed mantle plume beneath Marie Byrd Land [Luyendyk, et al., 2003; Weaver, et al., 1994]. This plume and its successor, a mantle plume still present beneath Marie Byrd Land, are interpreted to be the reason why Marie Byrd Land's elevation is ca. 1 km higher than

predicted by Airy isostasy [LeMasurier and Landis, 1996; Winberry and Anandakrishnan, 2004].

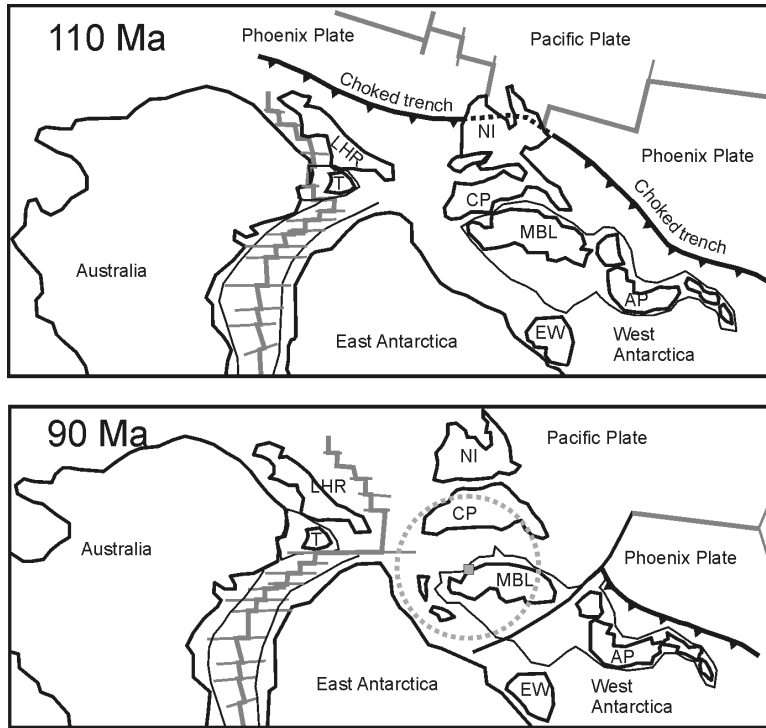


**Figure 3-2: Tectonic setting at the margin of East Gondwana at 90 Ma and 110 Ma illustrating the transition from convergent to divergent tectonics. Top: At 110 Ma, Phoenix Plate subducted beneath the entire margin, while seafloor spreading between the Phoenix Plate and the Pacific Plate is present. At this time, spreading also occurs between Lord Howe Rise and Australia, while Zealandia is still attached to East Gondwana. Only 20 Ma later, at 90 Ma (bottom), subduction beneath the Zealandia part of Gondwana has ceased and rifting controlled by the Marie Byrd Land plume between Zealandia and Marie Byrd Land has started. After Weaver et al. [1994] and Smith [1997].**

Abbreviations are: AP – Antarctic Peninsula, CP – Campbell Plateau, EW – Ellsworth-Whitmore-Land, LHR – Lord Howe Rise, MBL – Marie Byrd Land, NI – North Island.

Subduction beneath the part of East Gondwana which later became the Chatham Rise finally ceased when the Hikurangi Plateau collided with the Chatham Rise [Worthington, et al., 2006]. However, the timing of the collision and its relationship to the break-up between Zealandia and West Antarctica are still subject to debate. The time of the collision of the Hikurangi Plateau ranges from 105 Ma [Laird and Bradshaw, 2004] to 86 Ma [Worthington, et al., 2006], while the estimated time of the break-up (Figure 3-1) between Zealandia and West Antarctica ranges from 90 Ma [Eagles, et al., 2004; Larter, et al., 2002] to 79 Ma [Wood and Herzer, 1993]. With the collision of the Hikurangi Plateau, the subduction of the Phoenix Plate beneath Zealandia ceased, while the subduction proceeded along the Antarctic Peninsula for several tens of Ma [Eagles, et al., 2004]. The oldest seafloor spreading at the mouth of the Bounty Trough is interpreted at chron 34y (83 Ma) [Davy, 2006] and the youngest syn-rift sediments in the Great South Basin are 86.5 Ma old [Cook, et al., 1999]. The first seafloor spreading between Campbell Plateau and Marie Byrd Land occurred at chron 33o (79 Ma) [Davy, 2006; Sutherland, 1999]. Although the timing of a single event still varies, the order of the tectonic processes is without doubt.

The separation of Lord Howe Rise from Antarctica and Australia coincides with the separation of the Campbell Plateau from Marie Byrd Land [Schellart, et al., 2006]. The oldest seafloor anomaly southeast of Lord Howe Rise is chron 33o. Extensional phases within the Lord Howe Rise, leading to the opening of the New Caledonia Basin, are estimated to have occurred at 95 – 65 Ma and 62 – 56 Ma. In the second phase it was

probably associated with seafloor spreading in parts of the basin [Gaina, *et al.*, 1998b; Lafoy, *et al.*, 2005a].

The striking observation can be made that most of the regions mentioned above (West Antarctic Rift System, Lord Howe Rise, Campbell Plateau, Chatham Rise and parts of Marie Byrd Land) consist of extended continental crust [Cook, *et al.*, 1999; Davy and Wood, 1994; Shor, *et al.*, 1971; Trey, *et al.*, 1999; Winberry and Anandakrishnan, 2004]. However, for the plateaux of Zealandia, seismic evidence is very sparse. Major basement provinces can be traced throughout several of these regions [Adams, *et al.*, 2005; Bradshaw, *et al.*, 1997; Sutherland, 1999] (Figure 3-3). These common characteristics suggest a common history of the regions before breakup.

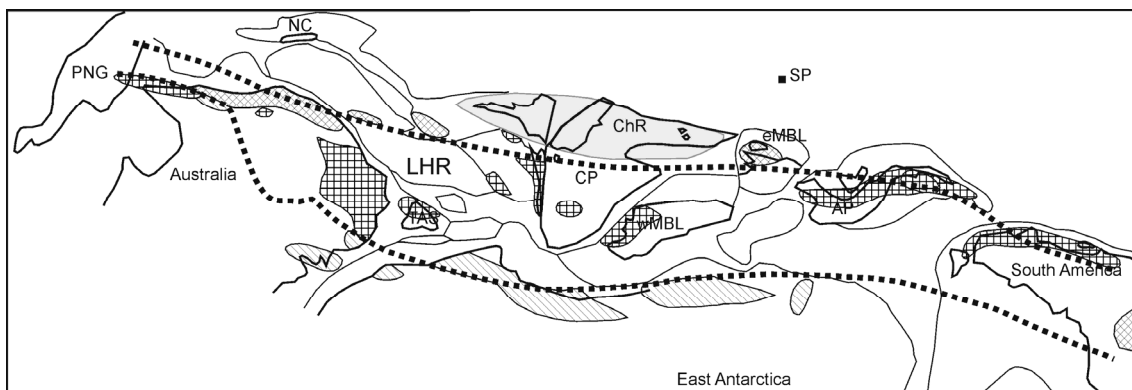


**Figure 3-3: Overview of the East Gondwana margin in the Late Triassic:** Terranes have been accreted along the entire margin. This leads to the observation that many terranes of present Zealandia have different origins depending on the time of accretion. Black dotted lines are continental margins at late Precambrian (bottom) and Palaeozoic (top). Hatched areas: Delamerian Fold Belt, cross-hatched areas: Lachlan Fold Belt, diagonally cross-hatched areas: New England Fold Belt, grey area: New Zealand Mobile Belt terranes. Thin black lines: submerged crustal fragments, black lines: coast lines. Abbreviations are: AP – Antarctic Peninsula, ChR – Chatham Rise, CP – Campbell Plateau, eMBL and wMBL – eastern and western Marie Byrd Land, TAS – Tasmania, NC – New Caledonia, PNG – Papua New Guinea, SP – South Pole. After Adams *et al.* [2005].

## 4 Geophysical methods and principles of interpretation applied

### 4.1 Seismic methods

The main method of geophysics used in this work is seismic refraction and wide-angle profiling. Its basic principle is to measure travel times of seismic waves that propagate through the earth's crust and uppermost mantle. The traveltime of a seismic wave travelling through the earth provides information on the compressional and shear wave velocity structure of the subsurface, in the case of turning rays mainly from the turning point of the wave because the gradient of a traveltime curve reflects the velocity of the turning point. The velocities of the seismic wave depend on the material properties and density of the medium and, therefore, contain information about the composition of the earth's crust. Temperature and pressure have an additional effect on the velocities as they alter density. Travel times of wide-angle reflections give information on the depth of the reflector which they interacted with, providing additional structural information of the subsurface. One of the strongest reflectors is the crust-mantle boundary, the Mohorovičić discontinuity (Moho). The depth of the Moho, crustal thickness and the velocity distribution help distinguish between continental and oceanic crust. Also, extensional and compressional processes change the crustal thickness. Conversely, knowing the crustal thickness gives evidence for large-scale processes changing the lithosphere.

#### 4.1.1 Raytracing

Raytracing forward-modelling and traveltime inversions are standard tools for modelling seismic refraction and wide-angle data. These methods offer a good combination of low time expenses and reasonable spatial resolution combined with a control of the quality of the model. They are based on asymptotic ray theory where rays are defined as normals of wave fronts. Raytracing has the advantage of great practicality and the disadvantage of assuming infinitely high frequencies. Models are layered and parameterised with velocity blocks. This means that models can be changed quickly and intuitively [Zelt and Ellis, 1988]. The degree of accuracy can easily be varied with the number of velocity and boundary nodes.

Snell's law at model boundaries, Fermat's principle and the elastic wave equation are the physical laws that build up the basic framework for raytracing. The elastic wave equation is approximated by the eiconal equation which is valid for high-frequency signals as long as the wavelengths of model changes are small compared to the wavelength of the seismic wave. According to Červený [1977], the system of differential equations, which are the basis of 2D-raytracing, can be written as follows:

$$\frac{dz}{dx} = \cot \theta \quad \frac{d\theta}{dx} = \frac{1}{v} \left( \frac{\partial v}{\partial z} - \frac{\partial v}{\partial x} \cot \theta \right) \quad (4-1)$$

$$\frac{dx}{dz} = \tan \theta \quad \frac{d\theta}{dz} = \frac{1}{v} \left( \frac{\partial v}{\partial z} \tan \theta - \frac{\partial v}{\partial x} \right) \quad (4-2)$$

with  $\theta$  as the angle between the  $z$ -axis and the tangent to the ray and  $v$  the 2D-velocity field. Boundary conditions applied at the starting point of the ray are:  $\theta = \theta_0$ ,  $x = x_0$  and  $z = z_0$ . A ray is emitted at the point  $(x_0, z_0)$  under the angle  $\theta_0$ . The raytracing equations are solved numerically. After the ray path is calculated, travel times are computed by integration of the velocity field along the ray path. As the velocity changes along the path and the ray path depends on the changing velocity path, the solution is a highly non-linear problem.

For the inversion of the traveltimes [Zelt and Smith, 1992], the traveltime vector  $\mathbf{t}$  can be written as a non-linear Function  $\mathbf{F}$  of the model parameters  $\mathbf{m}$  and a residual error  $\mathbf{e}$  between observed and measured travel times:

$$\mathbf{t} = \mathbf{F}(\mathbf{m}) + \mathbf{e} \quad (4-3)$$

The inversion aims to minimise the residual error in (4-3), so that the sum of the squares of the errors is minimal. This sum can be written as:

$$\mathbf{e}^T \mathbf{e} = [\mathbf{t} - \mathbf{F}(\mathbf{m})]^T [\mathbf{t} - \mathbf{F}(\mathbf{m})] \quad (4-4)$$

As (4-4) is non-linear, it has to be linearised in order to solve the equation with a least squares technique. The linearisation is done with a Taylor series expansion about a starting model  $\mathbf{m}_0$ , where higher-order terms are neglected. Consequently, a starting model is needed and the process must be executed iteratively. Then, the linearised equation can be written as

$$\mathbf{A} \Delta \mathbf{m} = \Delta \mathbf{t} \quad (4-5)$$

with  $\mathbf{A}$  the partial derivative matrix,  $\Delta \mathbf{m}$  the model parameter adjustment vector containing the elements  $\partial t_i / \partial m_j$  with  $t_i$  the  $i$ th observed traveltime and  $m_j$  the  $j$ th model parameter chosen for inversion. This can either be a velocity or a depth value.  $\Delta \mathbf{t}$  is the vector of residual traveltimes. The residual traveltimes and the partial derivatives are calculated during the raytracing. After each raytracing iteration, the parameter adjustment vector is computed and applied to the current model. In each particular modeling step, the derivations are calculated in a forward modeling step (raytracing) followed by an inversion in order to solve for  $\Delta \mathbf{m}$ .

A damped least-squares technique is well suited to solve over-determined inverse problems such as this [Aki and Richards, 1980]. The damped least-squares solution for  $\Delta \mathbf{m}$  can be written as

$$\Delta \mathbf{m} = \left( \mathbf{A}^T \mathbf{C}_t^{-1} \mathbf{A} + D \mathbf{C}_m^{-1} \right)^{-1} \mathbf{A}^T \mathbf{C}_t^{-1} \Delta \mathbf{t} \quad (4-6)$$

with  $\mathbf{C}_t$  and  $\mathbf{C}_m$  the estimated data and model covariance matrices and  $D$  an overall damping factor [Menke, 1984]. The covariance matrices consist of standard deviations which are the estimated uncertainty of the traveltimes measurement or alternatively an a priori estimate of the uncertainty of the model parameter. For crustal models, the estimated values are set to 0.1 – 0.2 km/s and 0.1 – 1 km [Zelt and Smith, 1992].

This process, consisting of inversion and forward modelling, allows a fast result together with a calculation of the model resolution. As the matrix is relatively small compared to the number of observed traveltimes and not very sparse, the inversion of the matrix can be carried out a lower-upper decomposition. The resolution matrix  $\mathbf{R}$  is then given by:

$$\mathbf{R} = \left( \mathbf{A}^T \mathbf{C}_t^{-1} \mathbf{A} + D \mathbf{C}_m^{-1} \right)^{-1} \mathbf{A}^T \mathbf{C}_t^{-1} \mathbf{A} \quad (4-7)$$

The diagonal elements of the resolution matrix  $\mathbf{R}$  represent the averaging of each model parameter compared to the true model, or, how many rays determine a particular model parameter. According to Zelt and Smith [1992], values greater than 0.5 indicate well resolved model parameters.

Finally, the a posteriori model covariance matrix can be written as [Tarantola, 1987]:

$$\mathbf{C} = (\mathbf{I} - \mathbf{R}) \mathbf{C}_m \quad (4-8)$$

with  $\mathbf{I}$  the identity matrix. The calculated standard errors (or uncertainties) can be calculated from the square root of the diagonal elements of  $\mathbf{C}$ . The values of the diagonal elements of  $\mathbf{C}$  together with the misfits normalised to the picking uncertainty ( $\chi^2$ ) and the rms-misfits are useful in assessing the quality of the model resolution. While the Chi-squared value describes the fit of the data within their assigned uncertainties without overfitting, the values of the resolution matrix describe the uncertainties of the model parameters. This does not necessarily lead to an interdependence of both values, but to a trade-off. When the pick uncertainties are large, the Chi-squared value is low (good), although a highly over-parameterised model leads to low (bad) model resolution. Conversely, too few model parameters lead to a high model resolution, while the misfit is bad. Chi-squared values greater than one normally indicate that the data reflect small-scale variations that are below resolution.

#### 4.1.2 Shear-wave models and Poisson's ratio

In general, velocity changes of a P-wave model can be caused by changes of the rock type: Different rocks have different P-wave velocities. However, finding a correlation between rock composition and P-wave velocity is very difficult, as many common rock types have very similar P-wave velocities [Birch, 1960, 1961]. In contrast to this, rocks with a similar P-wave velocity can have a different Poisson's ratio ( $\sigma$ ). This can be calculated from P- and S-wave velocities ( $v_p$ ,  $v_s$ ):

$$\sigma = 0.5 \frac{(v_p/v_s)^2 - 2}{(v_p/v_s)^2 - 1} \quad (4-9)$$

For example, Gabbro and Hornblendite have P-wave velocities of ca. 7.2 km/s at 600 MPa in laboratory measurements, but Gabbro has a  $\sigma$  of 0.295 and Hornblendite of 0.258 [Christensen, 1996]. It has been shown that, for some rocks, plagioclase feldspar and Si<sub>2</sub>O content influence  $\sigma$  as well as the grade of metamorphism and Fe-Mg-ratios of pyroxenes and olivines [Christensen, 1996]. As will be shown later on, the relatively large error in  $\sigma$  calculated from seismic wide-angle/refraction experiments allows only the broad distinction between mafic and felsic rocks.

Most ocean bottom seismometers deployed across the Bounty Trough recorded S-waves with high amplitudes, so that it was possible to derive an independent S-wave model. In the modelling process, the boundaries taken from the P-wave model were kept fixed and only the velocities were changed. S-waves are generated at geological boundaries where the impedance contrast is sufficiently high. As S-waves cannot propagate in liquids, the generation of S-waves occurs at the seafloor by P-to-S-conversion.

As  $\sigma$  is determined from two values affected by errors, the errors of  $\sigma$  depend on the errors of both input parameters. The error of a dependent function can be expanded into a Taylor series dropping the higher order terms and is then the sum of the partial derivatives multiplied by the individual errors.

$$\Delta\sigma = \sum_{i=1}^k \frac{\partial\sigma}{\partial x_i} \Delta x_i = \frac{\partial\sigma}{\partial v_p} \Delta v_p + \frac{\partial\sigma}{\partial v_s} \Delta v_s \quad (4-10)$$

Calculating the partial derivatives of  $\sigma$  yields:

$$\Delta\sigma = \frac{v_p/v_s^2}{((v_p/v_s)^2 - 1)^2} \Delta v_p - \frac{v_p^2/v_s^3}{((v_p/v_s)^2 - 1)^2} \Delta v_s \quad (4-11)$$

or:

$$\Delta\sigma = \frac{(v_p/v_s)^2}{\left(\left(v_p/v_s\right)^2 - 1\right)^2} \left[ \frac{\Delta v_p}{v_p} - \frac{\Delta v_s}{v_s} \right] \quad (4-12)$$

Although the ray coverage of the S-wave model is significantly lower than that of the P-wave model, and the pick uncertainties are higher, the uncertainties of the model velocity nodes are in the same order. For a simple evaluation of the error of  $\sigma$ , it seems tolerable to set both errors equal. Thus,  $\Delta v$  and  $V$  can be defined as:

$$\Delta v = \Delta v_p = \Delta v_s \wedge V = (v_p/v_s)^2 \quad (4-13)$$

This leads to a simplified equation of  $\Delta\sigma$  that is only dependent on the ratio of  $v_p/v_s$ , the error of the velocity models and the P-wave velocity. For an estimation of  $\Delta\sigma$ ,  $\Delta v$  is set to 0.2 km/s, which is at the upper boundary for model uncertainties:

$$\Delta\sigma = \frac{V}{(V-1)^2} \left[ \Delta v \frac{v_p - v_s}{v_p v_s} \right] = \frac{V(\sqrt{V}-1)\Delta v}{(V-1)^2 v_p} \quad (4-14)$$

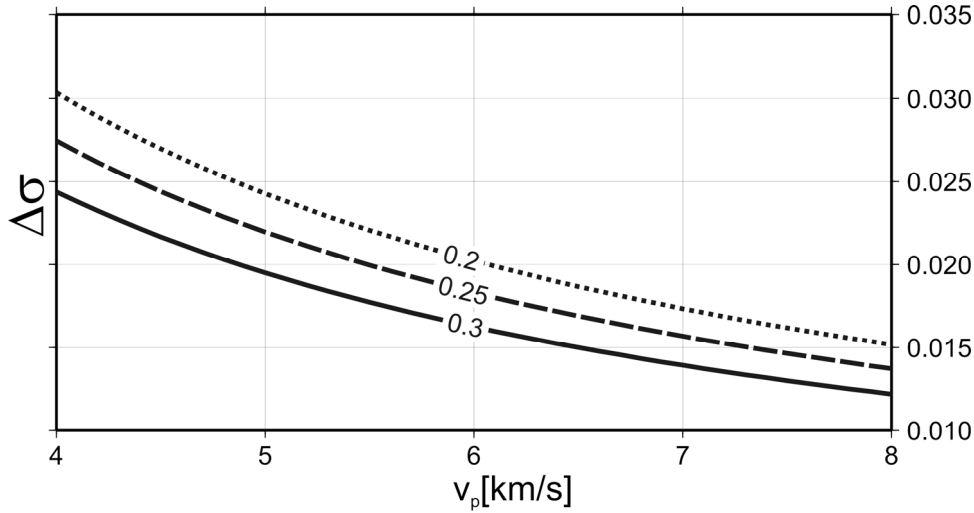


**Figure 4-1:** The error  $\Delta\sigma$  depending on the P-wave velocity for the Poisson's ratios of 0.2, 0.25, and 0.3. The Error decreases with increasing P-wave velocity and increasing  $\sigma$ .

Equation (4-14) shows that the error  $\Delta\sigma$  decreases with the ratio  $v_p/v_s$  and therefore with  $\sigma$ , and decreases with  $v_p$  (Figure 4-1). As higher P-wave velocities normally occur at greater depths,  $\Delta\sigma$  decreases with depth. Considering the range of seismic velocities and  $\sigma$ ,  $\Delta\sigma$  lies in the range of ca. 10 – 15% of  $\sigma$ .

In the study of the Bounty Trough model, a probability of rock composition was assigned to the nodes of the P- and S-wave velocity models. This does not mean that the probability could be quantified, but a qualitative statement was given. In order for this to be possible, the S-wave model had to have the same number of velocity nodes as the P-wave model to compute  $\sigma$  at each model node. This means that the S-wave model is highly over-parameterised. The smaller ray coverage in the S-wave model would normally yield a smoother model than the better covered P-wave model. An over-parameterised model has smaller values of the resolution matrix as it describes how many rays constrain a velocity node. This fact shows that the resolution matrix is a measure of the progress in modelling rather than a means to compare the quality of different models (e.g.  $v_p$ - and  $v_s$  models) with each other. As the ray coverage of the models of this work (Figures Figure 7-9 and Figure 7-11) is sufficiently high, a change in  $\sigma$  cannot lead to a sampling of differently assigned regions due to different ray-paths.

On the other hand, an additional  $v_s$ -model can add further constraints to a  $v_p$ -model that can only be quantified in a joint modelling process. Both datasets of the Bounty Trough show wide-angle reflections from the Moho ( $P_mP$ - and  $S_mS$ -phases). As the velocities of both models are modelled independently but with fixed interfaces, a good fit of the depth of the Moho in the  $v_s$ -model adds additional confirmation to the  $v_p$ -model.

### 4.1.3 Seismic experiments

The aim of the seismic dataset presented in this thesis was to give a detailed image of the earth's crust at the Campbell Plateau and its surrounding basins and troughs. This dataset was collected during the cruise SO-169 of R/V SONNE from Lyttleton to Auckland in January and February 2003 [Gohl, 2003]. The cruise included multichannel seismic and seismic refraction/wide-angle reflection experiments, gravity and magnetic measurements, and rock sampling from the seafloor (dredging).

For seismic refraction studies, a reasonable vertical resolution of deeper structures (ca. 1 km) with reversed travel paths can be achieved by ocean-bottom seismometers deployed in an average distance of ca. 10 – 18 km and an average source distance of ca. 150 m. We used an array of 20 VLF airguns with a total volume of ca. 52 l for profile AWI-20030001 and an array of eight G-Guns with a total volume of 48 l for profile AWI-20030002. The peak frequency of the sources was ca. 20 Hz, low enough to be recorded at far offsets. Additional onshore receivers were used on one of the profiles in order to connect the marine experiment to the onshore geology of New Zealand. Additional structural information about the sedimentary layers was gained by multichannel seismic profiles shot coincidentally or parallel to the refraction seismic profiles. This structural information was used to further constrain the modelling and interpretation of seismic refraction/wide-angle and gravity models, wherever the multichannel seismic data provided significant information.

## 4.2 Gravity methods and crustal thickness grid

### 4.2.1 Gravity methods

The crustal thickness grid is one of the main prerequisites for calculation of rotation poles as described in Chapter 9. Its overall quality relies on the quality and density of crustal thickness information. In the region of the submarine plateaux of New Zealand, the quantity of crustal thickness information based on refraction seismic data is too sparse, with only six lines in the Campbell Plateau and Chatham Rise area. In order to increase the crustal thickness information, gravity methods were employed. In addition to published gravity models, another 29 gravity profiles were modelled for the crustal thickness grid (Figure 4-2). The global dataset of Smith and Sandwell [1997] was used for gravity and the dataset of Sandwell and Smith [1997] for bathymetry information. The gravity and bathymetry data were extracted along previously published seismic reflection profiles from the global datasets, so that the sediment thickness could be used to constrain the gravity modelling process. In some regions of the Lord Howe Rise and New Caledonia Basin, no seismic reflection profiles were available. In these cases, the gravity profiles were extracted along the ridges and basins as this direction promised the fewest changes in sediment thickness.

As the only information to be gathered from the gravity modelling was the crustal thickness with a minimum structure, gravity models were generated. In this case this means that no lateral changes in density were allowed in the profiles and that the same densities for each layer were used for all models with the same number of layers. The number of sediment layers was taken from reflection seismic data, for the crust two layers were used and one for the mantle. Densities were estimated from profiles coincident with seismic refraction data [Groby, *et al.*, 2007; Groby, *et al.*, submitted]. For the profiles AWI-20030001 and 20030002, Bryan Davy modelled the gravity using the layers provided by the seismic refraction models. The densities used for these profiles were used for all gravity profiles modelled for the crustal thickness map. In a gravity inversion for the Challenger Plateau region, Wood and Woodward [2002] used constant densities for each layer, resulting in a mean gravity residual of  $0.24 \pm 4.10$  mgal. This shows that the assumption of constant densities throughout the model does not lead to very large errors.

### 4.2.2 Crustal thickness grid

The choice of a gridding algorithm depends mainly on the lateral sampling of the data to be gridded. The simple algorithm of a nearest neighbour gridding works best with a relatively dense net of data points. This gridding algorithm is a local technique. The value of a grid cell that has at least one neighbour within the search radius  $R$  is computed by averaging the values of its nearest neighbours. If there are no neighbours, no output is given. As the database for the crustal thickness grid has regions with dense data coverage (e.g. in the Challenger Plateau region) and regions with sparse (e.g. the

Campbell Plateau region) or very sparse coverage (e.g. the Lord Howe Rise), this technique would lead to gaps in the crustal thickness grid using a small search radius or to a blocky grid using a large search radius.

The value for a data point is given as a weighted mean of the nearest point from each sector inside the search radius. The distance-dependent weights  $w(r)$  are computed as follows:

$$w(r) = \frac{1}{1 + (3r/R)^2} \quad (4-15)$$

with  $r$  the distance from the node. As the reconstruction presented in Chapter 9 requires a complete and fine grid, this technique would make the reconstruction fail.

Hence, a global gridding algorithm, in contrast to a local algorithm, is necessary to compile the crustal thickness grid. The method applied here is an extension of the minimum curvature method widely used in earth sciences. Minimum curvature methods apply an interpolation scheme using continuous second-order derivatives, in which the integral of the squared curvature over the entire surface is minimised [Briggs, 1974]. The one-dimensional application of this interpolation scheme is well known as the natural cubic spline [Lancaster and Salkauskas, 1986]. However, this method can lead to large oscillations between controlling data points [Smith and Wessel, 1990].

It has been shown that the problem of oscillations can be reduced to a large extent, if the constraint of the global curvature is relaxed by the introduction of a tension of the surface [Smith and Wessel, 1990]. An increase of the tension parameter in turn reduces the weight of the constraint of minimum curvature, in the sense that the curvature is localised at the data points. In order to derive an interpolated data point  $z$  at position  $(x,y)$ , the following differential equation has to be solved:

$$(1 - T_I)^2 \nabla^2 (\nabla^2 z) - T_I \nabla^2 z = \sum_i f_i \delta(x_i - x; y_i - y) \quad (4-16)$$

with  $(x_i, y_i, z_i)$  as the constraining data. The function  $f_i$  has to be chosen so that  $z \rightarrow z_i$  as  $x \rightarrow x_i$  and  $y \rightarrow y_i$ , i.e. the interpolant has to fit the data at the control points. Additional constraints have to be followed for edges and corners. Setting the tension factor  $T_I$  to 0 leads to the minimum curvature algorithm without tension, setting  $T_I$  to 1 yields infinite tension. The solution of (4-16) has the important feature that it cannot have local extrema between the control points [Smith and Wessel, 1990]. This means, for the presented crustal thickness grid, that the gridding algorithm did not introduce any local extrema.

The calculation of the crustal thickness grid (Figure 4-2) is performed with a spacing of 3' x 3' using the algorithm of continuous curvature splines in tension. The grid cell size was a trade-off between resolution and calculation time. For the coarse grid search (Chapter 9), 2304 rotation poles were calculated. At a grid cell size of 1' x

1', the rotation of the grid took ca. 20 mins, at a grid cell size of 3' x 3' ca. 2 min. The region comprised all of Zealandia from 154° E to 170° W and 57° S to 17° S.

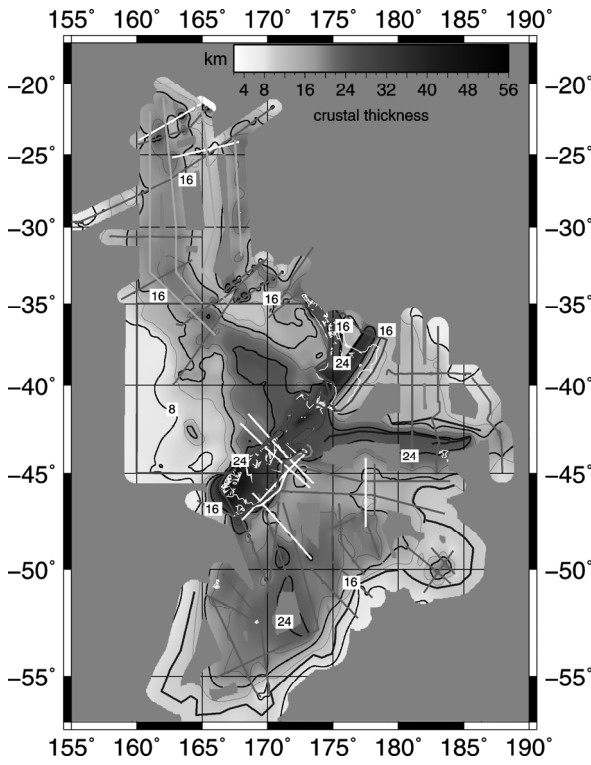


**Figure 4-2: Database of the crustal thickness grid.** The map shows the reliability of the crustal thickness grid (Chapter 9). Superimposed on the grid, which is calculated with a modified minimum curvature algorithm, is a mask that blanks out all grid nodes that have a distance to a data point of more than 75 km.

## 5 Structure of this thesis

This thesis deals with the break-up history of Zealandia from West Antarctica based on two seismic refraction/wide angle transects across Bounty Trough and the Great South Basin. Starting from the seismic observations, the work is completed with a tectonic reconstruction of Zealandia.

Chapters 2, 3, and 4 represent the background of the thesis. They deal with the previous knowledge of the geology of Zealandia and Marie Byrd Land and thus give a broad overview of the tectonic history and give an introduction to some basic concepts of geology and geophysics. On the geological side, the mechanisms of crustal extension are presented in spotlights, on the geophysical side the methods of modelling, particularly raytracing and gridding, and interpretation are presented.

Chapter 5 highlights the structure of this thesis, Chapter 6 shows my contributions to publications, and Chapter 7 is the reference list for chapters 2 – 4.

Chapter 7 and 8 focus on regional aspects of the geophysical data. In Chapter 9, the results of modelling the Bounty Trough transect are presented. Strong p- and S-wave and density anomalies as well as crustal thinning are found in the lower crust of the Middle Bounty Trough. They are interpreted as mafic intrusions and underplating. Combined with observations from seismic reflection data, a model of the Bounty Trough opening is developed invoking phases of back-arc extension, compression and rift-related extension. Comparison of the Bounty Trough opening with rift models of Kenya Rift and Oslo Rift shows that extension in Bounty Trough also comprised elements of the pure-shear and simple-shear model, the major extensional models.

Chapter 8 treats the seismic refraction profile as well as gravity and magnetic data from the Great South Basin and the Campbell Plateau. Again, crustal thinning and positive P-wave velocity anomalies are observed and interpreted as structures related to underplating. However, the Great South Basin did not experience the first extensional and the compressional phase and depicts a simple rift related basin. Geophysical observations are compared with the interpretations of magnetic anomaly systems in the region and lead to a re-interpretation of the origin of the magnetic anomaly systems in the respect that they either have a different origin or they developed differently over the time.

Chapter 9 is a synthesis of the investigations of Bounty Trough and Great South Basin leading to a reconstruction of Zealandia. Crustal thickness information of the basins suggested that previous plate-kinematic reconstruction would fail in this area of crustal thinning without seafloor spreading. Using the idea of crustal balancing, a new method for plate-kinematic reconstructions was developed. This novel method invokes the idea of hypothetical detachment faults in the regions of extended crust and the assumption of a pre-extensional crust with uniform thickness as a criterion for the best fit. In the basins, parts of the crustal thickness are assigned to each of the plates, so that the crustal thickness in total is preserved. After a plate rotation, the thickness is vertically summed up again and compared with the initial crustal thickness. This new reconstruction technique has re-determined the extension in the basins of Zealandia to

## STRUCTURE OF THIS THESIS

be far less than previously assumed and explained a number of geophysical observations addressed in literature and the previous chapters. It has shown that the extension in Bounty Trough and Great South Basin occurred simultaneously caused by the separation of Chatham Rise and the South Island from Antarctica.

Chapter 8 summarises this thesis by focussing on the main conclusions and addressing the questions raised in Chapter 1. It also deals with the opportunities resulting from the novel reconstruction technique of Chapter 9.

This thesis contains the original text, data and figures of three manuscripts that were submitted to peer-reviewed, international journals. The first manuscript (Chapter 7) is published in the *Journal of Geophysical Research B* (AGU, Washington), doi: 10.1029/2005JB004229. The second (Chapter 8) was submitted to *Tectonophysics* (Elsevier, Amsterdam) in December 2006, and the third manuscript (Chapter 9) was submitted to *G-cubed* (AGU, Washington) in May 2007. Due to its cumulative form, repetitions within the text and the figures cannot be avoided in this thesis.

## 6 Contributions to Publications

### **a. Is the Bounty Trough an aborted rift?**

Jan Grobys, Karsten Gohl, Gabriele Uenzelmann-Neben, Bryan Davy, Daniel H. N. Barker, Tara Deen, JGR, doi:10.1029/2005JB004229

Jan Grobys did the P- and S-wave seismic refraction modelling and most parts of the interpretation, Gabriele Uenzelmann-Neben processed the seismic reflection profile, Bryan Davy modelled the gravity profile and Tara Deen made the compositional model. All co-authors contributed to the interpretation

### **b. Extensional and magmatic nature of the Campbell Plateau and Great South Basin from deep crustal studies**

Jan Grobys, Karsten Gohl, Gabriele Uenzelmann-Neben, Bryan Davy, Daniel Barker, submitted to Tectonophysics

Jan Grobys did the P-wave seismic refraction modelling, Gabriele Uenzelmann-Neben processed the seismic reflection profile, and Bryan Davy modelled the gravity profile. All co-authors contributed to the interpretation.

### **c. Crustal balancing applied for plate-tectonic reconstruction of Zealandia**

Jan Grobys, Karsten Gohl, Graeme Eagles, submitted to G-cubed

Jan Grobys developed the method of pole rotations based on crustal thickness, modelled the satellite gravity profiles and did most of the interpretation. Karsten Gohl and Graeme Eagles contributed to the interpretation.

### **d. Neogene magmatic activity in the Bounty Trough**

Gabriele Uenzelmann-Neben, Jan Grobys, Karsten Gohl, Bryan Davy, Daniel Barker, submitted to GSA Bulletin

Gabriele Uenzelmann-Neben processed the seismic reflection profiles and did most of the interpretation, Jan Grobys contributed the seismic refraction background. All co-authors contributed to the interpretation.

## 7 Is the Bounty Trough, off eastern New Zealand, an aborted rift?

J. W.G. Grobys<sup>\*a</sup>, K. Gohl<sup>a</sup>, B. Davy<sup>b</sup>, G. Uenzelmann-Neben<sup>a</sup>, T. Deen<sup>c</sup>, D. Barker<sup>b</sup>,

<sup>a</sup>*Alfred Wegener Institute for Polar and Marine Research, Bremerhaven, Germany*

<sup>b</sup>*Institute of Geological and Nuclear Sciences, Lower Hutt, New Zealand*

<sup>c</sup>*ARC National Key Research Centre for Geochemical Evolution and Metallogeny of Continents, Department of Earth and Planetary Sciences, Macquarie University, Australia*

Published in *Journal of Geophysical Research, Solid Earth* (2007),  
doi:10.1029/2005JB004229

### Abstract

Remarkably little is known about the Cretaceous rifting process between New Zealand and Antarctica that affected the submarine regions within the New Zealand microcontinent. Bounty Trough provides insights into these break-up processes. Here we present results from a combined gravity, multichannel seismic and wide-angle reflection/refraction seismic transect across the Middle Bounty Trough and interpret these results on the basis of velocity distribution and crustal composition derived from Poisson's ratio and P-wave velocity. The lower crust exhibits a high-velocity ( $v_p \approx 7 - 7.7$  km/s,  $v_s \approx 3.9 - 4.5$  km/s), high-density ( $\rho = 3.02$  kg/cm<sup>3</sup>) body at the location of the thinnest crust on the profile. Here the crustal thickness is reduced to about 9 km from 22 - 24 km beneath Chatham Rise and Campbell Plateau. We interpret the high-velocity/density body as a magmatic intrusion into thinned continental crust. Our results show that the Cretaceous opening of Bounty Trough was very likely not the result of back-arc extension caused by collision of the Hikurangi Plateau with the Gondwana margin, but of continental break-up processes related to the separation of New Zealand from Antarctica. Rifting ceased in the Middle Bounty Trough at the onset of seafloor spreading. Comparisons with the Oslo Rift and the Ethiopian/Kenya Rift indicate, that all three rift systems show analogous extensional features. From this, we derive a stretching model for the Bounty Trough that combines elements of pure-shear and simple-shear extension.

## Keywords

continental rift, ocean-bottom seismographs, seismic refraction/wide-angle reflection, travel-time inversion, Gondwana break-up, Campbell Plateau, Chatham Rise

## 7.1 Introduction

Rift systems play a key role in the Wilson Cycle and give important insights into the processes and driving mechanisms that control the break-up of continents [Woodcock, 2004]. Many conjugate margins exhibit a distinct asymmetry that is often correlated with detachment faults accommodating large strains during extension [Whitmarsh, *et al.*, 2001]. Observations at rifts indicate that extension generally does not follow either of the accepted end-member extension models of “uniform stretching” or “simple shear” [Lister, *et al.*, 1986], but may consist of a succession invoking both [Ro and Faleide, 1992]. Quantifying the amount of crustal stretching allows refinement of plate-tectonic reconstructions, since most plate-kinematic reconstructions do not take account rifting prior to seafloor spreading.

The Bounty Trough is a bathymetric feature, up to 3 km deep, overlying a Cretaceous sedimentary basin in a submarine continental plateau. It separates the Campbell Plateau and Bounty Platform from the Chatham Rise (Figure 7-1). Thick (2 km) stratified sedimentary layers, which have mainly accumulated since the late Pliocene, characterize the modern Bounty Trough [Carter and Carter, 1987; Carter and Carter, 1993; Davey, 1977]. From seismic information, Carter *et al.* [1994] came to the conclusion that the Bounty Trough has a rift origin. Carter and Carter [1987] mentioned that new seafloor was not created within the rift, whereas Davy [1993] interpreted quasi-symmetric magnetic anomalies and rotated basement blocks as evidence for Permian back-arc/oceanic crust re-worked by Cretaceous extension.

A number of plate-tectonic reconstructions of the region have been made on the basis of geological observations [Kamp, 1986], palinspastic reconstructions [Gray and Norton, 1988] and magnetic data [Eagles, *et al.*, 2004; Sutherland, 1999]. While a Santonian to Campanian timing of Bounty Trough opening can be indirectly derived from geological and plate-tectonic evidence [Eagles, *et al.*, 2004; Wood and Herzer, 1993], the trough’s role in the regional plate-tectonic context is still poorly constrained.

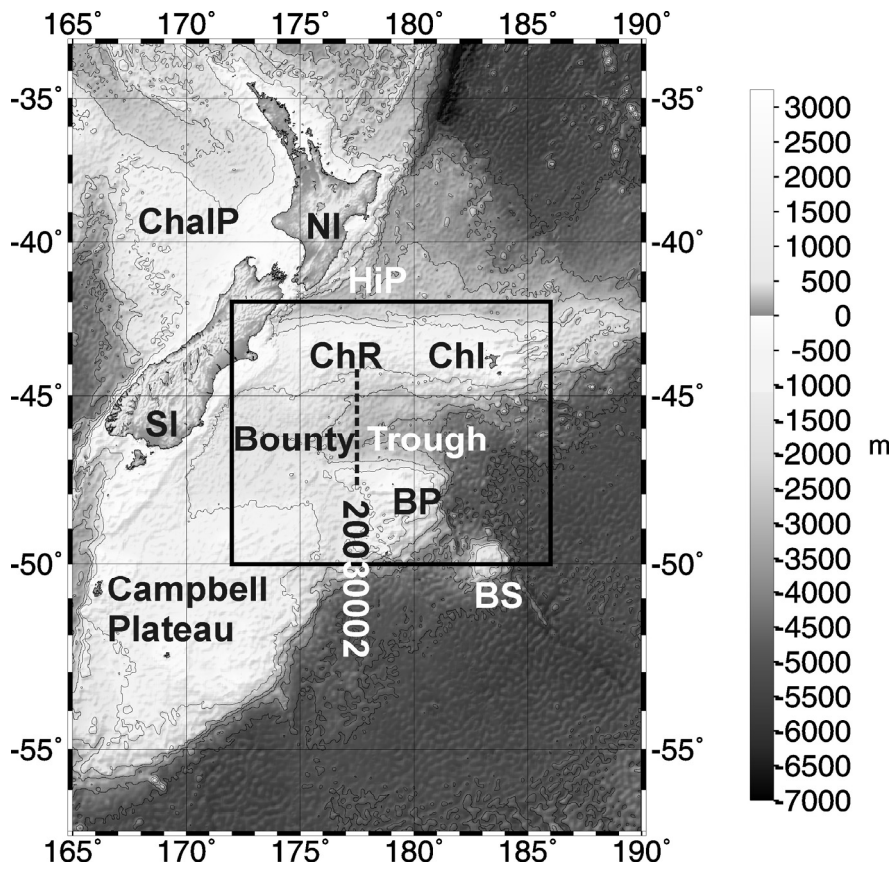


**Figure 7-1: Bathymetric overview map** [Smith and Sandwell, 1997] of the area southeast of the South Island of New Zealand and location of the CAMP experiment, showing location of seismic transect AWI-20030002 across the Bounty Trough (dashed). The black box shows the area of the gravimetric map (Figure 7-3). Abbreviations are: NI- North Island of New Zealand, SI – South Island of New Zealand, ChR – Chatham Rise, BP – Bounty Platform, BS – Bollons Seamounts, ChI – Chatham Islands, HiP – Hikurangi Plateau, ChalP – Challenger Plateau.

Knowledge of the regional rifting mechanisms may also improve the understanding of the differences between Marie Byrd Land and the New Zealand continent. Campbell Plateau and Chatham rifted from the Marie Byrd Land and Ellsworth Land sectors of Antarctica. All of these regions, appear to have a similar crustal composition [Wandres, *et al.*, 2004 and references therein], and crustal thickness (~ 25 km), but a different elevation relative to the sea surface [Ritzwoller, *et al.*, 2001]. While Chatham Rise and the Campbell Plateau are submarine plateaus at 500 m depth or deeper, Marie Byrd Land rises at least 500 m above sea level [Winberry and Anandkrishnan, 2004], while a uniform elevation of the four crustal blocks mentioned above prior to rifting [LeMasurier and Landis, 1996] is suggested. An improved knowledge of the crustal structure and rifting process should contribute to our understanding of the differential uplift and/or subsidence processes. Knowledge of the composition and the opening/extensional history of the Bounty Trough is important because of the trough's key position in the reconstruction of the Gondwana break-up between Antarctica and New Zealand [Eagles, *et al.*, 2004] (Figure 7-2). Whether the Bounty Trough is underlain by oceanic crust or thinned continental crust, and whether

the Bounty Trough is a back-arc basin or a failed rift arm of a triple junction at its mouth are questions that are still under debate [Davy, 1993; Sutherland, 1999]. A better knowledge of the roles played by these different processes will significantly improve plate-kinematic models of the New Zealand region and will contribute to understanding of the opening mechanisms of continental rifts worldwide.

Rift processes and elements of extension models (e.g. successive uniform stretching and simple shear) can be tested by means of deep crustal seismic surveys and potential field methods. To investigate the mechanisms of the Bounty Trough opening and its role in the early development of the southwest Pacific, the Alfred Wegener Institute for Polar and Marine Research (AWI), the Institute of Geological and Nuclear Science (GNS), and Macquarie University conducted deep penetrating seismic and potential field experiments (CAMP project) across the Campbell Plateau and the Bounty Trough. This paper focuses on the combined gravity, multichannel reflection, and refraction/wide-angle reflection seismic transect, AWI-20030002, running north-south across the middle Bounty Trough at 177.5° E (Figure 7-1). Our findings define the pre-rift size of the Campbell Plateau/Chatham Rise and thus help to further constrain reconstructions of the late Gondwana break-up.

## 7.2 Geological Setting

The Bounty Trough is a Cretaceous rift feature according to [Carter, *et al.*, 1994; Krause, 1966], interpreted by Davy [1993] as a feature of back-arc extension. It was formed during the late stages of Gondwana break-up [Eagles, *et al.*, 2004]. Running east-west for ~1000 km and with a width of ~350 km, the trough separates the Chatham Rise in the north from the Campbell Plateau with its northeastern part, the Bounty Platform.

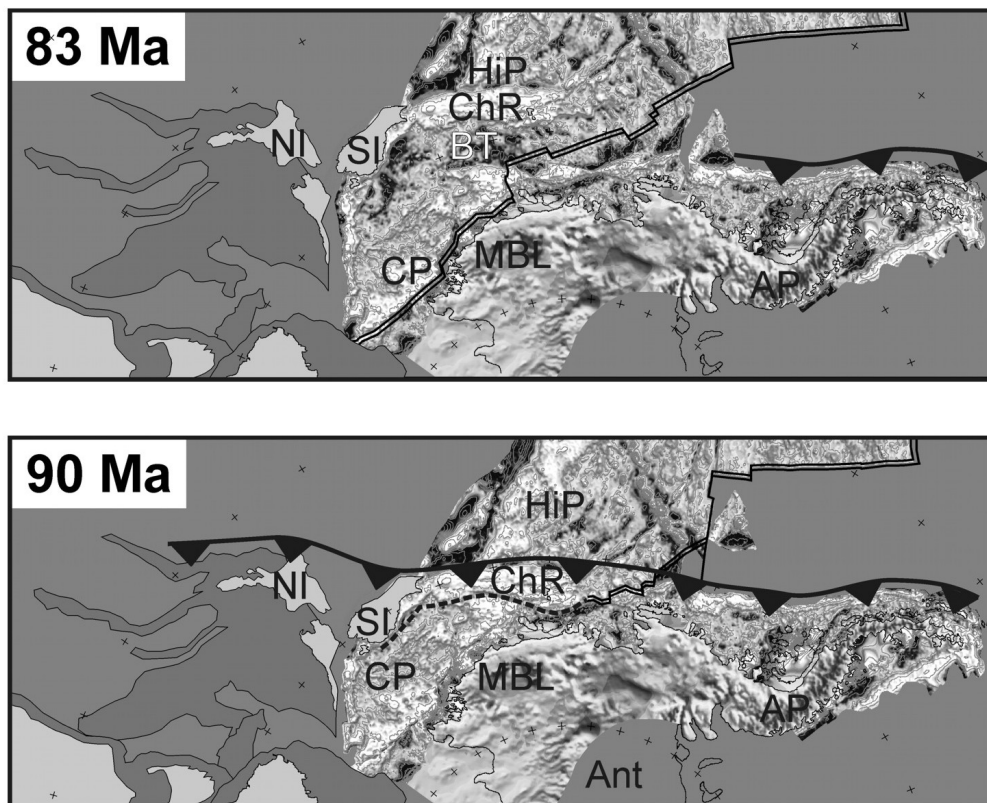


**Figure 7-2: Two time-slices from the reconstruction** of the opening of the southwest Pacific in the late Cretaceous, after Eagles *et al.* [2004]. Lower: Campbell Plateau and Chatham Rise are still parts of the same submarine plateau prior to 90 Ma. The black line marks the fossil subduction zone of the Phoenix Plate beneath the Chatham Rise, double lines indicate active extension or seafloor spreading. Dashed black line is the future Bounty Trough axis. Upper: At 83 Ma the Bounty Trough has opened, while Campbell Plateau is still attached to Marie Byrd Land. The reconstruction includes offshore free-air gravity anomaly data [McAdoo and Laxon, 1997; Sandwell and Smith, 1997] and data from the BEDMAP compilation for onshore Antarctica [Lythe, *et al.*, 2000]. Blue and green colors indicate negative free-air gravity values; orange, red and white colors indicate positive free-air gravity anomalies. Areas not included in the modeling process, or subducted areas, are shaded in solid gray. Abbreviations are: Ant – future Antarctic plate, AP – Antarctic Peninsula, BT – Bounty Trough, CP – Campbell Plateau, ChR – Chatham Rise, HiP – Hikurangi Plateau, MBL – Marie Byrd Land, NI – North Island of New Zealand, SI – South Island of New Zealand.

Bounty Trough deepens towards the Pacific Ocean in a series of broad terraces [Davy, 1977]. Two ca. 1 km high basement steps [Carter, *et al.*, 1994] separate the Bounty Trough into three subbasins. The steps can only be distinguished in bathymetry data (Figure 7-1), and give rise to no gravity anomalies in the satellite data (Figure 7-3). The prominent Bounty Channel, one of the world's major drainage channels, cuts deeply into the sediment fill along the axis of the Bounty Trough [Carter and Carter, 1987].

The timing of the Outer Bounty Trough opening is relatively well known: A linear magnetic anomaly immediately south of the Chatham Islands has been associated with oceanic crust. This anomaly might be the young end of anomaly 34, formed during the earliest seafloor spreading (~ 83 Ma) between Marie Byrd Land and New Zealand [Davy, 1993, Davy, in prep #277]. Carter *et al.* [1994] postulated that the basal sedimentary unit (D1) in the Outer Bounty Trough might be as old as early Cretaceous. East-west trending Mid-Cretaceous faults define the margin between Chatham Rise and the Bounty Trough. These faults imply a similar age of initial faulting and sedimentation in this region [Laird, 1993], too. Wood and Herzer [1993], using seismic data from the Chatham Rise area, interpreted Bounty Trough rifting as having ceased in late Campanian times (83.5 – 71.5 Ma). This is later than in a recent plate-tectonic reconstruction [Eagles, *et al.*, 2004], where the opening of Bounty Trough occurs prior to 83 Ma. Based on an investigation of the Otago Schist, Forster and Lister [2003] proposed two phases of extension in the eastern New Zealand region during the Cretaceous. A first phase occurred parallel to the margin of Gondwana at ca 115 Ma. At ca 110 Ma, extension rotated by approximately 90°, perpendicular to the Gondwana margin. Following the ideas of Bradshaw *et al.* [1996], Forster and Lister [2003] suggested that extension of the Bounty Trough occurred at ca 115 Ma and lasted until ca. 85 Ma. The zone of crustal extension is suggested to have continued across the then South Island of New Zealand.

Davy [1993] identified a set of quasi-symmetric magnetic anomalies that are aligned approximately parallel to the axis of Bounty Trough. The source rocks of these anomalies lie within the basement, which was suggested to consist of Permian to Triassic ocean crust because the onshore continuation of the anomalies lies in the Permian Dun Mountain Ophiolite Belt [Carter, *et al.*, 1994]. On newer maps of magnetic anomaly intensity in this region the linear nature of individual anomalies within the Bounty Magnetic Anomaly System is not so distinct [Sutherland, 1999]. A moderate correlation with some gravity anomaly structures, as seen in the satellite-altimetry derived dataset [Sandwell and Smith, 1997], suggests that the Bounty Trough magnetic anomaly pattern does not represent a remanent magnetization caused by field reversals. However, the magnetic anomalies in the Bounty Trough do raise the question of whether Bounty Trough opening followed any pre-existing Permian structure [Davy, 1993]. Alternatively, the magnetic anomalies might be related to Cretaceous igneous activity [Sutherland, 1999].

IS THE BOUNTY TROUGH, OFF EASTERN NEW ZEALAND, AN ABORTED RIFT?

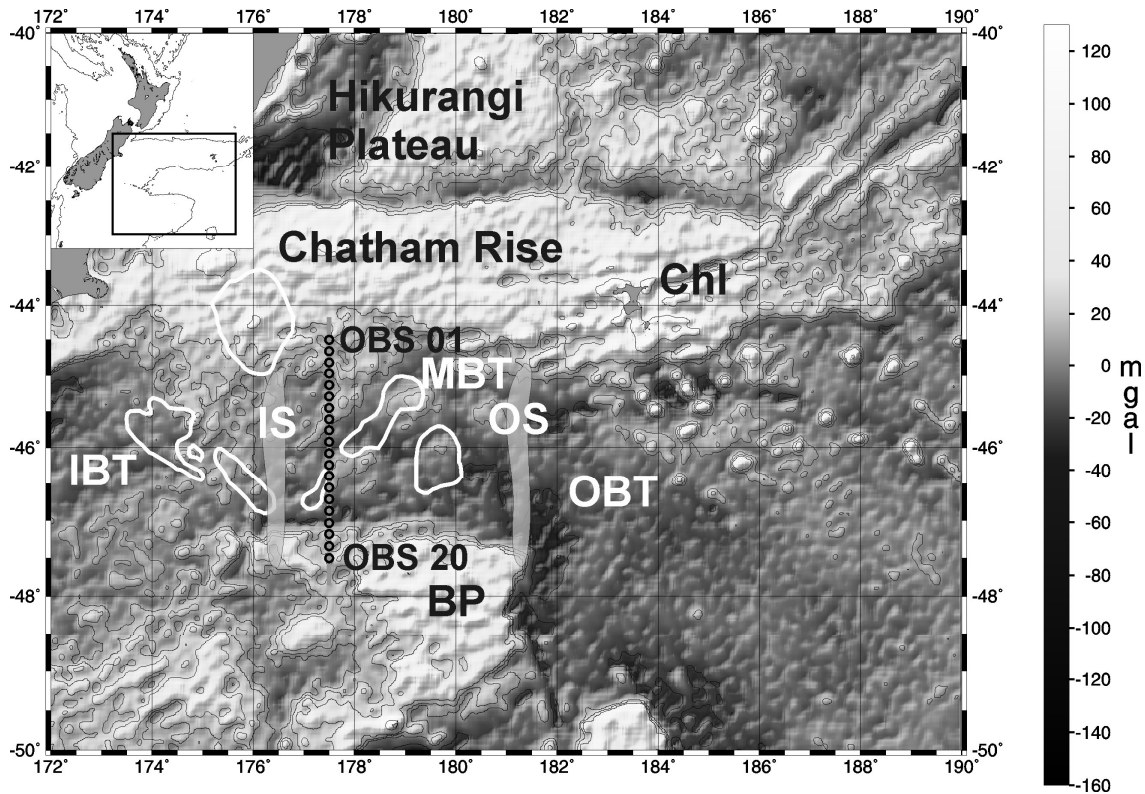


**Figure 7-3: Satellite gravity anomaly map** [Sandwell and Smith, 1997] of the Bounty Trough. Contour intervals are 20 mgal. Gravity lineaments trend at N45E, an angle of 45° to the Bounty Trough axis. In the Middle Bounty Trough, regional gravity anomalies match magnetic anomalies (white outlined areas, after [Sutherland, 1999]), while anomalies in the Inner Bounty Trough do not. The grey line indicates profile AWI-20030002, the black circles mark the positions of the OBS. IBT – Inner Bounty Trough, MBT – Middle Bounty Trough, OBT – Outer Bounty Trough, BP – Bounty Platform, ChI – Chatham Islands, IS – Inner Sill (basement step), OS – Outer Sill (basement step).

In the Middle Bounty Trough, sediments are underlain by highly fractured basement structures [Davey, 1977]. A block-faulted basement floors the Inner Bounty Trough. Cretaceous half-grabens face north within the basement of the Inner Bounty Trough [Wood and Herzer, 1993] in a 100 x 100 km area south of the trough axis near 174° E [Davy, 1993]. Elsewhere, wherever half-grabens are observed, they face dominantly to the south. East of 178.5° W, Davy [1993] has interpreted oceanic crust. Additional information about the crustal structure of the Bounty Trough can be inferred from examination of the crust of the adjacent plateaus, Chatham Rise and Bounty Platform. Chatham Rise is a submerged continental plateau, whose basement consists of Upper Paleozoic and Mesozoic schists and greywackes of the Torlesse Terrane [Adams and Robinson, 1977; Bradshaw, et al., 1981]. Dredged samples from near the Bounty Islands, on the Bounty Platform, are comparable with early Paleozoic metasedimentary rocks (e.g. Greenland Group) [Beggs, et al., 1990]. The Bounty Islands themselves are mostly composed of Early Jurassic granodiorites correlative to the Median Tectonic Zone (Median Batholith) [Beggs, et al., 1990; Kimbrough, et al., 1994]. Bradshaw [1991] supposed, from geological evidence, that the pre-opening crustal thickness of the present northern Campbell Plateau might have been approximately 40 km.

### 7.3 Data acquisition and processing

Line AWI-20030002 of the CAMP experiment is a 410 km long transect crossing the Bounty Trough from the Campbell Plateau to Chatham Rise. Along this line, we acquired a combined refraction/wide-angle reflection and multichannel seismic (MCS) dataset (Figure 7-1). The receiver arrays were a single 2150 m long streamer, and 20 GEOPRO ocean-bottom seismographs (OBS) equipped with three-component 4.5 Hz geophones and a hydrophone. An array of six G-Guns<sup>®</sup>, with a total volume of 48 l (2980 in<sup>3</sup>) [Gohl, 2003] generated the signals. OBS stations were spaced at ~17.5 km intervals; shot spacing was approximately 150 m. Bathymetry and water depths along the profile were recorded with R/V Sonne's onboard SIMRAD<sup>®</sup> EM-120 and Parasound systems. We converted the OBS data to SEG-Y format and applied corrections for the drift of the OBS clock. Exact OBS along track positions at the seafloor were relocated using direct wave arrivals. The maximum horizontal distance between an OBS deployment location and its position on the seafloor was 280 m.

To enhance the signal-to-noise ratio, the data were filtered with a time and offset dependent band-pass filter, deconvolved with a 200 ms spiking deconvolution, and FK-filtered at large-offset ranges to suppress wrap-around noise from previous shots. After each of these processing stages, we picked seismic phases. The resulting picks were carefully compared with each other for the highest signal-to-noise-ratio data in order to exclude phase-shifts caused by any of the three processing steps.

IS THE BOUNTY TROUGH, OFF EASTERN NEW ZEALAND, AN ABORTED RIFT?

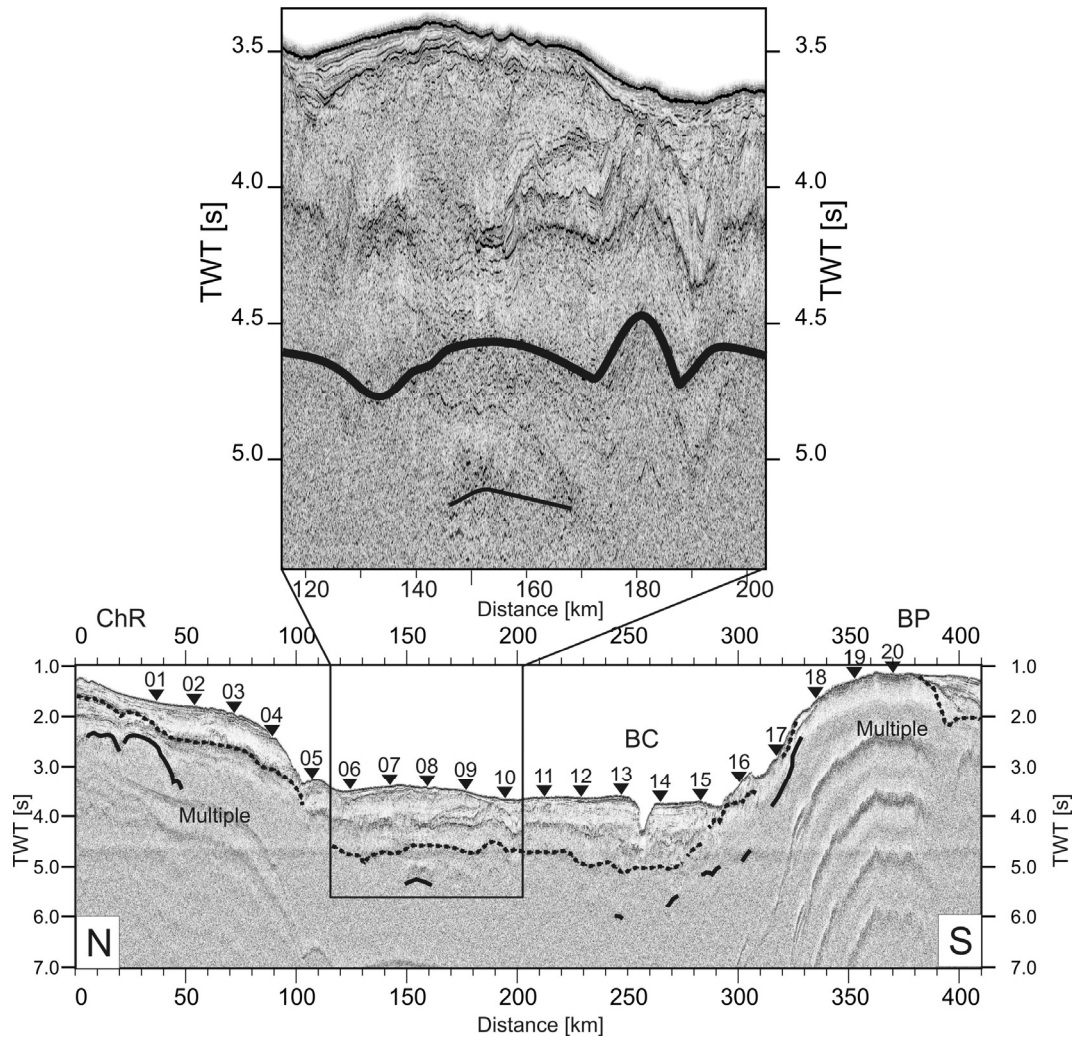


**Figure 7-4:** *Stacked multichannel seismic line AWT-20030002 across the Bounty Trough. Black solid line indicates the tentatively interpreted top of crystalline basement; the black dashed line marks the acoustic basement below stratified sedimentary layers. Triangles and numbers indicate the OBS locations along the transect.*

Multichannel seismic data were processed in a standard processing stream comprising sorting (50 m common-depth-point (CDP) interval), a detailed velocity analysis (every 50 CDPs), multiple suppression via a Radon transform, spike deconvolution to remove the bubble effect, corrections for spherical divergence and normal moveout, residual static corrections, stacking, and post-stack time and depth migration with an emphasis on enhancing of deep reflections. Further details of the processing and interpretation of these multichannel seismic reflection lines are given by Uenzelmann-Neben et al. [in review].

We obtained free-air gravity anomalies from a shipboard LaCoste & Romberg S-80 gravimeter recorded at 1-second interval. The measured values collected by the gravimeter are tied to the N.Z. Potsdam system (1959) via the gravity base station in Lyttleton, New Zealand.

## 7.4 Data description

### 7.4.1 Reflection seismic data

The seismic reflection data show a thick stratified fill (up to 2000m) (Figure 7-4) in the Bounty Trough. A strong reflector marks the bottom of the stratified layers. This transition to acoustic basement is visible in most of the MCS profile [Uenzelmann-Neben, *et al.*, in review]. Only a few discontinuous reflective patches can be seen beneath the acoustic basement reflector. The internal structure of this interpreted basement is poorly defined in the trough. Moho cannot be observed anywhere in the reflection seismic data.

### 7.4.2 Refraction seismic data

The vertical component of the OBS data record shows coherent P-wave phases at up to 120 km offset (Figure 7-5 and Figure 7-6). S-wave phases can be seen in the horizontal components of the OBS data at up to 70 km offset, with a lower signal-to-noise ratio than the vertical component recordings (Figure 7-7 and Figure 7-8). P-wave sections (Figure 7-5) consistently show high-amplitude wide-angle reflections from the Moho ( $P_mP$ ). A few records contain intracrustal reflections of low amplitude ( $P_cP$ ). An example of the  $P_cP$ -phase is displayed for OBS 05 (Figure 7-5d).

We identified refraction arrivals from two layers above and two layers below the acoustic basement. However, an exact separation into different crustal phases was impossible due to the strong influence of topography in the records. Apparent velocities of phases traveling through the middle and lower crust beneath the Bounty Channel are distinctly higher than the average apparent velocity over all stations, whereas phases traveling through the crust of the Bounty Platform are slower. On some of the OBS records, we observed weak  $P_n$  phases (refractions within the uppermost mantle) (Figure 7-5).

Horizontal component sections suffer from strong ringing and are thus of lower quality. However, a sufficient number of records show crustal refraction phases ( $S_g$ ) (Figure 7-7) and reflections from the Moho ( $S_mS$ ). Due to interfering P- and S-phases at small offsets (< 12 km), it was impossible to detect refractions from the sediment layer.

IS THE BOUNTY TROUGH, OFF EASTERN NEW ZEALAND, AN ABORTED RIFT?

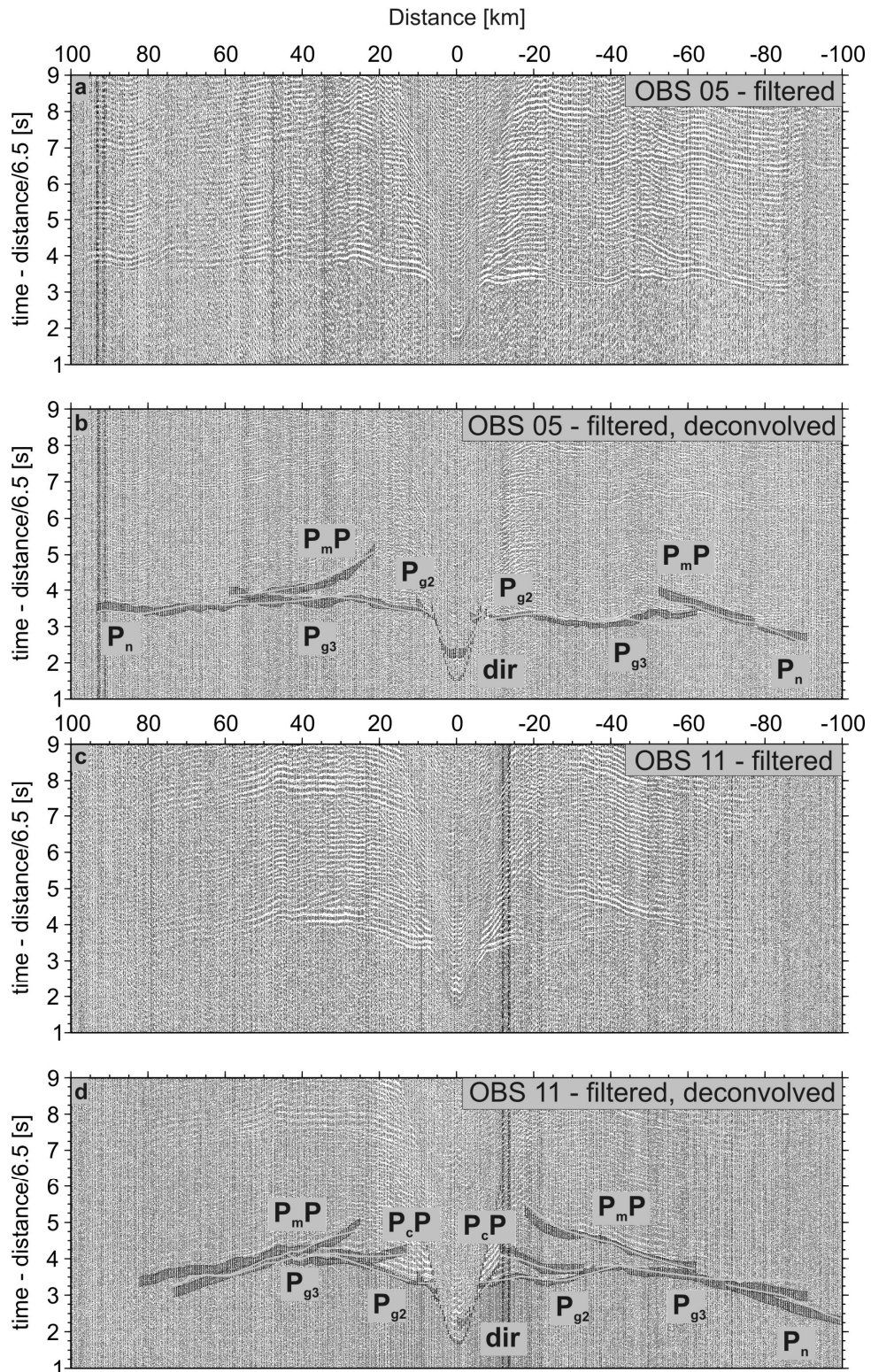


**Figure 7-5: Sample sections of vertical components of OBS records from stations 05 (top) and 11 (bottom).** All sections are plotted with a reduction velocity of 6.5 km/s applied. Sections a) and c) are filtered, sections b) and d) are deconvolved and filtered. Each lower section shows picked and calculated travel times, the size of the error bars indicates the assigned pick uncertainty. Light gray lines are modeled travel-times.

IS THE BOUNTY TROUGH, OFF EASTERN NEW ZEALAND, AN ABORTED RIFT?

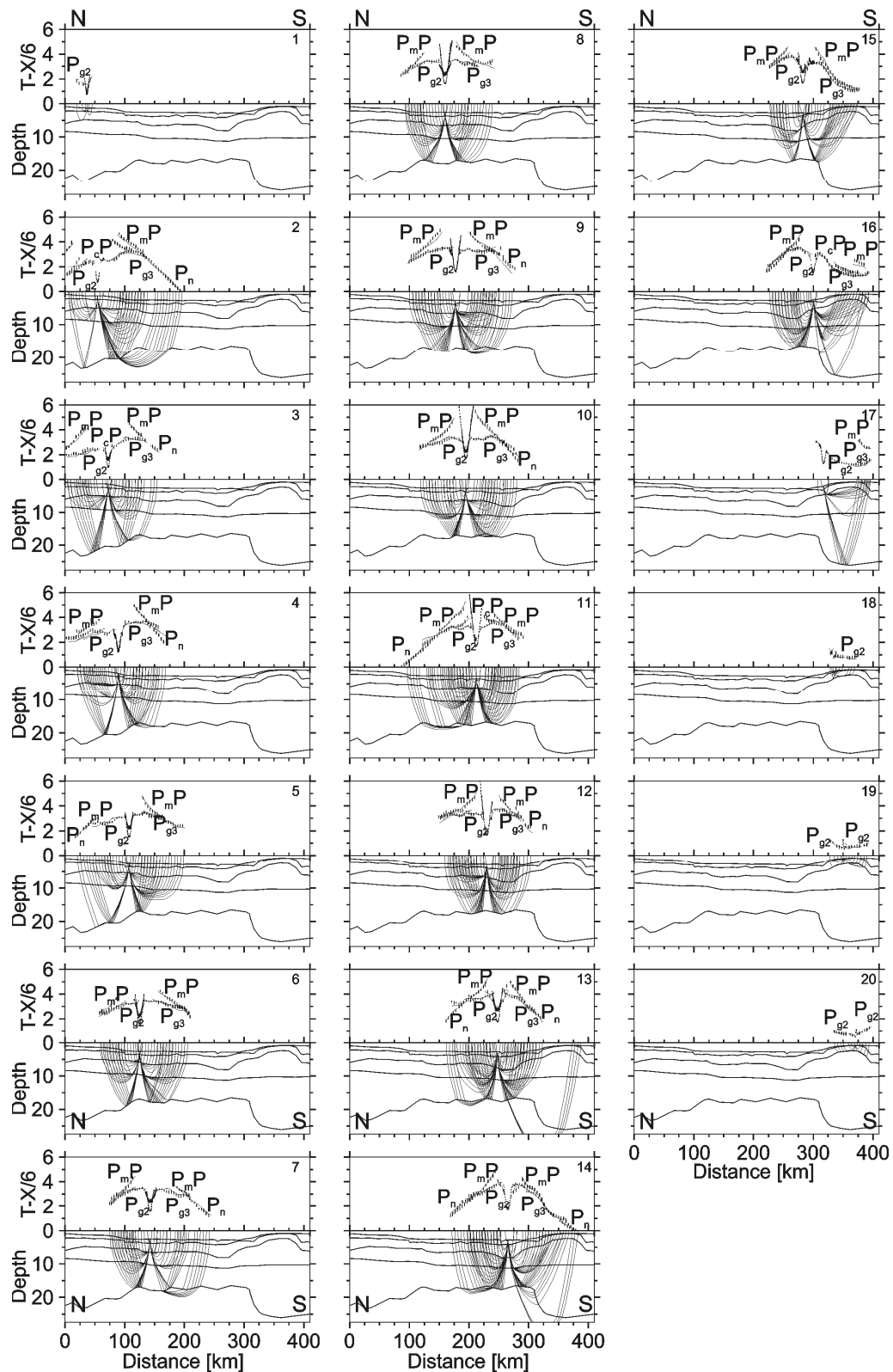


**Figure 7-6: Comparison of picked and computed travel times from the final P-wave model for each vertical component of an OBS station combined with the corresponding ray paths. OBS locations are in Figure 7-4. Depth in km, T-X/6 in s. Travel times are plotted with a reduction velocity of 6 km/s. Vertical error bars indicate observed times, the size of the bars corresponds to the assigned pick uncertainty. Calculated travel times are solid lines. Near-offset phases ( $P_{g1}$ ,  $P_{sed}$ , direct wave) are not labeled.**

## 7.5 Seismic travel-time modeling

We applied a layer-stripping procedure to refine the velocity-depth model by forward modeling. The MCS profile provided boundary conditions for the seafloor and acoustic basement depths. The forward modeling was followed by a successive travel-time inversion [Zelt and Smith, 1992] to fine-tune the model, using all P-wave reflected and refracted phases. At this stage we only allowed positive velocity gradients. As only very few shallow wide-angle reflections can be seen in the data, the top of acoustic basement taken from the MCS was retained. Another velocity interface was introduced into the middle crust of the model to provide a change in the velocity gradient only. Intracrustal reflections ( $P_cP$ ) associated with this interface, were recorded by only one OBS (station 16, Figure 7-6).

### 7.5.1 P-wave modeling

While the resolution of the velocity-depth model (Figure 7-9) can be calculated within the inversion scheme [Zelt, 1999], it is more difficult to quantify errors in phase identification and discrimination. Therefore we set the pick uncertainties from 40 ms to up to 125 ms depending on the signal-to-noise ratio [Zelt and Forsyth, 1994]. Although the true pick uncertainty might be lower than the assigned pick uncertainty, an estimate of the uncertainty in correct phase identification is included with this value [Berndt, *et al.*, 2001].

IS THE BOUNTY TROUGH, OFF EASTERN NEW ZEALAND, AN ABORTED RIFT?

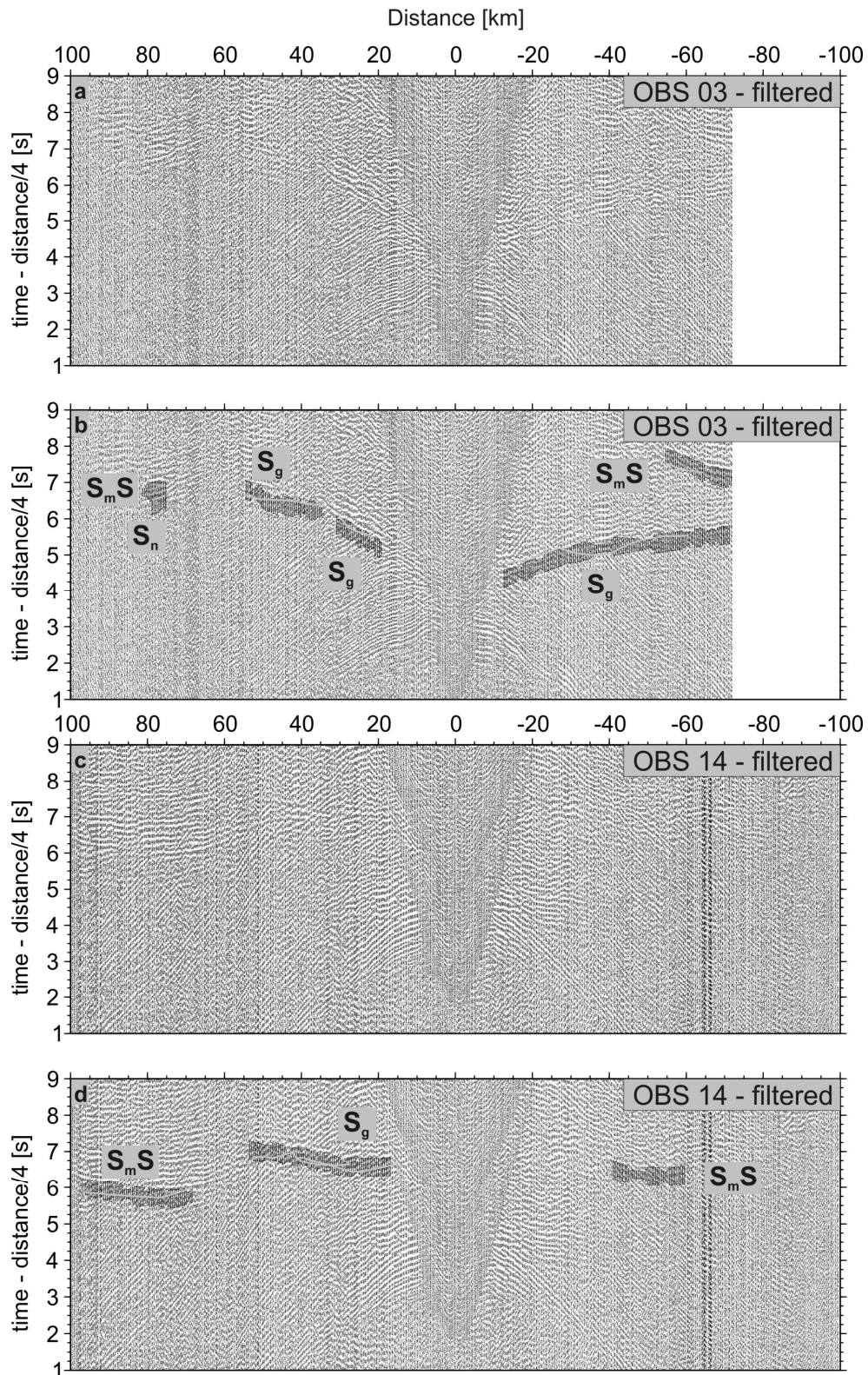


**Figure 7-7: Sample sections of horizontal components of OBS records from stations 03 (top) and 14 (bottom).** All sections are plotted with a reduction velocity of 4 km/s applied. Sections are filtered. Sections b) and c) show picked and calculated travel times, the size of the error bars indicate the assigned pick uncertainty. Light gray lines are modeled travel-times.

IS THE BOUNTY TROUGH, OFF EASTERN NEW ZEALAND, AN ABORTED RIFT?

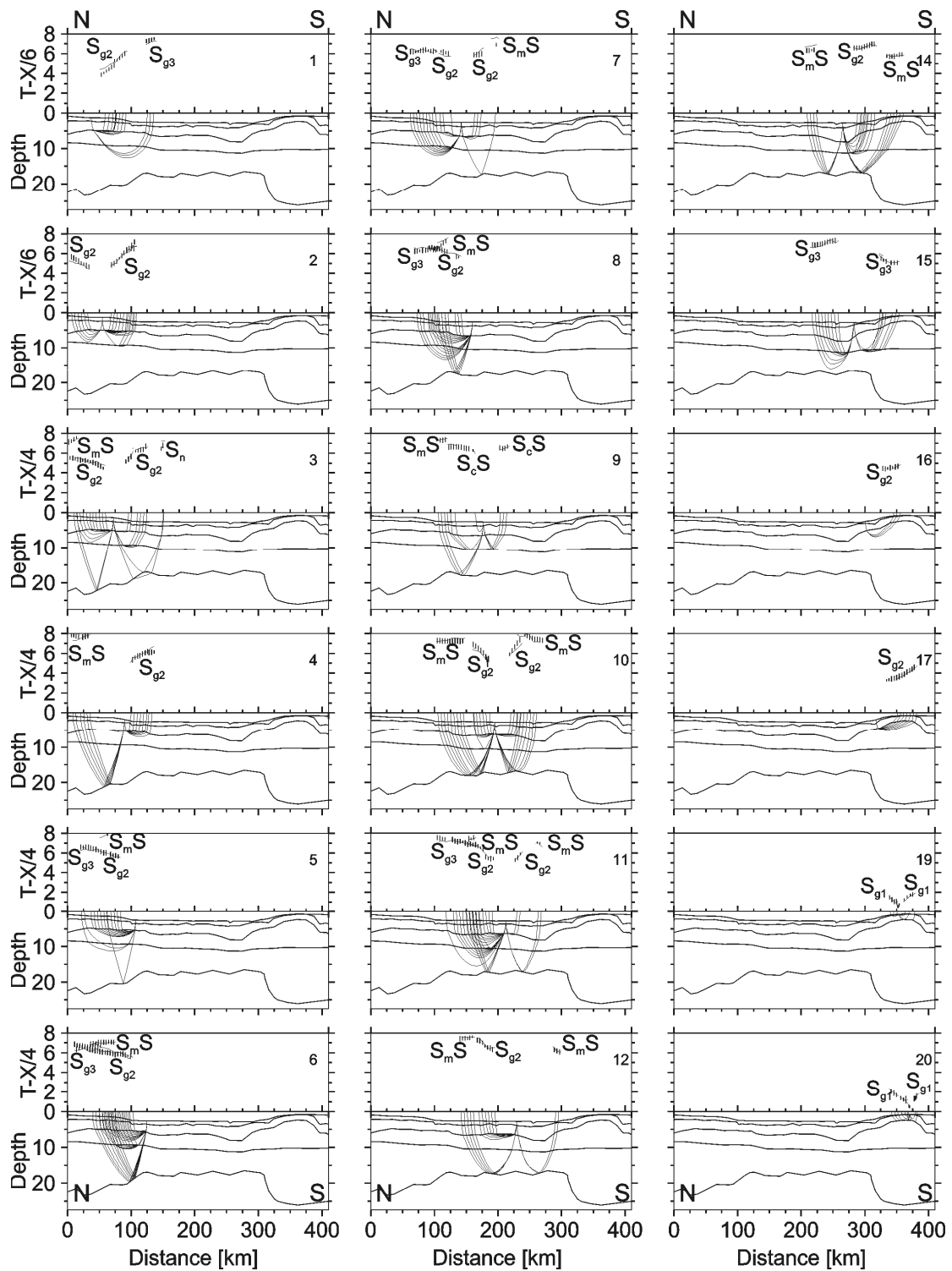


**Figure 7-8: Comparison of picked and computed travel times from the final S-wave model for each horizontal component of an OBS station combined with the corresponding ray paths. No coherent s-wave energy could be observed on stations 13 and 18. Travel times are plotted with a reduction velocity of 4 km/s. Depth in km, T-X/4 in s. Vertical error bars indicate observed times, the size of the bars corresponds to the assigned pick uncertainty. Calculated travel times are solid lines.**

## IS THE BOUNTY TROUGH, OFF EASTERN NEW ZEALAND, AN ABORTED RIFT?

The travel-time inversion process helps assess the model quality as it calculates rms-errors, model-based travel times and Chi-squared values for each branch of the travel-time curves (Table 7-1). With the uncertainties presented above we calculated travel time residuals and normalized Chi-squared values. These values accompanied by the number of picks are presented in Table 7-1. The overall rms-misfit is 0.138 s with a normalized Chi-squared value of 1.972, which is close to the optimum of 1. Figure 7-10 presents the values of the main diagonal of the resolution matrix of the P-wave velocity depth model. Maximum resolution is represented by a value of 1. Smaller values denote a spatial averaging of the true earth by a linear combination of model parameters [Zelt, 1999]. Resolution matrix values greater than 0.5 indicate well resolved nodes.

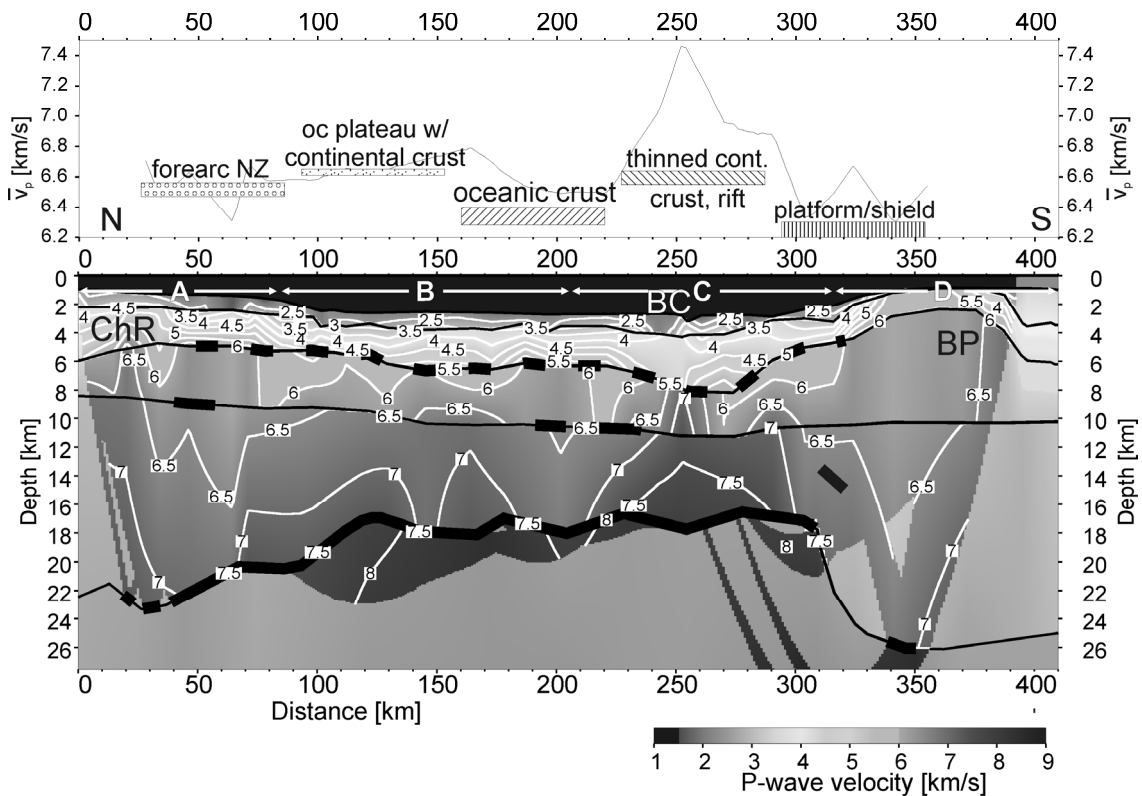


**Figure 7-9: Final P-wave velocity-depth model** overlain by a semi-transparent mask in areas without ray coverage. The top shows average crustal P-wave velocities in regions with ray coverage down to the Moho. The bars superimposed to the average crustal velocities show average crustal velocities for comparable crustal regions calculated from values of the CRUST2.0 model [Bassin, et al., 2000]. Bold sections of layer interfaces are constrained by wide-angle reflections. A high number of very short sections constrained by reflections are marked by the bold dashed layer interface interpreted as top of basement. Abbreviations are: BC – Bounty Channel, BP – Bounty Platform, ChR – Chatham Rise. Regions A–D span: A - Chatham Rise, B – northern Middle Bounty Trough, C – southern Middle Bounty Trough, D – Bounty Platform.

Phase	$t_{rms}$	Chi-squared	Number of picks
$P_{sed,1}$	0.147	5.650	64
$P_{sed,2}$	0.111	2.569	478
$P_cP$	0.166	3.048	405
$P_{g,1}$	0.123	1.960	2465
$P_{g,2}$	0.135	2.066	2565
$P_mP$	0.137	1.717	2626
$P_n$	0.193	3.069	850

**Table 7-1: Statistics of linear traveltime inversion for all phases within a particular modeling layer of the P-wave velocity-depth model. The water layer is not included in the statistics.**

Our P-wave model is best resolved (Figure 7-10) in the upper and lower crust over the range of the complete Bounty Trough and main parts of the Bounty Platform and Chatham Rise, where ray coverage is densest. As more rays turn in the upper part of a layer, this part is generally better resolved than the lower part of the layer. A reasonable (0.5 – 0.6) resolution is calculated for the uppermost mantle in the central part of the Bounty Trough. A change in the geometry of the Moho, and limited offsets, did not allow recording  $P_n$  phases at the flanks of the trough. Many regions of the velo-

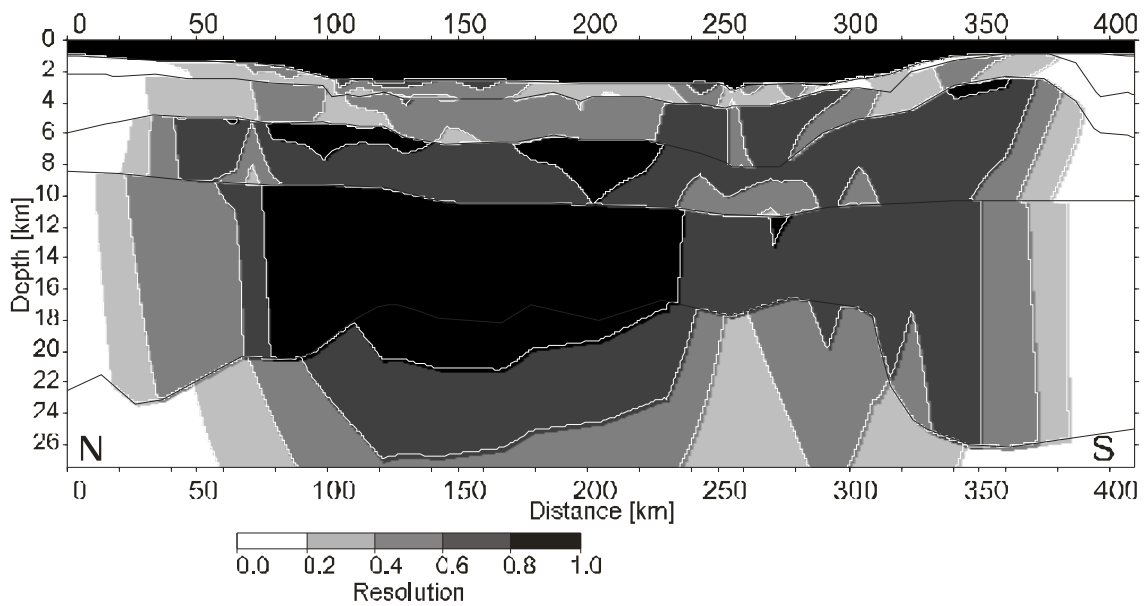


**Figure 7-10: Resolution values** calculated from travel time inversion for the P-wave velocity-depth model. Shading corresponds to resolution values. Contour line interval is 0.2. Resolution values of greater than 0.5 indicate a moderate to good resolution.

city model are less well resolved for the sediment layers. Due to smaller offset ranges and the masking effect of high-amplitude direct wave arrivals [White and Matthews, 1980] upper parts of the model are less covered with overlapping rays. Structural uncertainties in the upper layers are reduced by reference to the coincident MCS line. Intracrustal layer boundaries are not well resolved, but they were introduced to allow for changes in velocity gradient. In contrast to the intracrustal interfaces, the Moho is very well resolved due to a high number of  $P_mP$  phases. 91 % of the nodes have resolution values greater than 0.90, 82 % values greater than 0.97.

## 7.5.2 S-wave modeling

For this model (Figure 7-11) we assigned the same layer interfaces as in the P-wave model, assuming that the observed P- and S-wave energy was generated at the same seismic boundaries and that anisotropy is negligible [Musacchio, *et al.*, 1997]. We derived an initial S-wave velocity model by converting P-wave model velocities to S-wave velocities using constant Poisson's ratios for each individual layer. Most of the layers were converted with a standard value of 0.25, but for the sedimentary layer a value of 0.38 was used to allow for the significantly lower S-wave velocities in sediments [Digranes, *et al.*, 1998]. Subsequently we started a forward and inversion process analogous to the P-wave modeling using  $S_g$  and  $S_mS$  phases picked in the horizontal component sections. During these processes we only allowed the velocity nodes to vary in value.

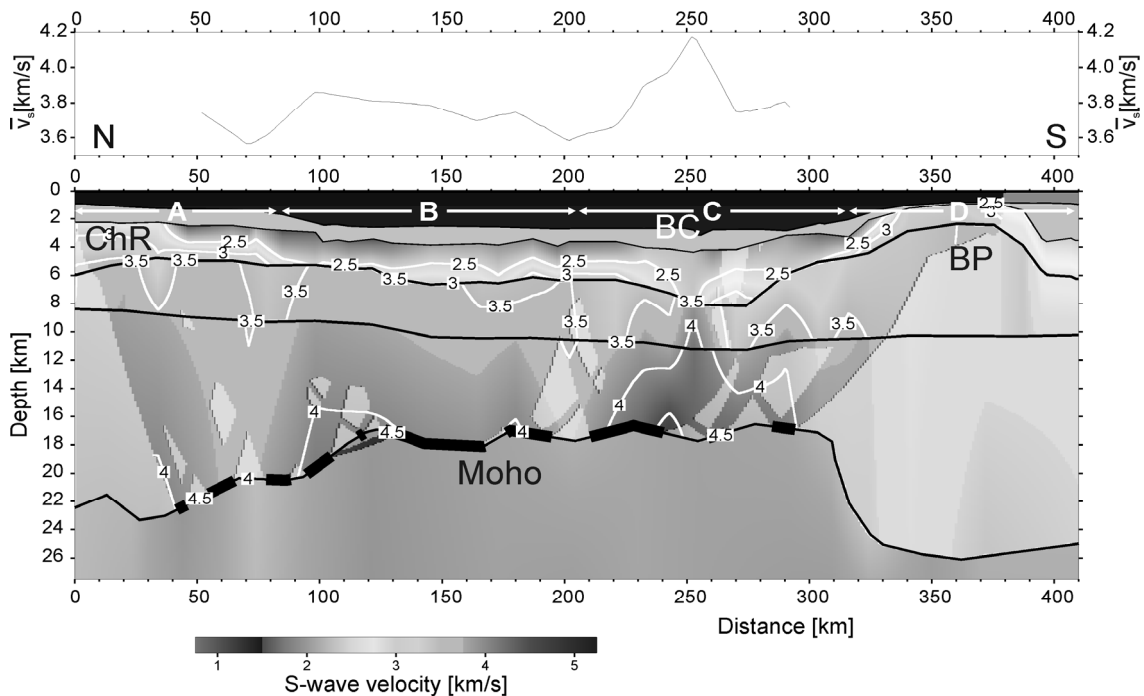


**Figure 7-11: Final S-wave velocity-depth model** overlain by a semi-transparent mask in areas without ray coverage and average crustal S-wave velocities. Bold sections of layer interfaces are constrained by wide-angle reflections. Due to the significantly fewer identified S-wave phases the ray coverage and resolution are less than those of the P-wave model. Abbreviations are: BC – Bounty Channel, BP – Bounty Platform, ChR – Chatham Rise.

Due to a low signal-to-noise ratio for S-wave phases we assigned pick uncertainties up to 250 ms. Therefore, we allowed for an increased ambiguity in the phase discrimination due to interference and possible intra-bed multiples. The number of interpreted S-wave phases is considerably smaller than the number of P-wave phases, resulting in fewer and smaller well-resolved areas (Figures 7-6 and 7-8). The overall rms-residual is 0.216 s with a normalized Chi-squared value of 1.334. In general, poorly resolved regions in the P-wave model have even worse resolutions in the S-wave model, whereas regions with a high resolution in the S-wave model also are well resolved in the P-wave model (Figure 7-12). In particular, the upper crust and the lower sedimentary layer in the northern Bounty Trough (50 – 220 km) exhibit high to very high resolution

values (0.6 – 1.0). The upper crust of the Bounty Platform (320 – 370 km) is also well resolved. However, the upper crust beneath the Bounty Channel and the sedimentary layers have a low resolution; here poor data quality is likely due to interference within the wave field and energy loss due to phase conversion at the seafloor. With only very few exceptions the only observed reflection phases are  $S_mS$  phases. Resolution values of the parts of the Moho covered by  $S_mS$  reflections lie mainly above 0.75. The  $S_mS$  phases can be fit very well using the Moho depth taken unchanged from the P-wave model. This fact adds additional confidence to the  $P_mP$  phase modeling results.

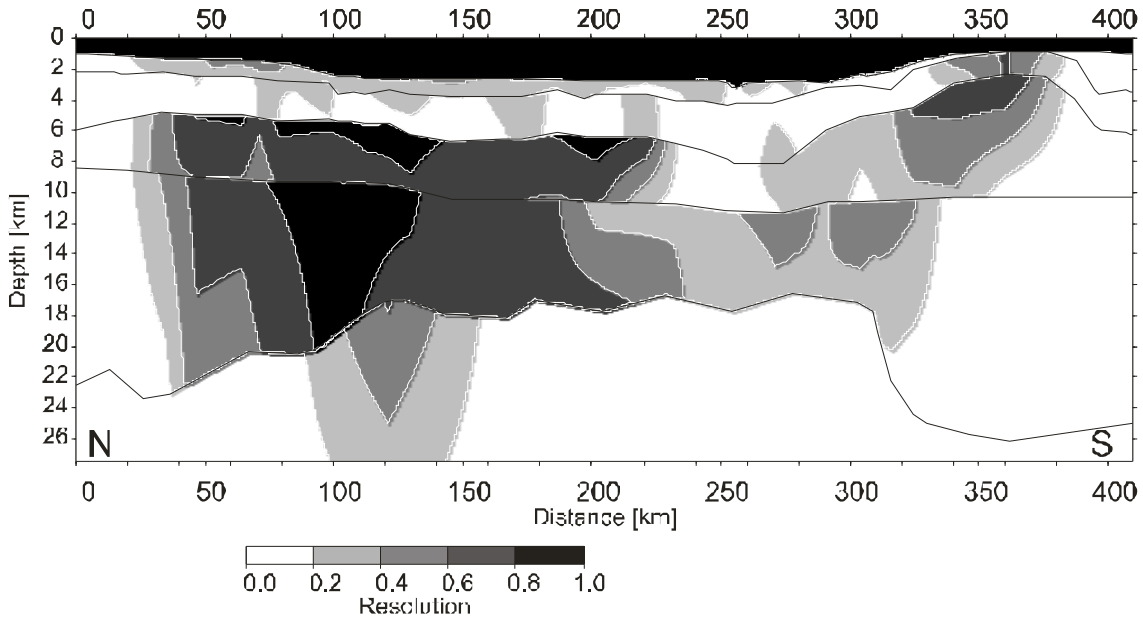


**Figure 7-12: Resolution values** calculated from travel time inversion for the S-wave velocity-depth model. Shading corresponds to resolution values. The resolution of the P-wave model is significantly better than the resolution of the S-wave model. Contour line interval is 0.2. Resolution values of greater than 0.5 indicate a moderate to good resolution.

Phase	$t_{rms}$	Chi-squared	Number of picks
$S_{sed,2}$	0.101	0.482	84
$S_cS$	0.273	1.669	15
$S_{g,1}$	0.221	1.362	1524
$S_cS$	0.099	0.170	33
$S_{g,2}$	0.202	0.963	336
$S_mS$	0.243	1.729	627
$S_n$	0.155	0.748	8

**Table 7-2: Statistics of linear travelttime inversion** for all phases within a particular modeling layer of the S-wave velocity-depth model. The water layer is not included in the statistics.

### 7.5.3 Poisson ratio model

The Poisson's ratio ( $\sigma$ ) is an expression of the ratio  $v_p/v_s$ .  $\sigma$  is strongly influenced by the mineralogy of rocks, in particular by the amount of plagioclase feldspar ( $\sigma=0.30$ ) and quartz ( $\sigma=0.09$ ), while pressure and temperature have only minor influence [Christensen, 1996]. In order to derive a model of  $\sigma$  (Figure 7-13) from the P- and S-wave model, we kept the number of velocity and depth nodes in both models the same. Subsequently we calculated  $\sigma$  for each single velocity node.

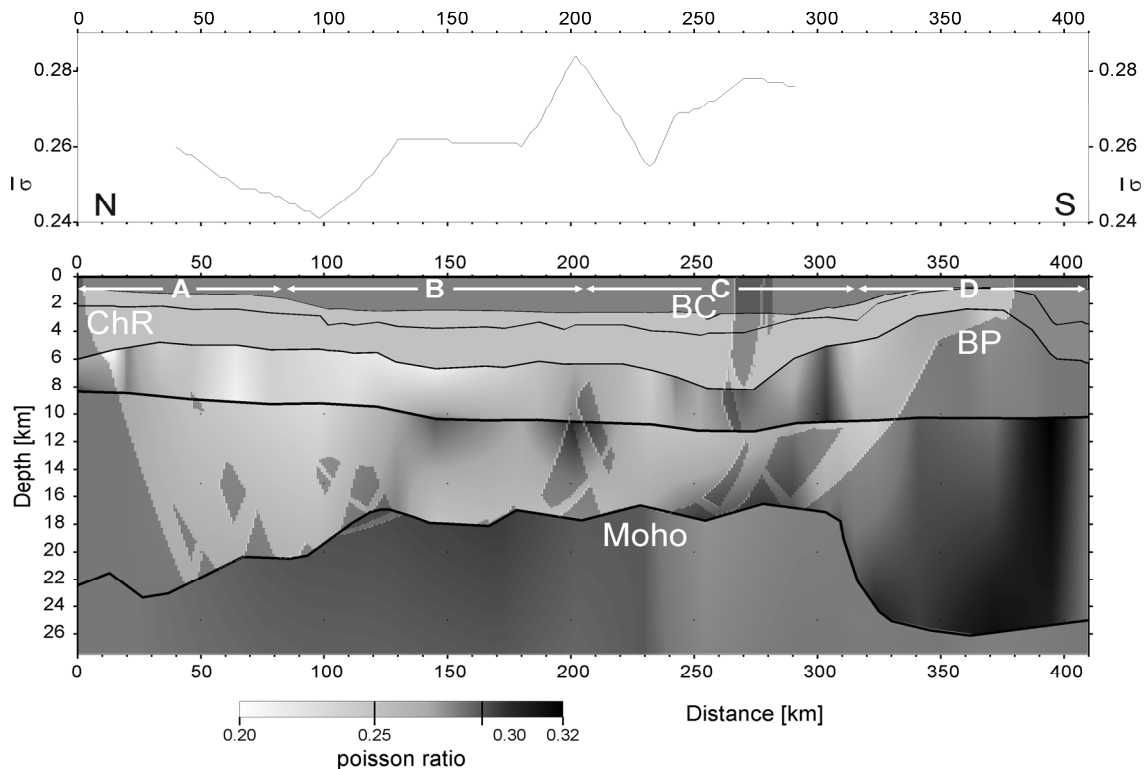


**Figure 7-13: Poisson's ratio model** and average Poisson's ratio across the Bounty Trough overlain by the semi-transparent mask of the S-wave model, as the smaller ray coverage of the S-wave model determines the resolution of the Poisson's ratio model. Poisson's ratio is calculated for each node. Abbreviations are: BC – Bounty Channel, BP – Bounty Platform, ChR – Chatham Rise.

$\sigma$  models often show a higher variability than separate  $v_p$  and  $v_s$  models. This reflects a higher sensitivity to changes in the lithology [Musacchio, *et al.*, 1997] and a larger error in model parameters. Errors of 2% in both  $v_p$  and  $v_s$  can result in an error of over 9% in  $\sigma$  [Christensen, 1996]. Therefore, we manually removed small-scale variations depending on values of adjacent nodes in the  $\sigma$  model. After the calculation of the  $\sigma$  model (Figure 7-13), we deleted obviously erroneous  $\sigma$ -values ( $< 0.20$  and  $> 0.32$ ) in short wavelength variations. The high number of remaining reasonable values gives additional indication for the reliability of the velocity models.

## 7.6 Discussion of seismic models

We calculated average crustal seismic velocities over those parts of the model, where the ray coverage reached down to the Moho. Seafloor topography, average crustal seismic velocity and velocity-depth models divide profile AWI-20030002 into four domains coinciding with Chatham Rise (A), the northern Bounty Trough (B), the southern Bounty Trough (C), and the Bounty Platform (D). Average crustal P-wave velocities range mainly from 6.4 – 6.6 km/s for Chatham Rise and Bounty Platform (A and D) and rise to 6.85 km/s and 7.3 km/s above the high velocity bodies in the northern and southern Bounty Trough (B and C) (Figure 7-9). Average crustal velocities, Moho depths, and Poisson's ratios at some positions of the profile are summarized in Table 7-3.

### 7.6.1 P-wave model

The upper sedimentary layer shows minor lateral velocity variations. Here, P-wave velocities range from 2 to 3.5 km/s in up to 2 km of stratified sediments, except for the Bounty Platform, where the sediment coverage reaches only less than 100 m. Davey [1977], using unreversed sonobuoy data from the Inner Bounty Trough, reported velocities from 1.9 to 2.2 km/s for the upper sedimentary layer and 2.7 to 3.9 km/s for the lower sedimentary layer, consistent with our sediment velocities.

P-wave velocities range from 3.3 to 3.8 km/s at the top of the lower sedimentary layer and 4.9 to 6 km/s at the bottom of the lower sedimentary layer with the highest values at the Chatham Rise. The situation at Bounty Platform is different with significantly higher velocities of 5.7 to 6 km/s and a low vertical gradient. There is only little control over the bottom of this layer across the Bounty Platform. It is most probable that the 5 km/s-velocity line across the Bounty Platform represents the transition between sediments and basement, suggesting that basement crops out at the Bounty Platform. The layer thickness averages 3 - 4 km. Davy [1993] reported higher velocity values of 5.9 to 6.5 km/s at depths of 1.5 – 3.5 km below the seafloor (b.s.f.) for the basement in the Bounty Trough in unreversed sonobuoy data.

The upper crustal layer thickens from 3 km under Bounty Trough to 8 km beneath the Bounty Platform. This layer has the strongest lateral velocity variations: Velocities range from 5.5 to 6.5 km/s beneath the Chatham Rise (part A). In the northern Bounty Trough (part B), P-wave velocities slow down in average, at the top of the layer the decrease to ca. 5 to 6.0 km/s, but are nearly the same at the base of the layer. In southern Bounty Trough (part C) beneath the Bounty Channel velocities increase to 6 to 7.2 km/s. Davey [1977] gave basement velocities of 5.0 to 5.6 km/s at depths of 2.5 – 3 km (b.s.f.) for the Middle Bounty Trough and about 6.2 km/s for the Inner Bounty Trough, which is consistent with our findings. The upper crustal velocity structure of the Bounty Platform is remarkably homogeneous, with velocities of 6 to 6.5 km/s and a low vertical velocity gradient. Generally, there is no distinct boundary between the upper and lower crust. It is merely a non-reflecting interface to allow measured gradient changes. The lower crust thins from 15 km thickness under Chatham

Rise and the Bounty Platform (regions A and D) to about 6 km under the Bounty Channel.

The lower crustal velocities of the Chatham Rise range from 6.2 to 7 km/s and increase to 6.8 to 7 km/s in northern Bounty Trough (part B). Further south, in the Bounty Trough, P-wave velocities increase to 7 to 7.7 km/s and slow down to 6.2 to 7 km/s beneath Bounty Platform (part D). On average, the lower crustal velocities of Bounty Trough (parts B and C) are 10 to 15 % higher than those of the Chatham Rise and the Bounty Platform.

The Moho can be defined by a large number of reflected phases and a few Pn phases. The entire crust thickens from 15 km under the Bounty Trough to 23 km under the Bounty Platform, and 22 km under the southern Chatham Rise. These findings agree very well with the results from gravity modeling by Davy and Wood [1994] who assigned a maximum crustal thickness of 23 – 26 km beneath the Chatham Rise. Velocities in the upper mantle vary from 7.7 km/s to 8.2 km/s.

### **7.6.2 S-wave model**

In general our S-wave model (Figure 7-11) images most of the main features of the P-wave model, while the crustal average shows only some trends. Above the high-velocity body in the lower crust of Bounty Trough (part C) the average crustal shear wave velocity rises to 4.2 km/s, but it drops to some 3.5 km/s elsewhere. Due to lower coverage, the average crustal shear wave velocity has only been calculated in regions with ray coverage down to the Moho.

The upper sedimentary layer has S-wave velocities of 0.9 to 1.4 km/s, but this layer is poorly resolved, so that these values should be regarded with caution. The same can be said for the lower sedimentary layer, except on Bounty Platform (part D). Velocities in the lower sedimentary layer range from 1.7 to 3.2 km/s in Chatham Rise and Bounty Trough (parts A – C), whereas the second layer from top at the Bounty Platform has S-wave velocities from 3.3 to 3.4 km/s.

S-wave velocities in the upper crust range from 3.2 to 3.6 km/s. They are homogenous throughout the complete layer, except for a small area under the Bounty Channel, a region of the model that is poorly resolved.

The lower crustal layer is the best-resolved part of the S-wave model for Chatham Rise and Bounty Trough (parts A-C); Bounty Platform (part D) is not resolved at all. Under the Chatham Rise velocities range from 3.5 to 3.9 km/s and increase to 3.6 to 4 km/s northern Bounty Trough (part B). Southern Bounty Trough (part C) shows the highest S-wave velocities ranging from 3.9 to 4.5 km/s under the Bounty Channel.

### 7.6.3 Poisson ratio and crustal composition models

As the resolution of the P-wave model is better than that of the S-wave model, the quality of the  $\sigma$  model (Figure 7-13) is mainly dependent on the S-wave model. The  $\sigma$  model shows some important trends. The northern part of the profile reveals low average values of  $\sigma$  in the crust that rise above the two zones of P-wave velocity highs. A peak, 200 km along profile, seems to result from low ray coverage at the shear wave model and a generally higher variability of the  $\sigma$ .

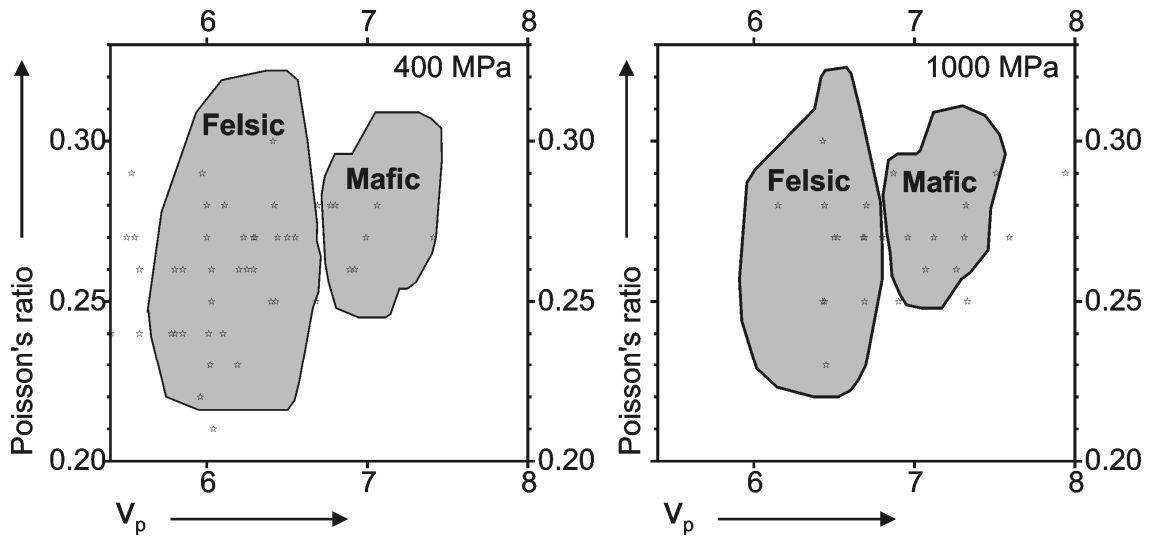


**Figure 7-14:**  $V_p$  and Poisson's ratio plotted in a combined graph. Plots show the fields of mafic and felsic rock composition for 400 MPa and 1000 MPa at middle and lower crustal depths. Gray areas of rock composition are plotted as a compilation of measurements by Christensen [1996]. Stars are values taken from the P-wave velocity and Poisson's ratio model of the Bounty Trough.

In the upper crust of Chatham Rise and northern Bounty Trough (parts A and B; 50 – 200 km along profile), the  $\sigma$  is relatively low at 0.22 to 0.24. These values extend down into the lower crust of Chatham Rise (part A). In contrast, the upper crust of southern Bounty Trough and Bounty Platform (parts C and D), and the lower crust everywhere except beneath Chatham Rise have  $\sigma = 0.26 - 0.30$ . The highest values are found under the Bounty Channel in the upper crust and the lower crust under the whole Bounty Trough. The two sedimentary layers beneath the seafloor are poorly resolved.

	without sediments	50 km	90 km	125 km	250 km	290 km	350 km
$\sigma$		0.256	0.244	0.257	0.270	0.276	0.280
$v_p$		6.56	6.58	6.38	7.37	6.87	6.45
$v_s$		3.76	3.76	3.81	4.13	3.81	3.53

**Table 7-3:** Average crustal velocity/ $\sigma$ -values at specific points of the velocity/ $\sigma$ -depth models. The sedimentary layers have not been included in the calculation of the average values.

Individually,  $v_p$ - and  $v_s$ -models, or  $\sigma$  models are considerably non-unique when interpreted for rock composition, because many rock types have similar P-wave velocities but different  $\sigma$  or vice versa [Christensen, 1996]. Nonetheless, comparisons of borehole samples with lithologies predicted by refraction velocities suggest that

refraction velocities can predict regional lithological trends [Digranes, *et al.*, 1996]. The non-uniqueness of  $\sigma$  models can be limited by comparing  $\sigma$  to  $v_p$ , and attempts to classify rock types by  $v_p$  and  $\sigma$  have enabled further constraints to be placed on the crustal composition [Christensen, 1996; Musacchio, *et al.*, 1997].  $\sigma$  and  $v_p$ , plotted in a graph for representative rock types after Christensen [1996] (Figure 7-14), show fields where rocks are more likely to be mafic or felsic [Musacchio, *et al.*, 1997]. In order to derive a crustal compositional model (Figure 7-15), each corresponding pair of nodes of the crustal layers of the P-wave model and the Poisson's ratio model was plotted against the fields of rock composition (felsic/mafic). Depending on the position in the graph, a rock composition was assigned to this node and plotted in the crustal compositional model. In cases where the assignment of the crustal composition was ambiguous, the values of the adjacent nodes guided the decision.

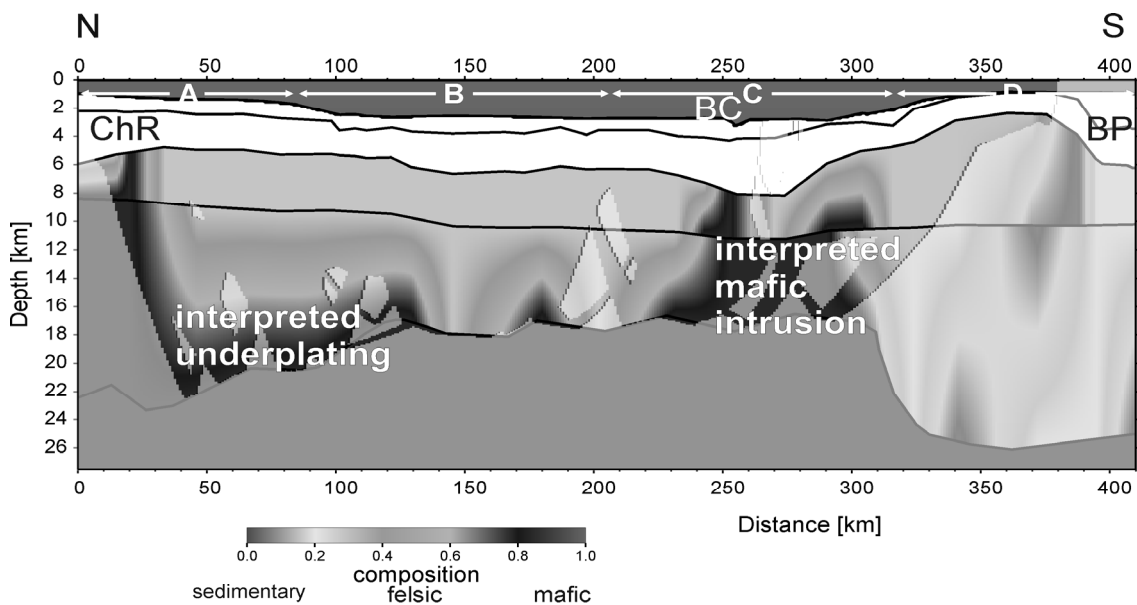


**Figure 7-15:** *The compositional model shows the likelihood of rocks to consist of more felsic or mafic material depending on Poisson's ratio and  $v_p$ . Abbreviations are: BC – Bounty Channel, BP – Bounty Platform, ChR – Chatham Rise.*

The compositional model (Figure 7-15) shows regions of high probability for felsic composition in most of the crust of the Bounty Trough. Three major exceptions from this observation exist in the lower crust: Our model reveals high probabilities for mafic composition in the base of the lower crust beneath Chatham Rise (part A), a portion of the base of the lower crust in northern Bounty platform (part B) and the entire lower crust and the base of the upper crust of southern Bounty Trough (part C). This mafic material in southern Bounty Trough (part C) can be correlated with the high-velocity and high-gravity bodies in the thin crust of the Bounty Trough. An area of 30 % of this profile across the Bounty Trough between 50 and 325 km is strongly affected by intrusions, or about 860 km<sup>2</sup> of this cross-section. We assume that 80 % of this intruded material is of mafic origin [Ilchenko, 1996]. If this represents an average amount of intrusion over the entire length of Bounty Trough, the volume of intruded mafic material is around 688,000 km<sup>3</sup>.

## 7.7 Discussion of gravity data

The gravity anomaly principally reflects the bathymetry of Bounty Trough, which, in turn, reflects crustal thinning beneath the Bounty Trough (Figure 7-16). The gravity model has been tied to an assumed oceanic crustal thickness south east of Chatham Rise, and is broadly constrained by refraction solutions for the top and the base of the crust. Crustal thinning, as well as the deepest water depth, is concentrated in the southern Bounty Trough with a sharp increase in crustal thickness south of 300 km where the profile crosses onto the Bounty Platform. Against the broader pattern of crustal thinning in the Bounty Trough, the gravity anomaly pattern reveals structures with a wavelength of 75 – 100 km.

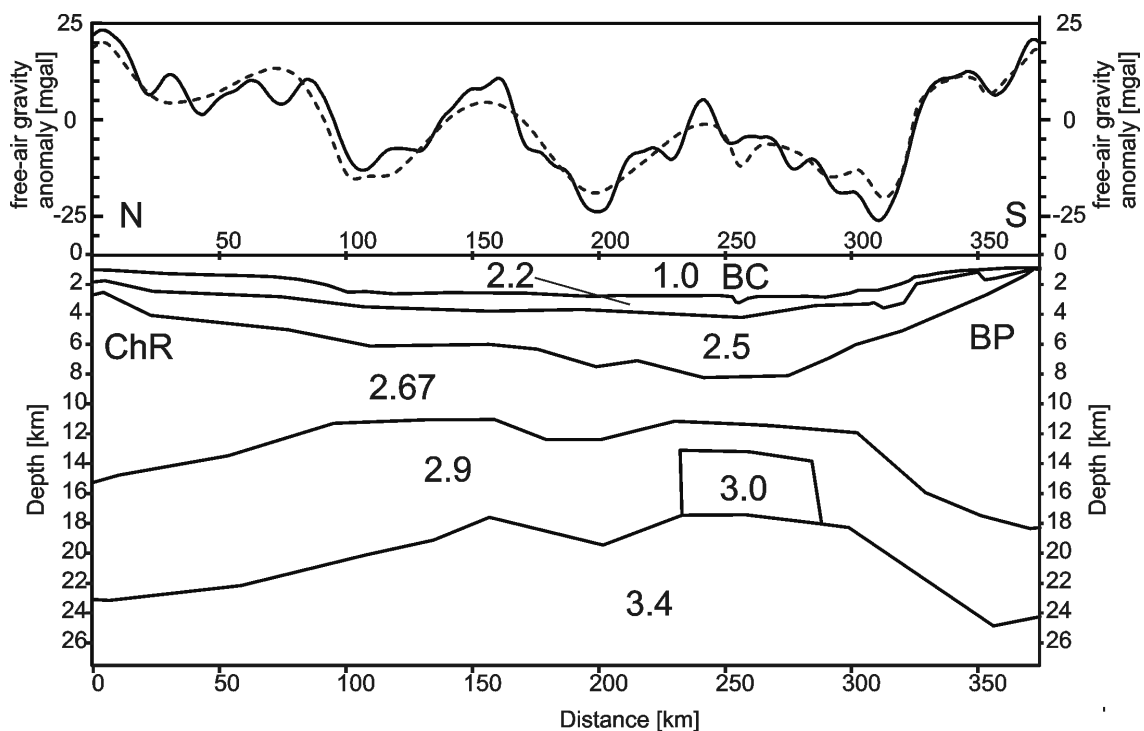


**Figure 7-16: Minimum structure gravity model**, with bodies striking orthogonal to the plane of the section and extending uniformly from each end of the section. Numbers are densities in  $\text{g}/\text{cm}^3$ . Above the gravity model measured (solid) and calculated (dashed) free-air gravity anomalies are plotted. The sedimentary and crustal thickness model has been guided by the seismic refraction model. Abbreviations are: BC – Bounty Channel, BP – Bounty Platform, ChR – Chatham Rise.

A broad, ca. 25 mgal, positive anomaly centered near the axis of the Bounty Trough is partly modeled by a high-density body of  $3.02 \text{ g}/\text{cm}^3$  reaching up into the middle crustal layer against a background value of  $2.9 \text{ g}/\text{cm}^3$  for the lower crust and  $2.67 \text{ g}/\text{cm}^3$  for the middle crustal layer (Figure 7-16). Similar anomaly variations further north have been principally modeled by variations in crustal thickness. Gravity highs observed in the ship-borne free-air gravity measurements correlate well with sub-parallel gravity lineations that can be seen in the satellite-gravity data set [Sandwell and

## IS THE BOUNTY TROUGH, OFF EASTERN NEW ZEALAND, AN ABORTED RIFT?

*Smith, 1997*]. Magnetic anomalies from marine magnetic measurements correlate well with some of the observed gravity anomalies (Figure 7-3), but not with others [*Sutherland, 1999*]. The better correlations appear in the Middle Bounty Trough, suggesting that potential field anomalies there could be attributed to mafic material intruded into the crust, whereas those in the Inner Bounty Trough may not.

## 7.8 Tectonic implications

Reflections from the Moho ( $P_mP$  and  $S_mS$ -phases), as well as the gravity model indicate a decreased Moho depth under the Bounty Trough and a strongly asymmetrical Moho topography with a steep southern flank and a gentle northern flank.

The MCS section of the Bounty Trough revealed rather well stratified upper sedimentary layers and almost transparent lower sedimentary layers that appear at first glance to be upper crystalline crust at this depth. However, our P-wave velocity-depth model revealed seismic velocities of ca. 3.7 - 5.4 km/s for this layer, too low for crystalline crust. Mortimer et al. [2002] observed acoustically transparent regions in the South East South Island (SESI) transect and interpreted them as weakly metamorphosed sediments (e.g. Murihiku Terrane). P-wave velocities for the Murihiku Terrane at shallow depths range from 4.7 to 5.4 km/s [Godfrey, et al., 2002; Godfrey, et al., 2001]. Therefore, we suggest a similar metasedimentary origin for the acoustically opaque zone in the Bounty Trough. The lack of stratification could be caused by periods in which the sediments have been mechanically and thermally reworked by alternating phases of extension and compression. Forster and Lister [2003] proposed the idea of a Cretaceous change in the direction of extension in the Bounty Trough. However, their model, based on the Otago Schist, does neither explain the rough topography of the acoustic basement nor the acoustically transparent layers beneath, as the compressional elements are lacking in their reconstruction.

The high-velocity body, in both P-wave and S-wave seismic models at 220 – 280 km, coincides well with a high-density body in the gravity model (Figures 7-9 and 7-16). As we cannot correlate observed gravity highs with basement highs interpreted in older single channel seismic (SCS) data [Davey, 1977], we rule out basement fault blocks as the source of the gravity highs. Our compositional model shows mafic rocks reaching up into the upper crust in southern Bounty Trough (part C) and at the base of the lower crust in northern Bounty Trough (part B). In continental rift zones, very similar crustal high-velocity/high-gravity bodies have often been interpreted as mafic intrusions [Ilchenko, 1996; Keranen, et al., 2004]. We interpret the high-velocity body of southern Bounty Trough (part C) as a mafic body intruded into the lower and upper crust and the high velocity zone, further north, as possible underplating at the base of the crust.

A gravity map of the Bounty Trough [Sandwell and Smith, 1997] shows several gravity lineations striking at ca. 45° to the Bounty Trough axis (Figure 7-3). Gravity highs and en echelon faulting in the Gulf of Aden strike at the same angle to the rift axis. Due to the position and strike direction of the gravity anomalies in the Gulf of Aden, these structures are interpreted as the expressions of magmatic cells related to incipient seafloor spreading [Dauteuil, et al., 2001]. Dauteuil et al. [2001] interpret the fact that the magmatic cells are arranged at an angle of ca. 45° to the axis of extension, as a sign of oblique rifting. We suggest that the gravity pattern in the Bounty Trough and, in turn, the mafic intrusions are comparable to those magmatic cells in the Gulf of Aden, indicating a NW-SE oblique rifting trend in the Bounty Trough.

Modeled seismic velocities and crustal thicknesses (Figure 7-9) indicate that the Chatham Rise and Bounty Platform are composed of continental crust, consistent with outcrop and dredge samples at the Chatham Islands and Bounty Island, where rocks of the Torlesse Terrane and Greenland Group have been found [Adams and Robinson, 1977; Beggs, *et al.*, 1990]. However, the seismic P-wave velocities beneath Bounty Platform and Chatham Rise are slightly higher than velocities modeled for the Torlesse Terrane in the SIGHT experiment at the eastern end of the Canterbury Basin [Van Avendonk, *et al.*, 2004a]. The results of the SIGHT lines [Scherwath, *et al.*, 2003; Van Avendonk, *et al.*, 2004a] modeled the lower crust as oceanic crust, based on the consistent observations of a deep intracrustal reflector and P-wave velocities of 6.9 – 7.1 km/s, with little lateral velocity variation. The velocity information is based on a few observed turning rays only. In our models, we do not observe this deep intracrustal reflector or the homogeneous velocity layer directly above the Moho, and therefore cannot associate the oceanic crust interpreted in the SIGHT lines with the rifting event interpreted in this paper, supported by the rejection of the interpretation of oceanic crust by Mortimer [2002].

The crystalline crust thins from 21 – 23 km at the flanks of the Bounty Trough to some 9 – 10 km under the trough. If this crustal thickness variation is the result of crustal thinning beneath the Bounty Trough, it indicates very high stretching factors ( $\beta$ ). As it is difficult to map the interface between the upper and lower crust, we calculated stretching factors for the entire crust. Calculated  $\beta$ -factors between 2.7 and 4.4 assume either an original thickness of 24 km, as observed under the Bounty Platform or 40 km as postulated by Bradshaw [1991]. A stretching factor of 3.3 is close to the value at which oceanic crust would form [Allen and Allen, 1990].

Our very high stretching factor and the fact that the interpreted magmatic intrusions reach far into the upper crust suggest that, at the location of our transect, rifting of the Bounty Trough ceased at or shortly after the onset of seafloor spreading. Depending on its timing, the location of rifting could have moved from the incipient Bounty Trough ocean to the later Campbell Plateau – Marie Byrd Land rift zone, as envisaged in the reconstructions of Eagles *et al.* [2004].

Davy and Wood [1994] modeled the Chatham Rise crust as ca. 25 km thick. The crust at the margin of the Bounty Platform is about 24 - 26 km (this paper). Crustal thickness at the center of the Campbell Plateau is about 27 km (Grobys *et al.*, manuscript in preparation, 2006). Moho depth beneath the formerly adjacent western Marie Byrd Land was estimated to be at least 25 – 30 km [Luyendyk, *et al.*, 2003; Ritzwoller, *et al.*, 2001]. In western Marie Byrd Land, observed dikes and faults strike at a high angle to the rifted continental margin [Luyendyk, *et al.*, 2003]. The extension direction these authors recorded for Colbeck Trough, formerly adjacent to Campbell Plateau, is almost perpendicular to the direction of initial seafloor spreading between Marie Byrd Land and the Campbell Plateau [Eagles, *et al.*, 2004]. The Colbeck Trough is attributed to intracontinental extension at 105 – 96 Ma [Fitzgerald, 2002; Luyendyk, *et al.*, 2003] that supposedly led to the formation of the West Antarctic and Ross Sea Rift system. From these indications, we suggest cautiously that the thinned crust of the Campbell Plateau and the Chatham Rise might be a result from the same event.

IS THE BOUNTY TROUGH, OFF EASTERN NEW ZEALAND, AN ABORTED RIFT?

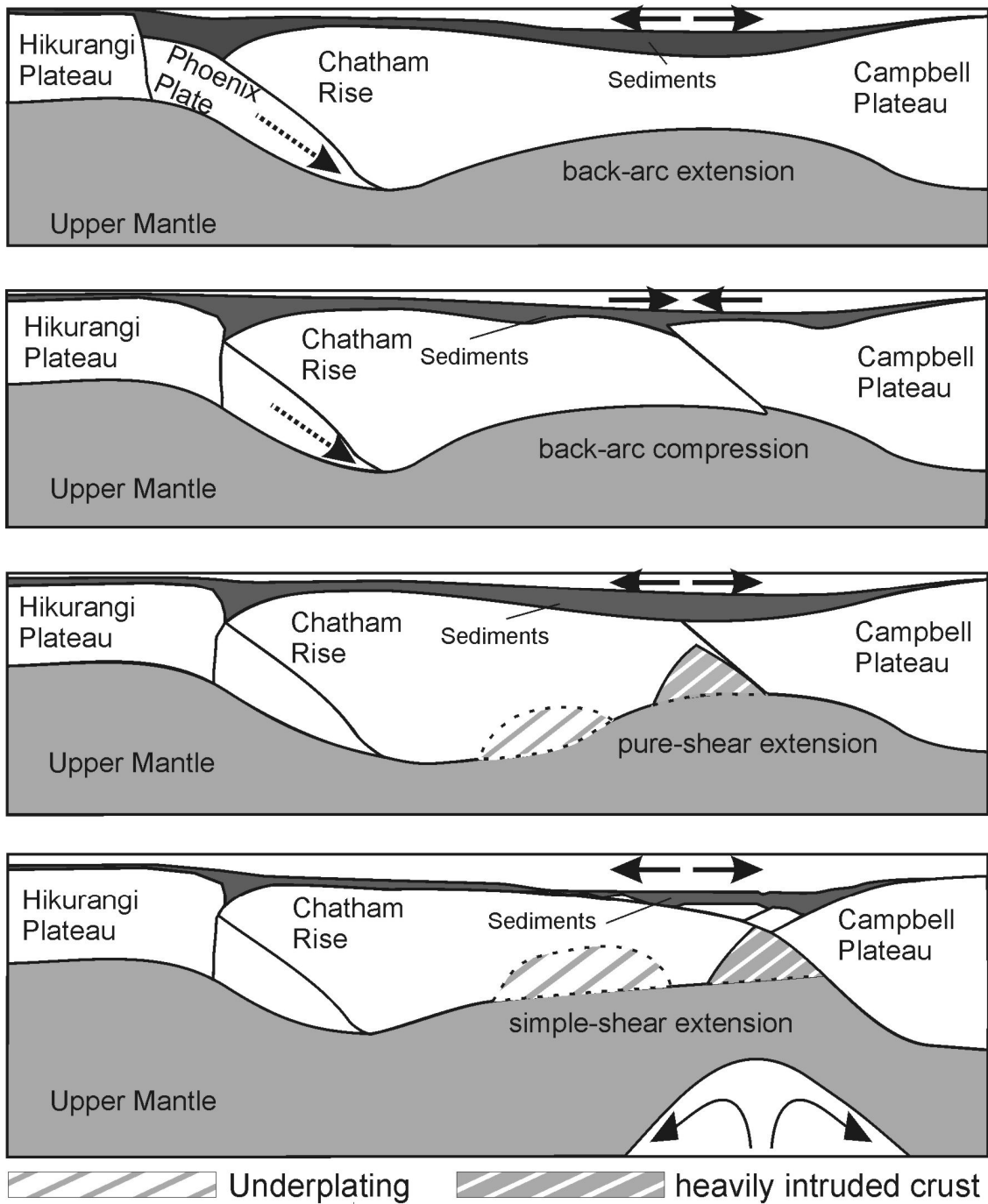


**Figure 7-17: Evolutionary tectonic model of the Bounty Trough.** Horizontal solid arrows show the direction of Bounty Trough deformation, dashed arrows the direction of the subduction of the Hikurangi Plateau, curved arrows indicate possible mantle flow pattern. a) Subduction of the Pacific Phoenix Plate causes back-arc extension Chatham Rise and Campbell Plateau. b) The collision of the Hikurangi Plateau with Chatham Rise turns the back-arc basin into compression. At this time, a weak metamorphism of previously deposited sediments occurs. c) End of collisional phase with the begin of extension. d) As rifting continues, extension style changes to simple shear extension with magmatic material underplating and intruding into the crust until the onset of seafloor spreading.

The Bounty Trough lies in a setting that has been influenced by a Cretaceous and older subduction zone situated north of the Chatham Rise [Fitzgerald, 2002] and seafloor spreading to the east (south of the Chatham Islands) (Figure 7-2). Both processes could have had an influence on Bounty Trough opening. Spörli and Ballance [1989] proposed that the early extension was the result of back-arc processes, whereas Carter and Carter [1987] call the Bounty Trough a failed rift-arm. In this context, we use the term “rifting” only for processes at divergent margins in contrast to extensional processes related to convergent margins, here addressed as “back-arc extension”.

The initial extension of a back-arc basin begins at the island-arc, as it is the most ductile part of the system [Tamaki, 1985]. This interpretation would require the Chatham Rise to be a former island arc. The most prominent expressions of arcs are volcanic activity [Herzer, 1995]. Chatham Rise consists of schist and greywacke of the Torlesse Terrane [Adams and Robinson, 1977; Bradshaw, et al., 1981] rather than arc volcanic deposits, and does not seem to have been a main zone of volcanic activity [Wood and Herzer, 1993]. Moho depths, and the velocity distribution over the Bounty Trough show a pronounced crustal thinning, consistent with the idea of a non-volcanic rift arm (Figure 7-9). The morphology of the Bounty Trough, a relatively broad sedimentary basin with steep flanks is a typical feature of an aulacogen [Burke, 1977]. What is more, the initiation of aulacogens is very often accompanied by the intrusion of igneous rocks [Burke, 1977] as indicated by high-velocity/high-density regions in the Bounty Trough.

The combined interpretation of geophysical data points to an interpretation of the Bounty Trough as a failed rift arm. It cannot be ruled out that the rifting of the Bounty Trough followed pre-existing zones of crustal weakness caused by the subduction of the Phoenix Plate under Chatham Rise. Sediments of the Torlesse Terrane were possibly deposited in a back-arc setting as suggested by Davy [1993]. Later on, they were thermally or mechanically reworked by phases of extension and compression. Albanian to Santonian (112 – 83.5 Ma) calc-alkaline volcanics and rhyolites, found in the Chatham Islands and South Island graben sequences, have chemistries that imply a change from a compressional to an extensional regime [Barley, et al., 1988]. This period of time coincides with the cessation of subduction of the Hikurangi Plateau [Davy, 2006]. It is possible that the subduction of the Phoenix Plate beneath the ancient Gondwana margin caused back-arc extension, as suggested by Forster and Lister [2003], and provided the depositional setting for pre-Cretaceous sediments in the Bounty Trough, while the collision of the Hikurangi Plateau caused the compressional forces that metamorphosed the pre-Cretaceous sediments (Figure 7-17).

## 7.9 Comparison with other rift systems

Comparisons of volcanic (Ethiopian Rift System, Red Sea, Oslo Rift) and non-volcanic (Gulf of Aden) rift systems at the early stage of development reveal a number of processes that may have operated during Bounty Trough opening. High-velocity zones are interpreted as cooled magmatic intrusions/underplating of similar spatial extent to those in the Bounty Trough. The Oslo Rift intrusions for example are estimated to have a volume of ca. 200,000 – 400,000 km<sup>3</sup> [Pedersen and van der Beek, 1994]. Dugda [2005] observed increased Poisson's ratios similar to those in areas of the Bounty Trough in parts of the Ethiopian rift zone. He suggested that they indicate a partial modification or replacement of the crust by mafic intrusions. Local gravity highs in a regional gravity low, as found in the Bounty Trough, have been observed for example in the Dniepr-Donets Basin where they are also explained as an intrusion of magmatic and ultramafic rocks [Yegorova, et al., 1999]. The strong similarities in the observations mentioned above at the Bounty Trough to other rift systems confirm the notion that the Bounty Trough was a typical large rift system.

Magmatic cells aligned oblique to the direction of extension in the East African Rift System and the Red Sea (e.g. [Ebinger and Casey, 2001]) are interpreted as the loci of extension within a nascent rift system [Dugda, et al., 2005]. This notion can also explain the correlated gravity-magnetic anomaly patterns in the Middle Bounty Trough. In the Inner Bounty Trough crustal thinning probably occurred to a lesser extent, because here gravity anomaly patterns do not correlate with magnetic anomalies. Gravity anomaly patterns as observed in the East African Rift System or the Red Sea are absent in the Outer Bounty Trough, where oceanic crust was formed. Based on the comparison with the gravity patterns mentioned above, it is reasonable to interpret the gravity patterns in the Middle Bounty Trough as the expressions of magmatic cells related to incipient seafloor spreading.

Evidence for large mafic intrusions in the Bounty Trough, as well as the strong structural asymmetry, do not comply well with the two end-member modes of extension. The pure-shear model, where extension is distributed through the lithosphere uniformly with depth, predicts a symmetric rift architecture and crustal thinning [Latin and White, 1990]. In contrast, in developing an extensional model to explain structural styles in Basin and Range, Wernicke [1982] suggested a lithosphere-scale detachment system. This model, along with other variations of simple-shear extension models, can explain strong structural asymmetry across the rift. Latin and White [1990] found that very little magma is produced by simple-shear extension. More recent studies [Louden and Chian, 1999; Ro and Faleide, 1992] have synthesized both extensional end-member models and proposed a multistage extension model that incorporates a transition from initial pure-shear extension to later simple-shear extension. This transitional model could well explain the rift-related features observed in the Bounty Trough, where we observe a strong asymmetry of the Moho as well as large intrusions into the crust, elements of both rift models (Figure 7-17).

## 7.10 Conclusions

The CAMP refraction survey and subsequent modeling have revealed much about the extensional processes associated with the Bounty Trough opening. Quantification of the amount of crustal stretching and intrusion contributes to an understanding of rift processes in general, and will improve plate-kinematic reconstructions of the southwestern Pacific in particular. This first combined wide-angle reflection/refraction and MCS line across the Bounty Trough provides the most detailed information on deep structures of the rift zone between Chatham Rise and Campbell Plateau. Our main results are:

- 1) The Moho depth decreases from 24 km b.s.f. under the Bounty Platform to about 12 km b.s.f. under the Bounty Trough. It increases again to 22 km b.s.f. underneath the Chatham Rise flank.
- 2) Two high-velocity bodies can be observed (Figures 7-9 and 7-12) in the P- and S-wave models: A distinct 60 km wide one is situated directly under the Bounty Channel.
- 3) P-wave velocities in the lower crust (Figure 7-9) rise from 6.2 – 7.0 km/s beneath Chatham Rise and Bounty Platform to 7.0 – 7.7 km/s under the Bounty Channel and for the upper crystalline crust, from 5.5 – 6.5 km/s to 6.0 – 7.2 km/s. Lower crustal S-wave velocities (Figure 7-12) increase from 3.5 – 3.9 km/s under the Chatham Rise to 3.9 – 4.5 km/s beneath the Bounty Channel.
- 4) Free-air gravity within the regional low of the Bounty Trough (Figure 7-9) is characterized by anomalies of about 25 mgal amplitude and 100 km wavelength. These anomalies can be modeled by crustal thickness variations and a high-density body, which is coincident with a high velocity body in the crust under the Bounty Channel.
- 5) A Poisson's ratio model (Figure 7-12) shows enhanced values ( $\sigma = 0.25 - 0.30$ ) in the whole crust beneath the Bounty Channel and reduced values ( $\sigma = 0.22 - 0.25$ ) in the crust under the northern Bounty Trough. Our compositional model (Figure 7-12c) indicates mafic crust in the area of the pronounced high-velocity body and at the base of the lower crust of the northern Bounty Trough.

All observations mentioned above support the interpretation of high-density/high-velocity bodies in the crust as magmatic intrusions into a thinned continental crust (Figure 7-17). We interpret the gravity patterns observed in the Middle Bounty Trough as the former locus of nascent seafloor spreading, in contrast to the Outer Bounty Trough where oceanic crust formed. The magmatic intrusions may have formed during a pure-shear extension phase that was followed by a simple-shear phase, which produced the overall asymmetry of the rift. Rifting ceased in the late Cretaceous. The fact that the Chatham Rise consists of continental crust, and that there are a large number of similarities in the structure and velocity distribution to modern rift systems, imply that the present Bounty Trough was not formed by back-arc extension but is a failed rift arm, which was possibly connected to a triple junction at the mouth of the Bounty Trough during the separation of New Zealand from Antarctica. However, the observation of acoustically transparent sediments suggests that an earlier process, possibly the subduction of the ancient Phoenix Plate beneath the Chatham Rise, caused

back-arc extension with sediment infill until the collision of the Hikurangi Plateau with the Chatham Rise led to successive compression.

## **Acknowledgements**

We are grateful to the captain and crew of RV *Sonne* during cruise SO-169 for their support and assistance. This project is primarily funded by the German Federal Ministry of Education and Research under BMBF contract no. 03G0169A as well as through contributions from AWI and GNS. The German Academic Exchange Service (DAAD) funded a visit of J.G. to GNS for two months. We thank Kristina Tietze for assistance with the S-wave modeling. Furthermore, we thank GeoPro GmbH (Hamburg) for their support in providing and operating the OBS equipment and Exploration Electronics Ltd. (Norwich) for providing and operating the seismic streamer system. Graeme Eagles and two anonymous reviewers helped to improve this manuscript. We thank Reinhard Werner, Kaj Hoernle, Fred Davey, and Nick Mortimer for fruitful discussions. Most of the figures were generated with Generic Mapping Tools [*Wessel and Smith, 1998*].

## 8 Extensional and magmatic nature of the Campbell Plateau and Great South Basin from deep crustal studies

J. W.G. Grobys<sup>\*a</sup>, K. Gohl<sup>a</sup>, G. Uenzelmann-Neben<sup>a</sup>, B. Davy<sup>b</sup>, D. Barker<sup>b</sup>,

<sup>a</sup>*Alfred Wegener Institute for Polar and Marine Research, PO BOX 120161, 27515 Bremerhaven, Germany, phone +49-471-4831-1237, fax +49-471-4831-1271*

<sup>b</sup>*GNS Science, 1 Fairview Drive, Avalon, Lower Hutt 5040, New Zealand*

\*Corresponding author: Jan Grobys, e-mail: jgrobys@awi-bremerhaven.de, phone: +49-471-4831-1237, fax: +49-471-4831-1271

### 8.1 Abstract

The Campbell Plateau is one of the largest submarine parts of the microcontinent of New Zealand. Although the opening of the Great South Basin played an important role in the late Gondwana break-up, the crustal structure of the basins and plateaus southeast of New Zealand are unknown to a large extent. Here we present results from a combined gravity, magnetic, multichannel seismic and wide-angle reflection/refraction seismic transect across the Great South Basin and parts of the Campbell Plateau and interpret this on the basis of velocity distribution and crustal thickness. The lower crust exhibits a zone of southeastward increasing P-wave velocities ( $v_p \approx 7.1 - 7.4$  km/s) beneath the central Campbell Plateau. In this area, crustal thickness averages to ca. 27 km. We interpret this high-velocity zone as underplating beneath a formerly extended crust. Our results hint that the extension of the Great South Basin was not accompanied by widespread magmatic activity, although signs of younger magmatism have been found across the Pukaki Rise and within the Great South Basin. Based on comparisons with nearby plateaus like the Lord Howe Rise and the Challenger Plateau, as well as probable paleo-positions of the magnetic anomaly systems of New Zealand and the Campbell Plateau, we suggest that an early phase of extension of the Campbell Plateau predated the opening of the Great South Basin.

### Keywords

Rift zones, ocean bottom seismographs, refraction methods, crustal thinning, Campbell Plateau, Great South Basin

### 8.2 Introduction

The Great South Basin (Figure 8-1) is the product of Cretaceous extension between the Campbell Plateau and the South Island [Eagles, *et al.*, 2004] leading to accumulation of up to 8 km of sediments [Carter, 1988a]. Syn-rift sediments were accumulated up to mid-Cretaceous time and rapid subsidence began thereafter [Beggs,

EXTENSIONAL AND MAGMATIC NATURE OF THE CAMPBELL PLATEAU AND GREAT SOUTH  
BASIN FROM DEEP CRUSTAL STUDIES

1993; Cook, *et al.*, 1999]. The Campbell Plateau (Figure 8-1) is a continental plateau [Davey, 1977] that at 100 Ma was situated between the South Island, Lord Howe Rise (Figure 8-1), Marie Byrd Land (present-day Antarctica) and the West Antarctic Rift System. The plateau lies mostly at less than 1000 m beneath sea level, rising up to 500 m at the Pukaki Rise and emerges at the Auckland and Campbell Islands.

The documented timing of the break-up of New Zealand from Antarctica and of the opening of the Great South Basin [Cook, *et al.*, 1999; Eagles, *et al.*, 2004] leaves a number of open questions. Gravity and bathymetry of the Campbell Plateau indicate a crustal thickness that is significantly reduced compared to regular continental crust. The tectonic processes leading to the extension of the Campbell Plateau are unknown, but it has suggested that this extension was related to an Early Cretaceous extensional or alternatively to the final break-up of New Zealand from Antarctica in the Late Cretaceous. Understanding these processes and their timing are important because they may explain the evolutionary history of some of the comparable plateaus in this region, e.g. the Lord Howe Rise and Challenger Plateau. Whether the Campbell Plateau underwent extension at the time of the extension of the Bounty Trough and Great South Basin or earlier is a subject of debate [Davey and Christoffel, 1978; Sutherland, 1999; Uruski and Wood, 1991]. Similarly, various theories exist about the origins of and the relationship between the two major magnetic anomaly systems over the plateau, the Stokes Magnetic Anomaly System (SMAS) and the Campbell Magnetic Anomaly System (CMAS). It is still unclear, for example if both anomaly systems are equivalents that have been offset by dextral strike-slip movement [Davey and Christoffel, 1978; Sutherland, 1999].

In order to investigate the mechanisms of Campbell Plateau extension and its role in the early opening of the southwest Pacific, the Alfred Wegener Institute for Polar and Marine Research (AWI) and GNS Science jointly conducted deep crustal seismic and potential field experiments across the Campbell Plateau, the Great South Basin and the Bounty Trough during RV *Sonne* cruise SO-169 in 2003 (project CAMP). This paper deals with the combined gravity, magnetic, multichannel seismic reflection (MCS), and the refraction/wide-angle reflection seismic transect of profiles AWI-20030001 and coincident AWI-20030013 running northwest-southeast across the Great South Basin and the northwestern part of the Campbell Plateau up to the Pukaki Rise.

EXTENSIONAL AND MAGMATIC NATURE OF THE CAMPBELL PLATEAU AND GREAT SOUTH BASIN FROM DEEP CRUSTAL STUDIES

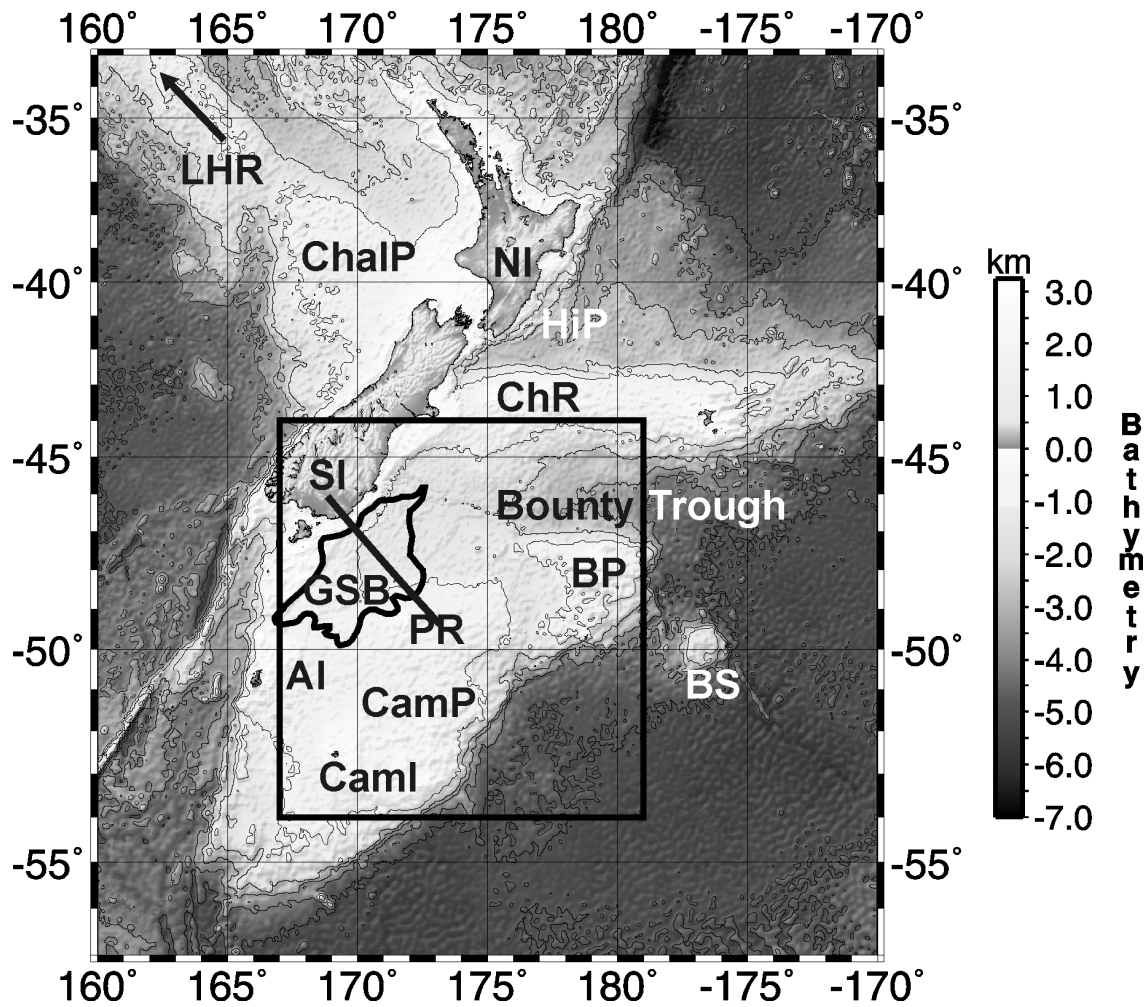


**Figure 8-1: Bathymetric overview map** [Smith and Sandwell, 1997] of New Zealand and location of the CAMP experiment, showing AWI-20030001 and coincident AWI-20030013 across the Bounty Trough (red). The black box shows the area of the gravimetric map (Figure 8-3). Abbreviations are: NI – North Island of New Zealand, SI – South Island of New Zealand, AI – Auckland Islands, BP – Bounty Platform, BS – Bollons Seamounts, CamI – Campbell Islands, CampP – Campbell Plateau, ChalP – Challenger Plateau, ChR – Chatham Rise, GSB – Great South Basin, HiP – Hikurangi Plateau, LHR – Lord Howe Rise, PR – Pukaki Rise.

### 8.3 Geological Setting

The Great South Basin is the largest and deepest sedimentary basin on the Campbell Plateau, New Zealand, encompassing an area of ca. 85,000 km<sup>2</sup>. The basin itself is not obvious in the bathymetry, but can be defined by the 2000 m sediment thickness isopach [Cook, *et al.*, 1999]. It is separated by basement highs from the Canterbury Basin to the north and from the Pukaki Basin to the south. Cook *et al.* [1999] interpreted the basement to consist of Cretaceous rocks, but they did not rule out the possible presence of older rocks or metamorphosed sediments beneath the Urutawan sediments (106.4 – 103.3 Ma) (Figure 8-2). Where the basement rocks have been drilled, they have been recognised as schists of Triassic to Jurassic ages, or granitic rocks of Cretaceous origin [Cook, *et al.*, 1999 and references therein]. Evidence for Cenozoic volcanism has been found in various clusters widely scattered over the Great South Basin and the Campbell Plateau. Although Farrar and Dixon [1984] suggested a time-dependent migration of volcanic activity over the Campbell Plateau, recent work has not been able to confirm this Werner *et al.* [in prep.].

Period	NZ Stage	Time	Group
Eocene		55.5	Rakiura group
Paleocene	Teurian	65.0	Pakaha group
Late Cretaceous	Haumurian	84.0	Hoiho group
	Piripauan	86.5	
	Teratan	89.1	
	Mangaotanean	92.1	
	Arowhanan	95.2	
	Ngaterian		
Early Cretaceous	Motuan	100.2	
	Urutawan	103.3	
		108.4	

**Figure 8-2:** Excerpt from stratigraphic timescale of New Zealand from Early Cretaceous to Eocene after Cooper [Cooper, 2004]. Width of bars representing the ages is not to scale.

Gravity modelling by Cook *et al.* [1999] suggests a minimum crustal thickness of 10 – 15 km in the central Great South Basin. The same gravity models indicate a maximum crustal thickness of about 29 km beneath the southeastern tip of the South Island and beneath the central Campbell Plateau. An assumed initial crustal thickness of ca. 35 km implies stretching factors of about 2 – 3 [Cook, *et al.*, 1999].

Ship- and airborne magnetic data collected over the South Island and the Campbell Plateau define two magnetic anomaly systems (Figure 8-3). The SMAS with

EXTENSIONAL AND MAGMATIC NATURE OF THE CAMPBELL PLATEAU AND GREAT SOUTH BASIN FROM DEEP CRUSTAL STUDIES

its northernmost component, the Junction Magnetic Anomaly (JMA), can be traced across the southern South Island and into the Great South Basin, where it decreases in amplitude and vanishes [Hunt, 1978; Sutherland, 1999]. The south-western part of the SMAS is attributed to plutonic complexes of the Median Tectonic Zone [Kimbrough, *et al.*, 1994], while the northern part, the JMA, marks the contact between the Caples and Maitai terranes [Cook, *et al.*, 1999]. The central anomaly of the SMAS is attributed to a source at moderate depths that underlies or intrudes the Murihiku Terrane greywackes [Mortimer, *et al.*, 2002]. Cook [1999] explains this body either as an old magnetic basement of at least Permian age or as a syn- or post-Murihiku (Jurassic) intrusion.

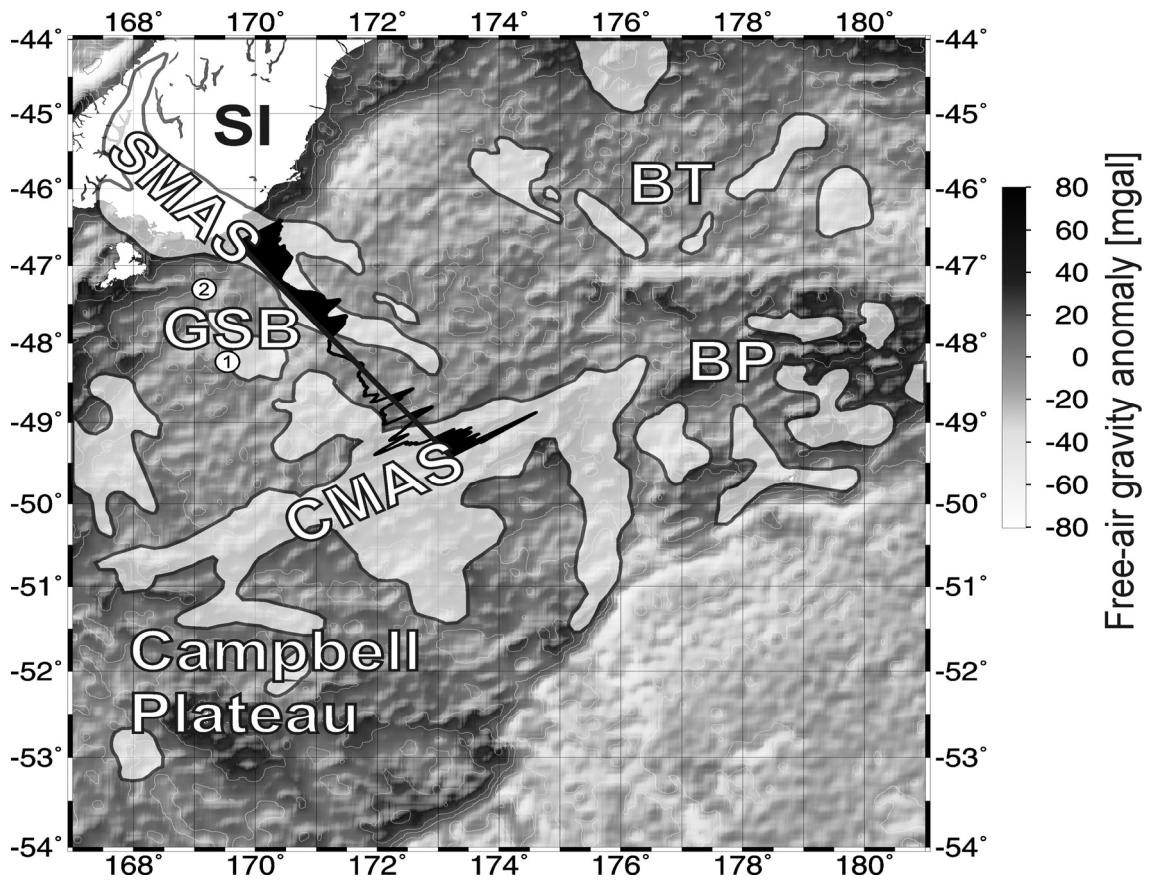


**Figure 8-3: Satellite gravity anomaly map** [Sandwell and Smith, 1997] of the Great South Basin and central Campbell Plateau. Contour intervals are 20 mgal. White outlined and shaded areas mark positive magnetic anomalies after [Sutherland, 1999]. Wiggle plot along the red ship's track shows the shipborne magnetic recording after IGRF removed. BT – Bounty Trough, BP – Bounty Platform, GSB – Great South Basin, SI – South Island, CMAS – Campbell Magnetic Anomaly System, SMAS – Stokes Magnetic Anomaly System.

Further south, a zone of high amplitude positive magnetic anomalies trends northeast across the central Campbell Plateau (Figure 8-3). This anomaly, the Campbell Magnetic Anomaly System, is interpreted to be caused by magnetic basement rocks [Davey and Christoffel, 1978]. They postulated that the CMAS was originally a continuation of the SMAS, which is now offset by a major shear zone. Later plate tectonic reconstructions [Kamp, 1986] estimated this offset to about 330 km, a value

EXTENSIONAL AND MAGMATIC NATURE OF THE CAMPBELL PLATEAU AND GREAT SOUTH  
BASIN FROM DEEP CRUSTAL STUDIES

that approximates the amount of extension in the Bounty Trough estimated by Kamp. A more recent plate tectonic reconstruction [Grobys, *et al.*, submitted] estimates the extension in the Bounty Trough to ca. 75 – 100 km.

A well-preserved stratigraphy of up to 8 km thick sediments down to the basement makes it possible to date the opening of the Great South Basin. Sediments of the Hoiho group (108.4 – 83.5 Ma) (Figure 8-2) lie above the interpreted basement. These sediments are heavily faulted along SW-NE trends and laterally discontinuous. The deposition took place in faulted depressions and sub-basins, suggesting syn-rift sedimentation. Piripauan (86.5 – 84.0 Ma) sediments show the beginning of a marine influence, and indicate that the basin's subsidence began at this time [Cook, *et al.*, 1999].

The Pakaha group sediments (83.5 – 55.5 Ma) contain relatively little evidence for continuous faulting. They are interpreted as having been deposited after normal faulting had ceased and during rapid subsidence of the basin. Cook *et al.* [1999] estimate a maximum of 1600 m syn-rift subsidence to and 2200 m post-rift subsidence took place [Cook, *et al.*, 1999]. Eocene sediments of the Rakiura group (55.5 – 34.3 Ma) mark the transition to open ocean conditions. In summary, this stratigraphic information contains the timing of the opening of the Great South Basin to have ceased in Piripauan time (86.5 – 84 Ma).

## 8.4 Data acquisition and processing

Seismic line AWI-20030001 of the CAMP Experiment is a 510 km long NW-SE-trending transect across the Great South Basin extending for a ca. 85 km onshore (Figure 8-1). The transect runs from the Pukaki Rise in the South to the vicinity of Gore, South Island. We acquired a coincident refraction/wide-angle reflection and multichannel seismic (MCS) dataset (Figure 8-3) as well as magnetic and gravity data along the offshore part of this line.

For the MCS, the receiver array was a single 2150 m long streamer. A source array of six G-Guns<sup>®</sup> with a total volume of 48 l (2980 in<sup>3</sup>) generated the signals. Approximate shot spacing was 50 m. The wide-angle reflection/refraction line was shot with a VLF airgun array of 20 airguns with a total volume 52 litres (3240 in<sup>3</sup>) at an average shot interval of 150 m. 20 ocean-bottom seismometers (OBS of GEOPRO<sup>®</sup> and University of Hamburg type), 4 ocean-bottom hydrophone systems (OBH of GEOMAR type), and 6 EARSS and ORION type seismic land stations recorded the shots of the VLF array. OBS/OBH stations were placed at between 13.5 and 27 km intervals, onshore stations were placed irregularly at intervals from 7 to 39 km. Bathymetry along the profile was recorded with the R/V *Sonne*'s SIMRAD<sup>®</sup> EM-120 and Parasound systems. We converted the OBS/OBH data to SEG-Y format and applied corrections for the drift of the OBS/OBH clock. Exact OBS/OBH positions along track at the seafloor were relocated using direct wave arrivals. The maximum horizontal distance between an OBS/OBH deployment location and its position on the seafloor was 384 m.

To enhance the signal-to-noise ratio, the data were filtered with a time and offset dependent band-pass filter, deconvolved with a spiking deconvolution at an operator length of 200 ms, and FK-filtered at large-offset ranges to suppress wrap-around noise from previous shots. After each of these processing stages, we picked seismic phases. The resulting picks were carefully compared with each other, in order to exclude phase-shifts caused by any of the three processing steps at the highest signal-to-noise ratio.

Multichannel seismic data of profile AWI-20030013 were processed in a standard processing sequence comprising sorting (25 m CDP interval), a detailed velocity analysis (every 50 CDPs), multiple suppression via a Radon transform, spike deconvolution to remove the bubble effect, corrections for spherical divergence and normal moveout, residual static corrections, stacking, and post-stack time migration.

We obtained free-air gravity anomalies from a shipboard LaCoste & Romberg S-80 gravimeter recorded at 1-second intervals. The measured values collected by the gravimeter are tied to the N.Z. Potsdam system (1959) via the gravity base station in Lyttleton, New Zealand.

Magnetic data were recorded by a Geometrics G-801 proton free precession magnetometer towed ca. 150 m behind the ship. The magnetic anomaly values were calculated by subtracting the IGRF reference field from the observed total field measurements.

## 8.5 Data description

### 8.5.1 Seismic reflection data

The seismic reflection data show an up to 7000 m thick fill of generally well-stratified layers over the Great South Basin (Figure 8-4). A channel can be identified as deep as 2 s TWT below the seafloor (b.s.f.). It has migrated 20 km southeastwards in the period from late Eocene to late Paleocene (ca. 20 Ma). The channel's northern levee is well developed, the southern levee is ~100 ms TWT thinner. A distinct unconformity cuts across the levee sediments, above which the channel starts to fill. Basement can be tentatively traced at a depth of ~350 m (b.s.f.) in the southeast. Only patches of basement can be observed anywhere else along the profile. By correlation with the Hunt lines B-210, B-214 and F-14 (Hunt Petroleum, 1972), we were able to correlate four main reflectors from the top of Cretaceous, top of Palaeocene, top of mid Eocene and top of late Eocene.

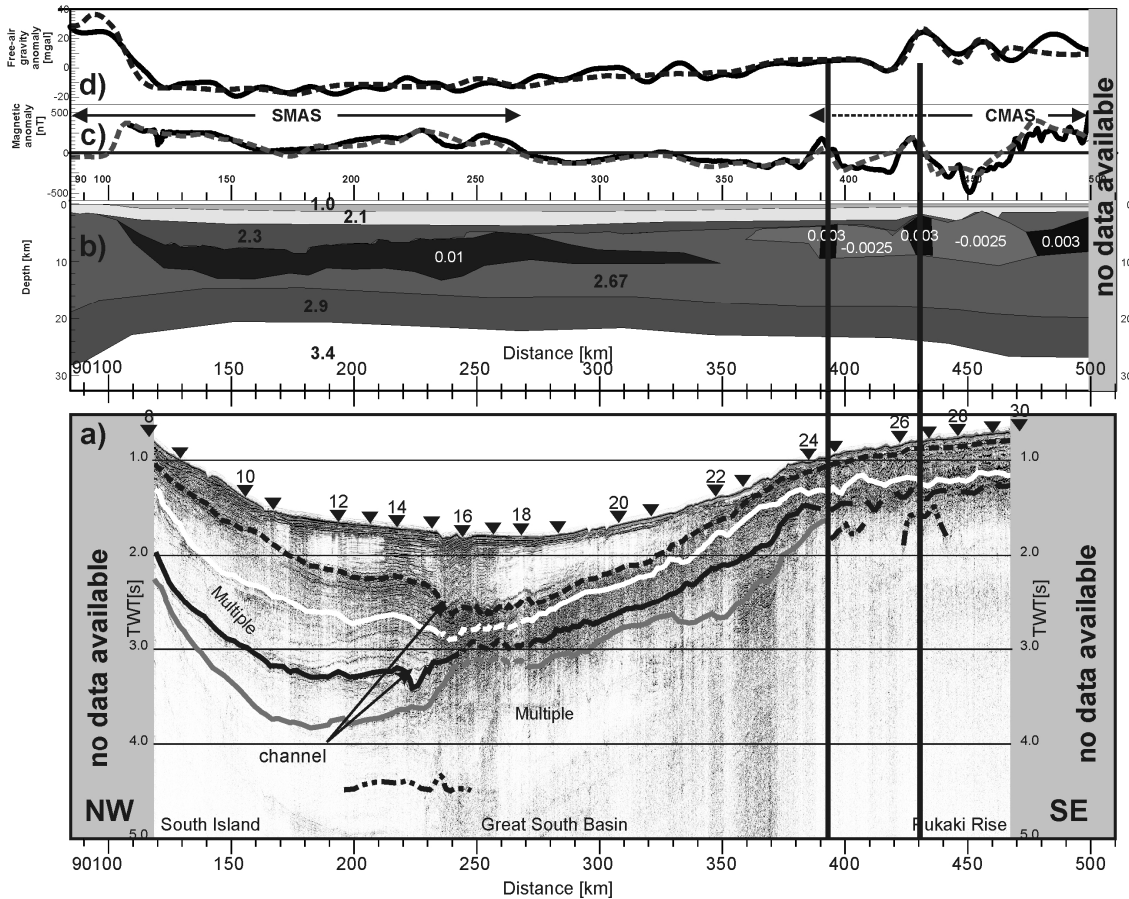


**Figure 8-4:** a) Stacked multichannel seismic line AWI-20030013 across the Great South Basin. Triangles and numbers indicate OBS locations along the transect. Colours of the reflectors are: dashed black – top of Eocene, white – mid of Eocene, solid black – top Palaeocene, grey – top of Cretaceous, dotted dashed black line – tentatively interpreted basement. b) Minimum structure gravity and magnetic model, with bodies striking orthogonal to the plane of the section and extending uniformly from each end of the section. White numbers are susceptibilities in SI-units, black numbers densities in  $\text{g}/\text{cm}^3$ . Above the gravity model (b) measured (solid) and calculated (dashed) free-air gravity anomalies (d) as well as measured (solid) and calculated (dashed) magnetic anomalies (c) are plotted.

Between 200 and 250 km, the reflection patterns change. Layers are well-stratified northwest and southeast of this area, whereas the layering is more hummocky in between. Northwest of the channel, which abuts this hummocky region, Paleocene reflections continue with high amplitude and moderate continuity in a more chaotic pattern. However, reflections can be traced up onto the Pukaki Rise. No intra-basement reflector or Moho reflection can be observed anywhere on profile AWI-20030013.

### 8.5.2 Seismic refraction data

The vertical components show coherent P-wave phases at up to 100 km offset (Figure 8-5 and 8-6). The signal-to-noise-ratio differs strongly from one station to another. Weak S-wave phases can be seen at short offsets in the horizontal components of a few OBS/OBH recordings only. Most P-wave sections (Figure 8-5) show high-amplitude wide-angle reflections from the Moho ( $P_mP$ ). In addition to the inner part of the Great South Basin, weak wide-angle reflections from the basement ( $P_bP$ ) as well as intra-crustal wide-angle reflections ( $P_cP$ ) can be observed.

Phase	$t_{rms}$	Chi-Squared	Number of picks
$P_{dir}$	0.030	0.439	447
$P_{sed1}$	0.071	2.290	287
$P_{sed1}P$	0.154	2.473	32
$P_{sed2}, P_{sed3}$	0.092	2.027	977
$P_{sed2}P$	0.128	1.735	131
$P_{sed3}P$	0.102	0.876	346
$P_{sed4}$	0.111	1.926	1854
$P_{bas}P$	0.158	2.946	225
$P_{g1}$	0.174	2.450	7364
$P_{g2}$	0.195	2.940	1582
$P_cP$	0.153	1.509	744
$P_mP$	0.169	1.782	4257
$P_n$	0.168	1.732	1343

**Table 8-1: Statistics of linear travelttime inversion for all phases within a particular modeling layer of the P-wave velocity-depth model.**

While the resolution of the velocity-depth model (Figure 8-7) can be calculated within the inversion scheme [Zelt, 1999], it is more difficult to quantify errors in phase identification and discrimination. Therefore, we set the variable pick uncertainties in the range 40 ms to 150 ms depending on the signal-to-noise ratio. Although the true pick uncertainty might be lower than the assigned pick uncertainty, an uncertainty in correct phase identification is included with this value [Berndt, et al., 2001].

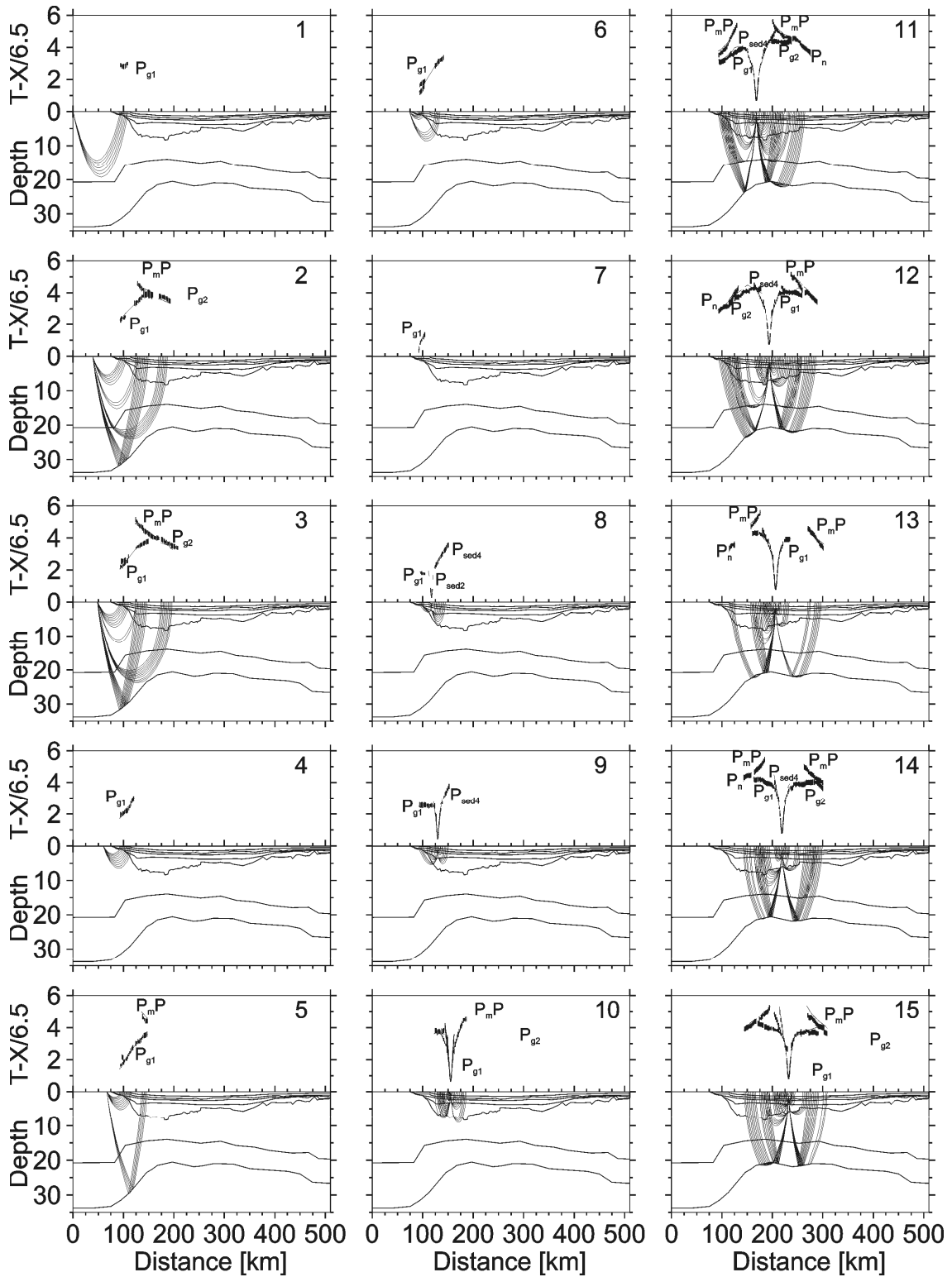


We identified refraction arrivals from three to four sedimentary layers ( $P_{\text{sed1}} - P_{\text{sed4}}$ ), and two crustal layers ( $P_{\text{g1}}, P_{\text{g2}}$ ). A separation into different sedimentary phases was feasible due to strong first order velocity discontinuities and laterally homogeneous apparent velocities within the layer, whereas a moderate signal-to-noise ratio enabled an exact separation of the two crustal refractions. We observed weak  $P_n$  phases (refractions within the uppermost mantle) (Figure 8-5 and 8-6) on some of the OBS records within the basin and on the Pukaki Rise.

## 8.6 Seismic travel-time modelling

We applied a layer-stripping procedure to refine the velocity-depth model by forward modelling. The forward modelling was followed by a travel-time inversion [Zelt and Smith, 1992] to fine-tune the model, using all P-wave reflected and refracted phases. At this stage we only allowed positive velocity gradients except for one high-velocity lens in one sedimentary layer. As only very few shallow wide-angle reflections can be seen in the data and basement was only visible in patches in the MCS data, the top of basement taken from gravity modelling was retained. We introduced another velocity interface (Figure 8-7) into the middle crust of the model. This interface is constrained by wide-angle reflections in the southeastern part of the profile and provides a change in the velocity gradient.

EXTENSIONAL AND MAGMATIC NATURE OF THE CAMPBELL PLATEAU AND GREAT SOUTH BASIN FROM DEEP CRUSTAL STUDIES



EXTENSIONAL AND MAGMATIC NATURE OF THE CAMPBELL PLATEAU AND GREAT SOUTH BASIN FROM DEEP CRUSTAL STUDIES

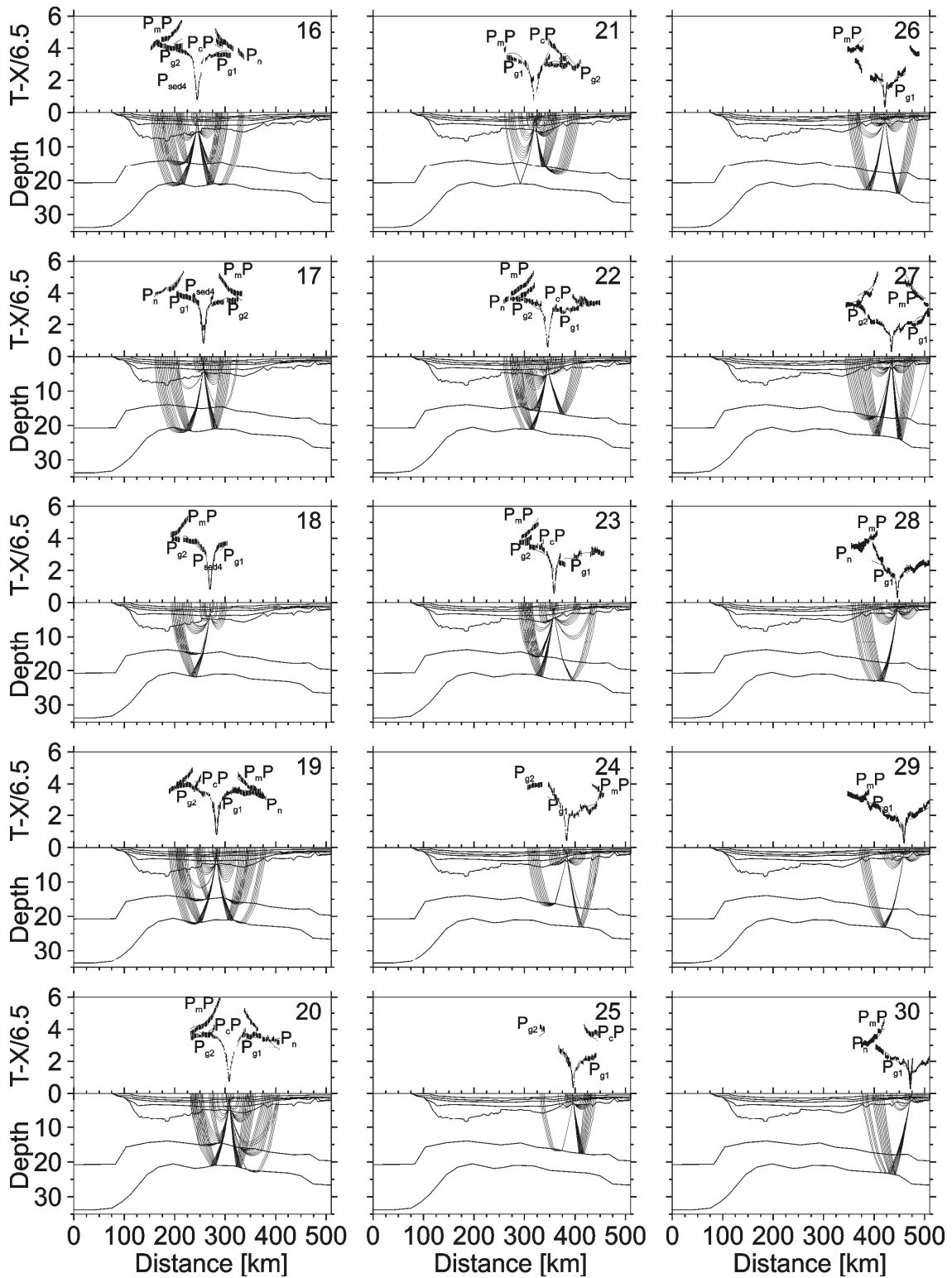


**Figure 8-6:** Comparison of picked and computed travel times from the final P-wave model for each vertical component of an OBS station combined with the corresponding ray paths. Station locations are shown in Figure 8-4. Depth in km,  $T-X/6.5$  in s. Travel times are plotted with a reduction velocity of 6.5 km/s. Vertical error bars indicate observed times, the size of the bars corresponds to the assigned pick uncertainty. Calculated travel times are solid lines. Near-offset phases ( $P_{sed1-3}$ , direct wave) are not labelled.

EXTENSIONAL AND MAGMATIC NATURE OF THE CAMPBELL PLATEAU AND GREAT SOUTH BASIN FROM DEEP CRUSTAL STUDIES

The travel-time inversion process helps assess the model quality as it calculates rms-errors, model-based travel times and Chi-squared values for each branch of the travel-time curves (Table 8-1). With the uncertainties presented above we calculated travel time residuals and normalised Chi-squared values. These values accompanied by the number of picks are presented in Table 8-1. The overall rms-misfit is 0.160 s with a normalised Chi-squared value of 2.113, which is close to the optimum of 1. Figure 8-8 presents the values of the main diagonal of the resolution matrix of the P-wave velocity depth model. Maximum resolution is represented by a value of 1. Smaller values denote a spatial averaging of the true earth by a linear combination of model parameters [Zelt, 1999]. Resolution matrix values greater than 0.5 indicate well resolved nodes. In general, the rms-misfits and Chi-squared values are significantly smaller in the northwestern part of the profile than in the southeast, because the southeastern end of the profile exhibits very rough basement and disturbed reflectors.

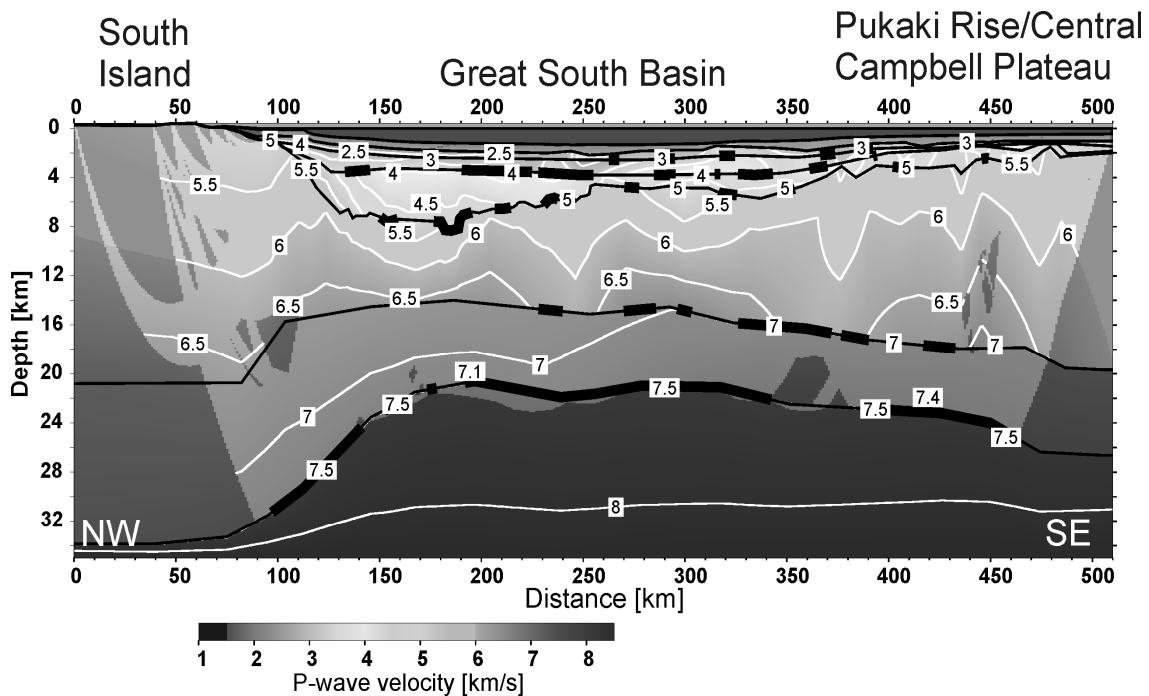


**Figure 8-7: Final P-wave velocity-depth model** overlain by a semi-transparent mask in areas without ray coverage. Bold sections of layer interfaces are constrained by wide-angle reflections.

Our P-wave model is best resolved (Figure 8-8) in the upper and lower crust over the Great South Basin and parts of the Pukaki Rise, where the resolution values lie well above 0.8. Ray coverage is densest in this region. As more rays turn in the upper part of a layer, this part is generally better resolved than the lower part of the same layer. The resolution for the uppermost mantle in the central part of the model is good (0.6 – 0.8). A change in the topography of the Moho, and limited offsets, meant that no  $P_n$  phases were recorded beneath the South Island. Many regions of the velocity model are less resolved for the sediment layers. Due to smaller offset ranges and the masking effect of high-amplitude direct wave arrivals [White and Matthews, 1980], upper parts of the model are less covered with overlapping rays. Structural uncertainties in the upper layers are reduced by reference to the coincident MCS line. The Moho and the

EXTENSIONAL AND MAGMATIC NATURE OF THE CAMPBELL PLATEAU AND GREAT SOUTH  
BASIN FROM DEEP CRUSTAL STUDIES

mid-crustal layer boundary are well resolved in the middle of the profile. Between 323 and 390 km, the mid-crustal layer boundary has resolutions greater than 0.65, between 196 and 449 km, the Moho has resolution values greater than 0.65.

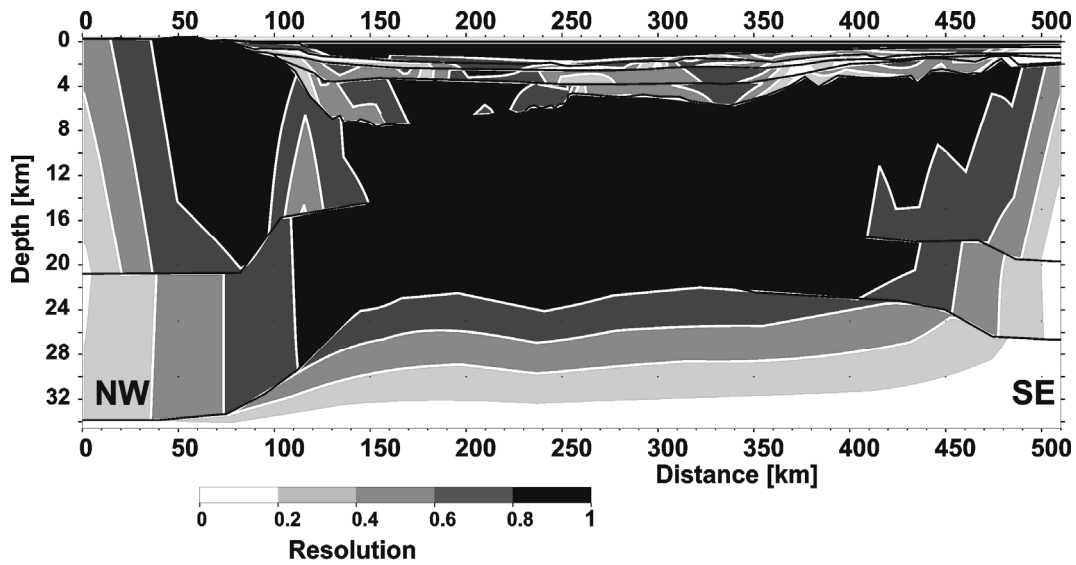


**Figure 8-8:** Resolution values calculated from travel time inversion for the P-wave velocity-depth model. Shading corresponds to resolution values. Contour line interval is 0.2. Resolution values of greater than 0.5 indicate a moderate to good resolution.

## 8.7 Discussion of seismic and gravity models

The refraction seismic P-wave velocity-depth model (Figure 8-7) shows four layers above the basement that have little lateral velocity variation except for the second from top layer. Parts of the layer interfaces are constrained by wide-angle reflections marked as bold lines. The uppermost layer has velocities ranging from 2 km/s at the top to 2.5 km/s at its base, with a maximum thickness of 0.75 km. P-wave velocities of the second layer range from 2.2 km/s to 2.5 km/s at the top of the layer to 2.5 km/s to 3.0 km/s at the base. However, in the area between 245 km and 260 km the basal velocities are significantly increased to 3.8 to 4.0 km/s. Turning rays of three OBS stations cover this area. The thickness of this layer reaches 0.9 km.

The third layer from top has velocities of 2.6 to 3 km/s at the top of the layer and 3.0 to 4.0 km/s at its base. P-wave velocities in the area of 245 km to 260 km are in the same range, thus producing a velocity inversion in this area. The maximum thickness of this layer is 1.1 km. Seismic velocities in the fourth layer from top range from 3.7 km/s to 4.4 km/s at its top and from 5.0 to 5.6 km/s at the bottom of the layer. Seismic velocities are slightly decreased in the Great South Basin compared to values at its flanks and the central Campbell Plateau.

The upper crustal layer has velocities from 5.0 km/s to 5.5 km/s at the top of the layer and 6.5 km/s to 7.1 km/s at its base. A slight increase in velocities can be observed from the South Island to central Campbell Plateau. The thickness of this layer decreases from 22 km beneath the coast of the South Island to only ca. 7 km beneath the inner Great South Basin, before increasing to 24 km again beneath the central Campbell Plateau. Velocities derived from data of one unreversed sonobuoy [Davey, 1977] northeast of the Pukaki Rise are 6.6 km/s for the basement. This value seems to be too high and may be due to the sonobuoy's unreversed nature

The thickness of the lower crustal layer is modelled as 10 km beneath the coast of the South Island, decreasing to ca. 6 km beneath the central Campbell Plateau. Its velocities are between 6.6 km/s –and 7.1 km/s at the top of the layer and 7.5 km/s at its bottom. Again, in this layer seismic velocities increase from NW to SE. The thickness of the crystalline crust totals 30 km beneath the coastline of South Island, 13 km beneath Great South Basin, and 24 km beneath the central Campbell Plateau.  $P_n$  phases constrain a velocity of 7.6 –7.7 km/s in the uppermost mantle.

The gravity anomaly pattern (Figure 8-4) principally represents the bathymetry of the Great South Basin and the Pukaki Rise/central Campbell Plateau as well as the crustal thinning beneath the Great South Basin (Figure 8-4). The gravity model has been tied to an assumed crustal thickness of the South Island and the central Campbell Plateau [Cook, *et al.*, 1999] and confirmed by refraction solutions for the top and base of the crust. The model crust is thinned beneath the entire Great South Basin, with a sharp increase in thickness towards the South Island northwest of 140 km. Traversing southwest onto the Pukaki Rise, the increase of modelled crustal thickness is gentler in comparison. A small number of anomalies with a wavelength of ca. 20 km over the

EXTENSIONAL AND MAGMATIC NATURE OF THE CAMPBELL PLATEAU AND GREAT SOUTH  
BASIN FROM DEEP CRUSTAL STUDIES

central Campbell Plateau can be modelled by variations in the basement-depth that can be tentatively traced in the MCS section as well.

The magnetic anomaly pattern (Figure 8-4) shows two sets of magnetic anomalies over the Great South Basin and the Campbell Plateau. The long-wavelength anomaly system of ca. 200 nT beneath the Great South Basin can be modelled by an elongated magnetic body at ca. 8 km depth (b.s.f.). The two magnetic anomalies of 400 nT amplitude and a wavelength of ca. 15 - 20 km near the Pukaki Rise can be well modelled by two small-scale (~ 5 km wide) dike-like intrusions. In the MCS profile, two patches of reflections can be seen coinciding with these magnetic anomalies at 1.8 s (TWT) (Figure 8-4). Further southeast, at the Pukaki Rise, a number of short-wavelength (~2km), low amplitude (80 -100 nT) anomalies are observed. As the magnetic profile extends 33 km further than the MCS profile, these structures cannot be found in the MCS data.

## 8.8 Interpretation

A high-velocity structure of 15 km extent was modelled in the second layer below the seafloor at ca. 250 km. The velocity of this area reaches 4.0 km/s at 750 – 1000 m depth (b.s.f.) compared to P-wave velocities of 2.7 – 3.0 km/s in the lateral vicinity. In the MCS section, a region of increased amplitudes and decreased reflector continuity coincides well with the high-velocity body of the seismic refraction model. The top reflector interpreted from this area correlates with the top of Eocene reflector on other profiles (e.g. F-14 and B-218) [Cook, *et al.*, 1999]. Salt, an intrusion or apron sediments could cause a zone of high-velocities in this area. Salt would cause higher velocities of ca. 4 km/s, but a salt body would rather have a diffuse pattern of low amplitude reflections. Moreover, no large occurrences of salt have been reported from the Great South Basin [Cook, *et al.*, 1999]. Apron sediments could have been deposited by channel-like features like those mentioned by Cook [1999] and observed in the MCS data (Figure 8-4). Higher compaction, or a different grain size, could likely cause the observed high-velocity lens. Similar velocities for clastic apron sediments were reported, for example, by Grevemeyer *et al.* [2001]. A depositional feature would also be consistent with the moderately chaotic reflection patterns.

A magmatic intrusion could be another possible reason for the high-velocity zone. The p-wave velocities of max. 4 km/s in this region are at the lowermost limit for intrusive rocks, but the magnetic profile shows a broad low amplitude positive anomaly of 30 – 35 km wavelength over this part of the profile. Although this form speaks in favour of a somewhat deeper source, with the level of the high-velocity zone in MCS data is consistent with the interpretation of the Foveaux volcanic sediments of dating to Late Eocene – Miocene times [Carter, 1988b]. However, the features observed here are ca. 180 km southeast of the Foveaux volcanic sediment province. In summary, the observations of this high-velocity structure are too ambiguous to make a clear interpretation of its origin, but on the basis of the seismic velocities, we favour interpreting this structure as a sedimentary feature.

Reflections from the Moho, as well as the gravity model, indicate a very thin (ca. 13 km) crystalline crust beneath the Great South Basin in contrast to the 30 km thickness beneath the coastline of the South Island and 22 km beneath the central Campbell Plateau. The modelled crustal thickness (without sediments) beneath the Great South Basin compares very well with that suggested by Cook *et al.* [1999], while our crystalline crustal thickness of the central Campbell Plateau is slightly (ca. 2 km) less than that of Cook *et al.* [1999]. The total crustal thickness with sediments (27 km), and velocity structure ( $v_p = 5.5 - 6.8$  m/s) of the upper crust of the Campbell Plateau indicate very strongly that this crust is of continental origin [compare e.g. Holbrook, *et al.*, 1994].

Collins [1991] derived an average total crustal thickness of 30 – 45 km for continental crust in Australia. This crust is mainly undeformed, has similar lithologic characteristics to the crust in New Zealand and was adjacent to it in Cretaceous time. A similar pre-breakup crustal thickness is assumed for the Ross Sea, that was also adjacent to the Campbell Plateau [Trey, *et al.*, 1999]. If, using similar assumptions to that of

Bradshaw [1989], we assume a thickness prior to deformation of 35 - 40 km for the Campbell Plateau crust, we would thus calculate stretching factors of 1.6 – 1.8 for the central Campbell Plateau and 2.7 – 3.0 for the Great South Basin. If, on the other hand, the Campbell Plateau had its present thickness already prior to Great South Basin formation, then stretching factors of the Great South Basin would be ca. 2. Considering the pre-stretching thickness of the Great South Basin to have been the same as that of the central Campbell Plateau, the unstretched Great South Basin would have had a width along this profile of ca. 75 km compared to ca. 150 km today.

The crustal thickness beneath the coast of the South Island of New Zealand corresponds well to the thickness modelled by Scherwath et al. [2003]. Throughout the profile, we observe crustal velocities from 5.5 to 6.6 km/s in the upper crust, except beneath Pukaki Rise, where the velocities are slightly higher at 5.5 to 7.1 km/s. The observed velocities are, in the upper crust, slightly higher (0.2 km/s) than the velocities indicated by Scherwath et al. [2003]. However, the seismic lines of the SIGHT experiment [Scherwath, et al., 2003; Van Avendonk, et al., 2004a] extend into the Canterbury Basin rather than into the Great South Basin, so it is questionable whether their results for the Pacific end of the profile can be compared with the results of the line presented here.

In the southeastern part of our profile (260 km – 430 km, below the central Campbell Plateau), we observe strong intracrustal reflections from the boundary between upper and lower crust. This reflector lies ca. 6 km above the Moho reflector. Scherwath et al. [2003] and Van Avendonk et al. [2004a] reported an intracrustal reflector at the same depth beneath the Canterbury Basin from the SIGHT profiles. Such mid-crustal reflectors are not observed beneath the Great South Basin. The observation of this reflector beneath the central Campbell Plateau coincides with a lateral increase in p-wave velocities of the lower crust by ca. 0.3 – 0.4 km/s, whereas p-wave velocities beneath the Canterbury Basin are not increased [Scherwath, et al., 2003; Van Avendonk, et al., 2004a]. Smith et al. [1995] interpreted the lower crust beneath the Canterbury Basin as old oceanic crust overlain by Caples and Torlesse metasedimentary rocks. The SIGHT profiles extend less distance from the coast than our profile and cross the Canterbury Basin instead of the Great South Basin. Adopting this earlier interpretation of the mid-crustal reflector for the Campbell Plateau would mean that the northwestern Campbell Plateau was underlain by oceanic crust. However, we found no indication for oceanic crust beneath the Great South Basin, in either the seismic velocity field or reflection patterns. Similarly, drill sites in the Great South Basin, e.g. sites Tara-1 and Pakaha-1, found gneiss or granite at the upper surface of the basement [Cook, et al., 1999].

The significant increase in seismic velocities of the lower crust and the reflector at the top of the high-velocity body of the central Campbell Plateau suggest that this high-velocity lower crust could instead be caused by underplating. Underplating has been described at various rifted passive margins, e.g. at the US Atlantic margin or the Vøring Plateau [Holbrook, et al., 1994; Mjelde, et al., 1997]. At the Atlantic margin, Holbrook et al. [1994] present evidence for a ca. 24 km thick crystalline transitional crust in parts of their profiles. The lower part of this crust has high (7.2 – 7.5 km/s) P-wave velocities, similar to those on our findings (7.2 – 7.4 km/s). At the Vøring Plateau, Mjelde et al. [1997] show an underplated body with velocities of 7.2 – 7.4 km/s at the

EXTENSIONAL AND MAGMATIC NATURE OF THE CAMPBELL PLATEAU AND GREAT SOUTH  
BASIN FROM DEEP CRUSTAL STUDIES

base of a ca. 23 km thick crust. The top of this underplating is constrained by a distinct mid-crustal reflector. Based on these similarities, we suggest that the high-velocity body in the lower crust beneath the Pukaki Rise should be interpreted as intruded/underplated crust. If such a 6 km thick underplate exists beneath the entire Campbell Plateau, as defined by the 1000 m isobath, its volume totals ca. 2,500,000 km<sup>3</sup>. If just the central Campbell Plateau, confined by the 750 m isobath, was underplated, the volume would be ca. 1,000,000 km<sup>3</sup>. Our profile covers only parts of the Campbell Plateau, so the estimation of the volume of underplating is based on an extrapolation and states maximum values.

If, instead, the CMAS is attributed to the underplated body, then it does not geographically coincide with it completely. The northwestward limit of the CMAS is at 380 km along the profile, while the high velocities begin at ca. 300 km (Figure 8-4 and 8-7). The CMAS differs from the SMAS in displaying higher frequencies. Interpretations vary as to how far the CMAS and the SMAS can be interpreted as dextrally-offset parts of the same anomaly system [Davey and Christoffel, 1978; Sutherland, 1999]. The high-frequency parts of the CMAS along our magnetic profile can be modelled by shallow dike-like structures. Two coincident positive free-air gravity anomalies additionally indicate intrusions or shallow basement highs to be present. Due to the data quality of the MCS section, it is not possible to distinguish between these two possibilities. As the MCS section does not continue over Pukaki Rise (Figure 8-4) dating of these intrusional structures by means of seismic data is not possible. Rock samples dredged from the Pukaki Rise yield ages up to 4.3 Ma (Werner, pers. comm.). We cannot rule out that this younger magmatic activity may be related to underplating beneath the Campbell Plateau. The implied differences in magmatic activity and the observed variability in the style of the magnetic and associated gravity anomalies (Figure 8-3) suggest that either the sources of the CMAS and SMAS have different origins, or that they were modified in different ways following strike-slip separation proposed by Davey and Christoffel [1978].

It is unclear why the proposed underplating would occur only beneath the Campbell Plateau but not beneath the Great South Basin, as this is the thinnest and weakest part of this region off southeastern New Zealand. One explanation would be that the underplating was related to an extensional event that took place prior to the Great South Basin opening.

Most continental rift systems (e.g. Diepr-Donetsk-Basin, East African Rift System or Bounty Trough) [Ebinger and Casey, 2001; Grobys, et al., 2007; *The DOBREfraction'99 Working Group, et al., 2003*] show underplating and/or intrusions at the rift axis, whereas underplating along our profile is interpreted beneath the flanks of the rift system. This phenomenon has been observed at only a very few other rift systems: The Hebrides Shelf in the vicinity of the volcanic northeastern Rockall Trough [Klingelhöfer, et al., 2005] is underlain by a ca. 6 km thick underplate, whereas the seaward Rockall Trough itself consists of extended continental crust that has a thickness of between 12 and ca. 19 km and no underplate, similar to the Great South Basin. Klingelhöfer et al. [2005] did not remark on this arrangement.

Most recent plate-tectonic reconstructions suggest that the Campbell Plateau, Lord Howe Rise, the Challenger Plateau and the Ross Sea were adjacent prior to the late

EXTENSIONAL AND MAGMATIC NATURE OF THE CAMPBELL PLATEAU AND GREAT SOUTH  
BASIN FROM DEEP CRUSTAL STUDIES

Gondwana break-up [*Wandres and Bradshaw, 2005*]. All these geographic features show similar crustal thickness [*Sundaralingham and Denham, 1987; Trey, et al., 1999; Wood and Woodward, 2002*]. Underplating is interpreted to have occurred beneath Lord Howe Rise and the Challenger Plateau [*Wood and Woodward, 2002*], and the crust of the Ross Sea is interpreted to be intruded by mafic rocks [*Trey, et al., 1999*]. For this reason, we assume that crustal thinning and underplating beneath the four formerly adjacent areas are related to one event, which we identify as Early Cretaceous or Jurassic thinning prior to the break-up [*Uruski and Wood, 1991; Wood, 1993*]. Consistent with this, Sutherland [1999] relates the source of the CMAS and SMAS either to Median Tectonic Zone volcanism at ca. 130 Ma [*Kimbrough, et al., 1994*] or to even older volcanic arc related rocks. The reconstructions of Fitzgerald [2002] and Wandres and Bradshaw [2005], based on New Zealand and Antarctic tectonostratigraphy, indicate an extensional phase in the vicinity of these submarine plateaux in the Early Cretaceous at ca. 120 Ma. Forster and Lister [2003] proposed a first extension in the South Island at ca. 110 Ma from onshore geology. With the data presented here, it is not possible to discriminate between these events or refine the proposed timing.

## 8.9 Conclusions

The CAMP reflection/refraction seismic profiling and gravity/magnetic survey and ensuing modelling have revealed much about the extensional structures of the Campbell Plateau. Quantification of the crustal extension during Cretaceous Great South Basin opening will help in refining plate-kinematic reconstructions of the southwestern Pacific. This first combined refraction/wide-angle reflection and MCS survey across a large part of the Campbell Plateau provides new detailed information about the Campbell Plateau extension and the timing of this extension. Our main observations are:

- 1) The Moho shallows from 33 km (b.s.f.) beneath the coast of the South Island to 21 km (b.s.f.) underneath the Great South Basin. It deepens again to 27 km under the central Campbell Plateau.
- 2) In the P-wave model, a high-velocity body in the lower crust can be observed beneath the central Pukaki Rise. The velocities of this body gently rise towards the central Campbell Plateau. The boundary between the upper and lower crust is highly reflective beneath the Campbell Plateau, while this mid-crustal reflector does not occur beneath the Great South Basin or the coast of the South Island.
- 3) P-wave velocities in the lower crust rise from 6.7 – 7.1 km/s under the South Island and the Great South Basin to 7.1 – 7.4 km/s beneath the Pukaki Rise. In the upper crust, P-wave velocities range from 5.1 – 6.5 km/s beneath the South Island to 5.8 – 7.0 km/s under the Pukaki Rise. Four sedimentary layers in the Great South Basin could be recognized in the refraction/wide-angle reflection record, with velocities in the ranges 1.7 – 2.2 km/s, 2.3 – 2.9 km/s, 2.4 – 4.0 km/s and 4.0 – 4.8 km/s.
- 4) The long wavelength free-air gravity anomaly of the Great South Basin has an amplitude of ca. 40 mgal. It can be modelled by crustal thickness variations. Across the Campbell Plateau, a number of anomalies with a wavelength of ca. 20 km and an amplitude of ca. 200 mgal can be related to shallow basement structures.
- 5) The high-velocity body beneath the northwestern Campbell Plateau is interpreted as an underplated body with a possible maximum volume of ca.  $1.0 - 2.5 \times 10^6 \text{ km}^3$ , if it is assumed to occur beneath large parts of the Campbell Plateau. The high P-wave velocities of this body, the fact that it is enclosed by prominent reflectors and comparisons with formerly adjacent submarine plateaus are strong indications of an underplated continental crust. The reduced crustal thickness of the Great South Basin compared to Campbell Plateau indicates a high stretching factor of ca. 2. Assuming instead that both features formed by stretching of crust with an initial thickness of 35 – 40 km yields a

$\beta$ -factor of 2.7 – 3.0 for the Great South Basin and 1.6 – 1.8 for the Campbell Plateau.

The CMAS differs significantly from the SMAS in wavelength. The CMAS correlates with short-wavelength gravity anomalies, and may be associated with underplating and shallow basement structures beneath the central Campbell Plateau. It seems most likely that the two magnetic anomaly systems have different origins and/or developed histories. Rock samples dredged from the seafloor suggest ongoing magmatic activity that persisted at least into Pliocene time. Underplating occurred underneath the northwestern Campbell Plateau but not beneath the Great South Basin and is also thought to have affected neighbouring plateaus like the Lord Howe Rise and Challenger Plateau. This extension and underplating may have occurred at the same time, when all the plateaus were adjacent probably in the Early Cretaceous at ca. 135 – 110 Ma or even in Jurassic time.

### **Acknowledgements**

We are grateful to the captain and crew of RV Sonne during cruise SO-169 for their support and assistance. This project is primarily funded by the German Federal Ministry of Education and Research under BMBF contract no. 03G0169A as well as through contributions from AWI and GNS. The German Academic Exchange Fund (DAAD) funded a visit of J.G. to GNS for two months. Furthermore, we thank GeoPro GmbH (Hamburg) for their support in providing and operating the OBS equipment and Exploration Electronics Ltd. (Norwich) for providing and operating the seismic streamer. We had useful discussions with Reinhard Werner, Rupert Sutherland and Nick Mortimer. Graeme Eagles greatly improved this manuscript. Most of the figures were generated with Generic Mapping Tools [*Wessel and Smith, 1998*].

## 9 Crustal balancing applied for plate-tectonic reconstruction of Zealandia

Jan W.G. Grobys<sup>\*</sup>, Karsten Gohl, Graeme Eagles<sup>a</sup>

*Alfred Wegener Institute for Polar and Marine Research, PO BOX 120161, 27515 Bremerhaven, Germany, phone +49-471-4831-1237, fax +49-471-4831-1271*

<sup>\*</sup>Corresponding author: Jan Grobys, e-mail: jangrobys@bwb.org, phone: +49-471-4831-1237, fax: +49-471-4831-1271, now at Federal Armed Forces Research Centre for Underwater Acoustics and Geophysics, Klausdorfer Weg 2-24, 24148 Kiel, Germany.

<sup>a</sup> now at: Royal Holloway, University of London, Egham Hill, EGHAM, TW20 0EX, United Kingdom

### 9.1 Abstract

Zealandia is a key piece in the plate reconstruction of Gondwana. The positions of its submarine plateaus are major constraints on the best fit and breakup involving New Zealand, Australia, Antarctica and associated microplates. As the submarine plateaus surrounding New Zealand consist of extended and highly extended continental crust, classic plate tectonic reconstructions assuming rigid plates and narrow plate boundaries fail to reconstruct these areas correctly. We present a plate-tectonic reconstruction based on crustal balancing, an approach that takes into account the rifting and thinning processes affecting continental crust. In a first step, we computed a crustal thickness map of Zealandia using seismic, seismological and gravity data. The crustal thickness map shows the submarine plateaus to have a uniform crustal thickness of 20 – 24 km and the basins 12 – 16 km. We assumed that a reconstruction of Zealandia should close the basins and lead to a most uniform crustal thickness. We used the standard deviation of the reconstructed crustal thickness as a measure of uniformity. The reconstruction of the Campbell Plateau area shows that the amount of extension in the Bounty Trough and the Great South Basin is far smaller than previously thought. Our results indicate that the extension of the Bounty Trough and Great South Basin occurred simultaneously.

## Keywords

New Zealand, Antarctica, plate-kinematics, geodynamics, crustal thickness, continent-ocean boundary, crustal thinning

## 9.2 Introduction

Plate-kinematic reconstructions cannot be expected to give precise results where magnetic seafloor spreading anomalies and fracture zones of oceanic crust are not observed, as these are the major constraints for calculating rotation parameters and the timing of plate motions. Areas where these data might be missing include oceanic crust overprinted by large volume magmatic extrusions, and thinned continental crust where extension did not reach the stage of seafloor spreading. In this paper, we present a novel approach to plate tectonic reconstructions by applying a crustal balancing method which takes into account continental rifting and extension at plate and micro-plate boundaries. This method reduces the errors caused by inappropriate identification and characterisation of the continent-ocean boundary. Crustal extension processes can be highly variable. In our approach, we apply the two important end-member models: pure-shear and simple-shear [*Latin and White, 1990; Wernicke and Burchfiel, 1982*]. In both models, plates in areas of extension and compression, delineated by detachment and thrust faults, can be considered overlapping or underlapping. This extension or compression is difficult to simulate without invoking crustal thickness, meaning here and throughout the entire paper the thickness of the crystalline crust. On a grid showing crustal thickness, the crust can be divided vertically so that a certain percentage of the crustal thickness in a plate boundary region can be assigned to one plate and the remaining part to its conjugate. An important prerequisite is knowledge of the present crustal thickness of the deformed and undeformed parts of the plates.

It has been shown that the basins and troughs around New Zealand are partly or entirely underlain by highly extended continental crust [*Grobys, et al., 2007; Grobys, et al., submitted; Lafoy, et al., 2005a; Laird, 1993; Scherwath, et al., 2003; Van Avendonk, et al., 2004a*]. With its large extended continental plateaus and basins (Figure 9-1), Zealandia is a good example of the results of extensional processes and a good area for testing their consequences and demands for making plate-kinematic reconstructions.

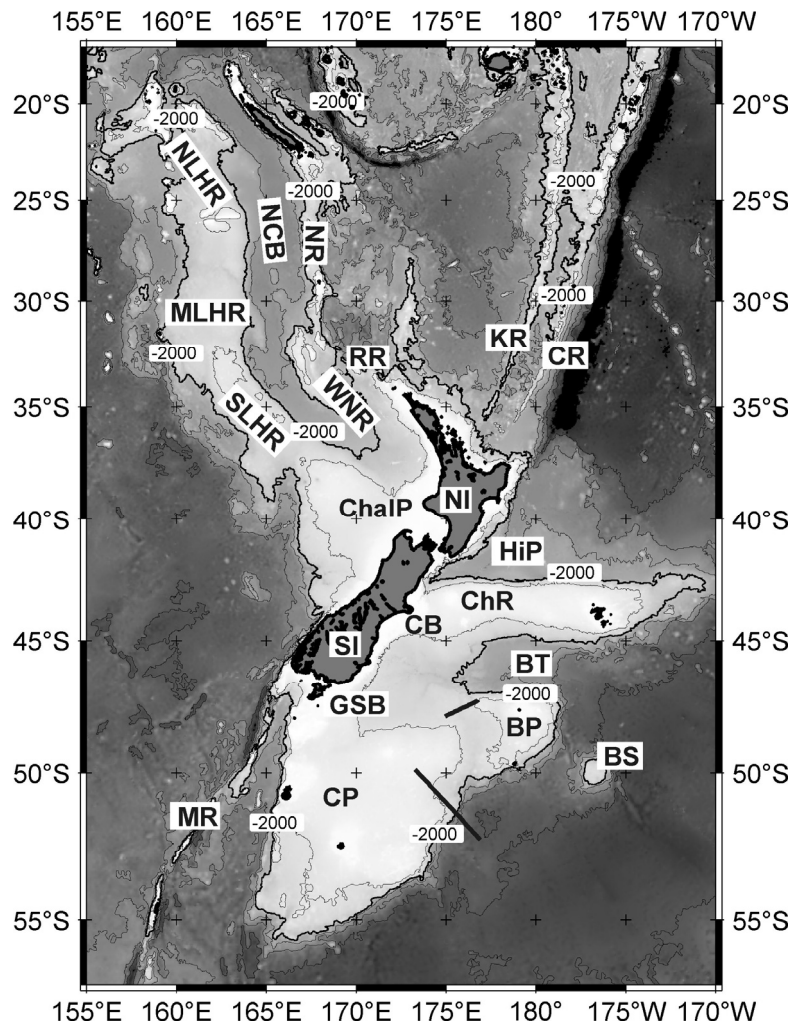


**Figure 9-1: Bathymetric overview map** [Smith and Sandwell, 1997] of Zealandia. Abbreviations are: NI – North Island of New Zealand, SI – South Island of New Zealand, CB – Canterbury Basin, ChR – Chatham Rise, HiP – Hikurangi Plateau, BT – Bounty Trough, BP – Bounty Platform, BS – Bollons Seamounts, CP – Campbell Plateau, MR – Macquarie Ridge, GSB – Great South Basin, ChalP – Challenger Plateau, SLHR – Southern Lord Howe Rise, MLHR – Middle Lord Howe Rise, NLHR – Northern Lord Howe Rise, NCB – New Caledonia Basin, NR – Norfolk Ridge, WNR – West Norfolk Ridge, RR – Reinga Ridge, KR – Kermadec Ridge, CR – Colville Ridge.

A plate-kinematic reconstruction of Zealandia and Marie Byrd Land of West Antarctica can give important insights on how a compressional plate boundary turns into an extensional one and how seafloor spreading starts [Bradshaw, 1989; Luyendyk, 1995]. Understanding these processes in general and for this region in particular will help improving reconstructions of the global plate circuit, which consists of two large, almost decoupled, sub-circuits (Pacific and Gondwana [Cande and Stock, 2004a]), mainly by constraining the regional tectonic setting at the time Zealandia started to separate from Antarctica.

### 9.3 Tectonic introduction

The West Gondwana continental margin between the Ross Sea and Marie Byrd Land sectors underwent a transition from a convergent to a passive margin regime. The Pacific Plate subducted beneath Chatham Rise, which originally lay north of eastern Marie Byrd Land, until the Hikurangi Plateau collided with it in Cretaceous times. Shortly after the cessation of seafloor spreading at Osborn Trough, Chatham Rise started separating from West Antarctica, opening Bounty Trough and Great South Basin [Mortimer, *et al.*, 2006]. Extension followed subduction and collision very closely, with estimates of their respective timings often overlapping. According to Worthington *et al.* [2006], spreading at Osborn Trough and subduction beneath East Gondwana ceased at ca. 86 Ma, while Chatham Rise is interpreted to have separated from Thurston Island and Marie Byrd Land at ca. 90 Ma [Eagles, *et al.*, 2004; Larter, *et al.*, 2002], as the Bounty Trough and Great South Basin opened [Eagles, *et al.*, 2004]. Bounty Trough is interpreted to have undergone a first back-arc extensional phase during the subduction of the Phoenix Plate followed by tectonic inversion when the Hikurangi Plateau collided with Chatham Rise [Grobys, *et al.*, 2007], which in turn was followed by a second extensional phase in late Cretaceous times [Eagles, *et al.*, 2004]. The youngest syn-rift sediments in the Great South Basin are of Cretaceous age [Cook, *et al.*, 1999; Grobys, *et al.*, submitted] dating the end of extension to 86.5 Ma. The oldest seafloor spreading southeast of the Chatham Islands is marked by anomaly 34y (83 Ma) [Davy, 2006]. Campbell Plateau, further west, started to separate from West Antarctica during chron 33r (83.0 – 79.1 Ma) [Larter, *et al.*, 2002]. While Mukasa and Dalziel [2000] suggested a segmentation of Campbell Plateau into an eastern and a western part, it is widely accepted that the Plateau can be considered a single unit in a plate-kinematic sense (e.g. [Wandres and Bradshaw, 2005]).

The opening history of the New Caledonia Basin is by far less well known than those of the Bounty Trough and Great South Basin. While the Lord Howe Rise is considered to consist of thinned and intruded continental crust [Shor, *et al.*, 1971; Woodward and Hunt, 1971], the New Caledonia Basin has been interpreted to consist partly of thinned continental crust and partly oceanic crust. Evidence for extended continental crust is stronger in the northern and southern parts than in the central part [Auzende, *et al.*, 2000; Uruski and Wood, 1991; Vially, *et al.*, 2003; Wood and Woodward, 2002]. Lafoy *et al.* [2005a] assumed oceanic crust in the Central New Caledonia Basin on the basis of broad and diffuse magnetic anomalies. It is interpreted that a first basin-forming phase occurred in the New Caledonia Basin region between 95 and 65 Ma [Lafoy, *et al.*, 2005a]. A second phase of extension, possibly associated with seafloor spreading, occurred in the New Caledonia Basin at 62 – 56 Ma [Gaina, *et al.*, 1998b; Lafoy, *et al.*, 2005a].

Zealandia underwent a major reorganization phase in the period from ca. 45 Ma onward [Cande and Stock, 2004b; Sutherland, 1995]. After the cessation of spreading along the Tasman Ridge at ca. 52 Ma [Gaina, *et al.*, 1998b], spreading began in the Emerald Basin south of New Zealand [Kamp, 1986; Sutherland, 1995]. As the instantaneous pole of relative motion between Australia and the Pacific plate moved gradually southward, the spreading direction became more and more oblique

[*Sutherland, 1995*]. At ca. 22 – 21 Ma, key elements of the present plate boundary through New Zealand had developed [*King, 2000*]. A further major change in the pole of relative motion between Australia and the Pacific plate occurred at ca. 6-5 Ma, when it moved northwestwards, causing the initiation of today's transpressional plate boundary.

An extensional event in prior to New Zealand's separation from Marie Byrd Land has been reported for the period ca. 140 – 100 Ma. Evidence for this event comes from metamorphic core complexes in the South Island [*Forster and Lister, 2003; Spell, et al., 2000*] and from the upper Jurassic – Cretaceous stratigraphy of the Taranaki Basin [*Uruski, 2003*]. The younger (125 – 100 Ma) extensional events in New Zealand coincide with the development of a core complex in Marie Byrd Land [*Luyendyk, et al., 1996*], and the older events (140-125 Ma) have been linked extensional events in a precursor of the West Antarctic Rift System [*DiVinere, et al., 1995; Müller, et al., 2000*]. An accurate reconstruction of the New Zealand – Antarctic sector of Gondwanaland (e.g. [*Wandres and Bradshaw, 2005*]) allows an estimate of the timing of crustal extension of the submarine plateau margins.

## 9.4 Crustal thickness grid

Crustal thickness grids help define and characterise tectonic units within a region. In this study, we use the crustal thickness grid as the basis to compute rotation parameters, by assuming a constant crustal thickness applied in a region prior to its extension.

Name	Methods	Reference
Bounty Trough	Seismic Refraction, Sediment thickness, Gravity	[Davy, 1993; Grobys, <i>et al.</i> , 2007]
Campbell Plateau	Gravity, Sediment thickness	[Davey, 1977, this work]
Challenger Plateau	Gravity	[Wood and Woodward, 2002]
Chatham Rise	Seismology, Gravity	[Davy and Wood, 1994; Reyners and Cowan, 1993]
Great South Basin	Seismic Refraction, Sediment thickness, Gravity	[Cook, <i>et al.</i> , 1999, this work; Davey, 1977; Grobys, <i>et al.</i> , submitted]
Lord Howe Rise & New Caledonia Basin	Gravity, Sediment thickness, Seismic Refraction	[Davey, 1977; Herzer, <i>et al.</i> , 1997; Jongsma and Mutter, 1978; Lafoy, <i>et al.</i> , 2005a; Lafoy, <i>et al.</i> , 2005b; Van de Beauque, <i>et al.</i> , 1998]
North Island	Gravity	[Beanland and Haines, 1998]
South Island & Canterbury Basin	Seismic Refraction, Seismology	[Godfrey, <i>et al.</i> , 2001; Kohler and Eberhart-Phillips, 2002; Mortimer, <i>et al.</i> , 2002; Scherwath, <i>et al.</i> , 2003; Van Avendonk, <i>et al.</i> , 2004a]

**Table 9-1: Database of information used to constrain the crustal thickness**

We combined published and new 2D and 3D models of crustal thickness to generate a gridded regional crustal thickness map (Figure 9-3). 3D-models of crustal thickness already exist for the North and South islands of New Zealand, and the Challenger plateau (Figure 9-1). We modelled 29 new minimum-structure 2D gravity profiles (e.g. Figure 9-2) together with the various previously published gravity, seismic refraction and seismological models. We extracted free-air gravity values from a global satellite-derived dataset [Smith and Sandwell, 1997], and bathymetric information was derived from either the seismic profiles or from satellite altimetry [Sandwell and Smith, 1997]. A number of ship soundings contributed to the bathymetry grid in the Zealandia area, reducing the risk of using a circular method. Wherever possible, sedimentary layers were constrained for the gravity profiles using multichannel seismic data. Sediment thickness data were not available for some areas of the Lord Howe Rise and New Caledonia Basin. Here, we estimated sediment thicknesses on the basis of geological and bathymetric information. Given the minimum structure criterion for the gravity models, we used the same densities in each one.

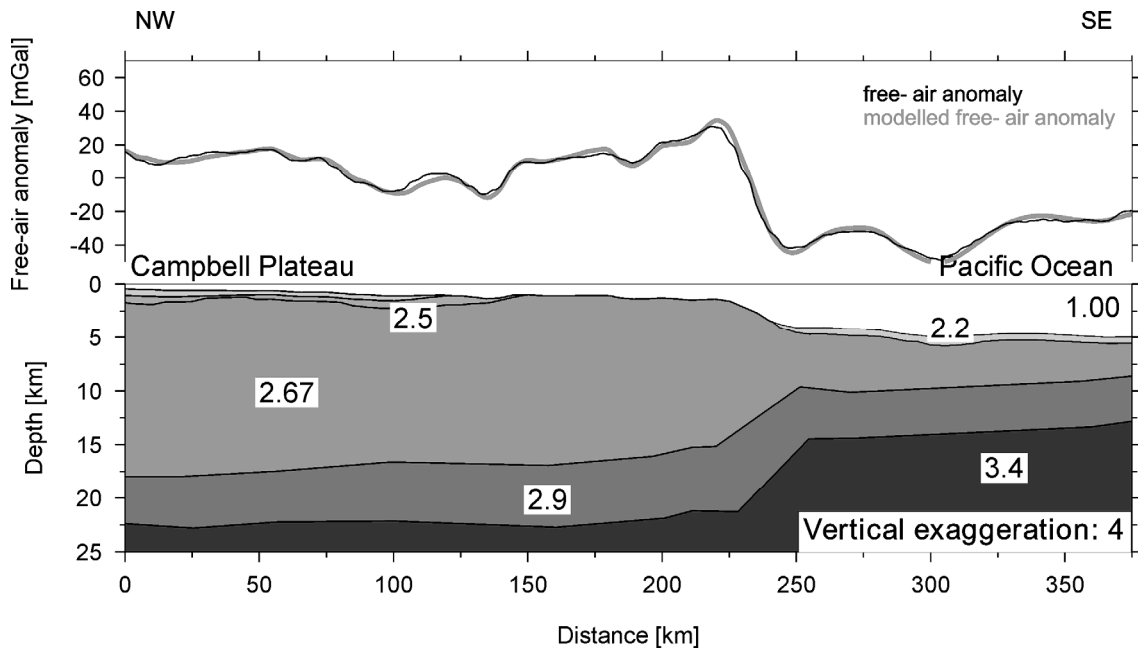


**Figure 9-2: Example gravity model across the Campbell Plateau:** Minimum structure gravity model, with bodies striking orthogonal to the plane of the section and extending uniformly from each end of the section. Observed gravity data are taken from Smith and Sandwell [1997]. Black numbers are densities in  $g/cm^3$ .

The crustal thickness models had to be adjusted for the differences in crustal thickness yielded using different techniques. To do this, we used the interfaces in seismic refraction models of the Great South Basin, Bounty Trough, Canterbury Basin and New Caledonia Basin as a reference (Figure 9-3). Seismic refraction lines connected by gravity profiles showed a consistent crustal thickness. Only the crustal thickness of the South Island, which is based on seismological data [Kohler and Eberhart-Phillips, 2002] had to be reduced by 8 km in order to fit the refraction data. After depth corrections, line and grid data were interpolated at 5 km intervals and gridded with a spacing of 3 x 3 min, using a continuous curvature gridding algorithm [Smith and Wessel, 1990]. The resulting grid extends from 57°S to 17° S and from 157°E to 175°W.

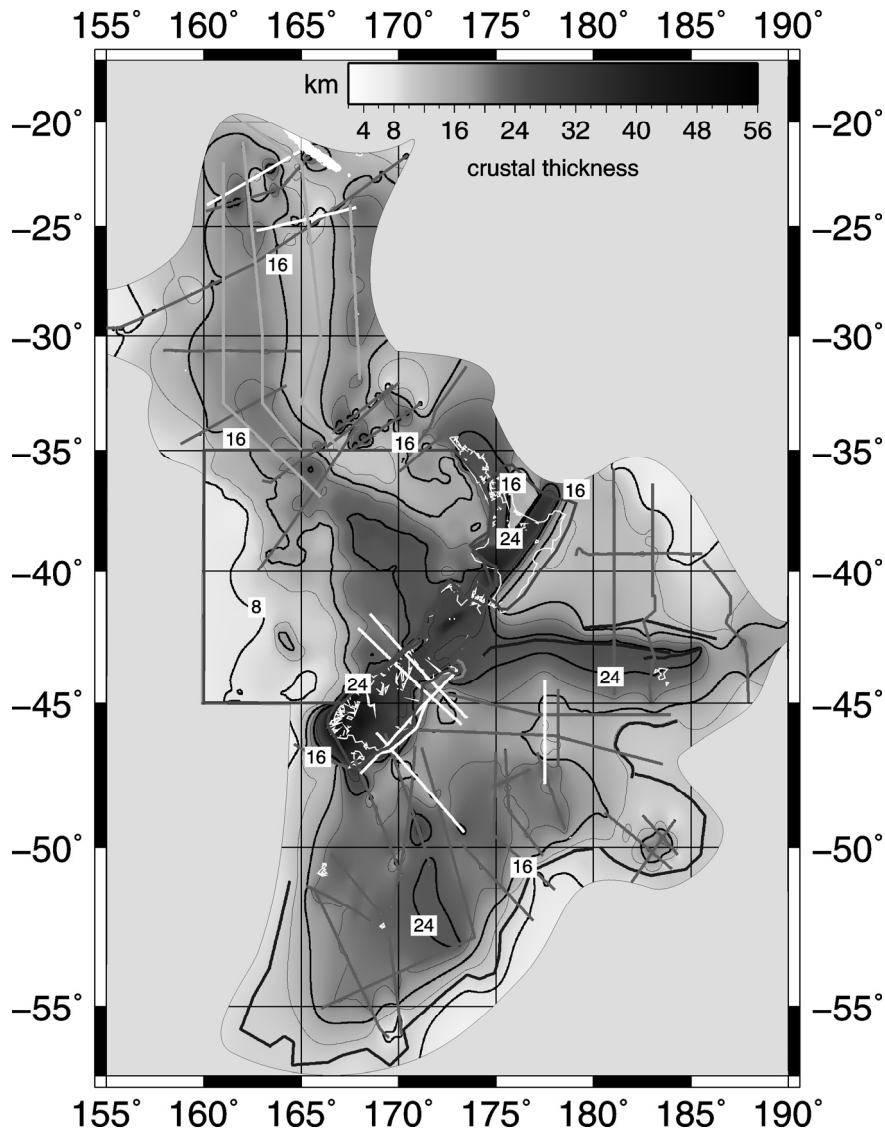


**Figure 9-3: Crustal thickness map of Zealandia.** The crustal thickness map of Zealandia shows the main features of the microcontinent. Unconstrained areas are masked. Abbreviations are: NI – North Island of New Zealand, SI – South Island of New Zealand, BP – Bounty Platform, BS – Bollons Seamounts, BT – Bounty Trough, CampP – Campbell Plateau, ChalP – Challenger Plateau, ChR – Chatham Rise, GSB – Great South Basin, HiP – Hikurangi Plateau, LHR – Lord Howe Rise, PR – Pukaki Rise, StI – Stewart Island.

We estimate that the lateral error involved in digitizing published crustal thickness data from paper journals should not be larger than ca. 10 km. The sparse data coverage in the Lord Howe Rise area and at the margins of the plateaus is a second source of errors. Therefore, we were not able to map the Macquarie, Colville, and Kermadec ridge systems, as their small size would have required denser coverage. In general, the accuracy of the crustal thickness map decreases from the centre of a plateau towards its margins (Figure 9-3). Crustal thickness for the deep sea was extrapolated from a few known areas (e.g. seafloor around Bollons Seamount [Davy, 2006]).

The crust southeast of New Zealand, Campbell Plateau, Bounty Platform, Chatham Rise and Bollons Seamount has a uniform thickness of 20 – 24 km (Figure 9-3). The crustal thickness increases to ca. 26 km at Pukaki Rise, on the central Campbell Plateau. Pukaki Rise cannot be mapped entirely due to insufficient data coverage. However, patches of increased thickness are arranged along a line tentatively suggesting the location of Pukaki Rise. The map shows the crustal thickness decreasing from the Inner Bounty Trough (ca. 18 km) towards the Outer Bounty Trough (ca. 10 km). Two small areas with decreased thicknesses (ca. 14 km) are shown in the Canterbury and the Great South basins (Figure 9-3).

The map resolution in the Challenger Plateau region is much higher, as this area was taken from the grid of Wood and Woodward [2002], where denser profile data were available. The three ridge systems east of the New Caledonia Basin tend to be merged in the map, because the ridges are covered by a few lines only and some of the lines do not extend across all three ridges (Figure 9-3). The crustal thickness west of the New Caledonia Basin decreases northwards from the Challenger Plateau (ca. 24 km). The lowest crustal thickness can be found at the midpoint of Lord Howe Rise between 33° S and 27° S (ca. 18 km). Further north, the thickness increases again to ca. 22 km. The part of New Caledonia Basin adjacent to the Middle Lord Howe Rise (33° S - 27° S) is the region that Lafoy [2005a] suggested to consist of oceanic crust. However, in our map, the New Caledonia Basin has a uniform crustal thickness of ca. 14 km, except between 35° S and 37° S, where it decreases to ca. 11 km. The step from the New Caledonia Basin to the Norfolk, West Norfolk and Reinga ridges appears to be mapped well, while the eastern margins of the Norfolk and Reinga ridges are not imaged. For this reason, we masked this region in Figure 9-3. Where they are well imaged, the three ridges have a range of crustal thickness of ca. 18 – 24 km. The West Norfolk and Reinga ridges have the higher thicknesses of ca. 20 – 24 km, while the Norfolk Ridge has a maximum thickness of ca. 21 km and is thinnest (ca. 18 km) opposite the (thin) Middle Lord Howe Rise.

## 9.5 Method of fitting plate-kinematic boundaries

Common plate-kinematic reconstructions are based on the assumption that a) continental and oceanic plates and plate segments are rigid and b) that they are and were always separated by well-defined first-order discontinuity boundaries. It has been shown e.g. for the East Greenland Volcanic Margin [Voss and Jokat, 2007] that the transition zone between continental crust unaffected by rifting and pure oceanic crust can be as wide as 180 km. Similarly, Grobys et al. [2007] showed that the ca. 350 km wide Bounty Trough in New Zealand, which did not reach the seafloor spreading stage, is in large parts underlain by highly extended continental crust.

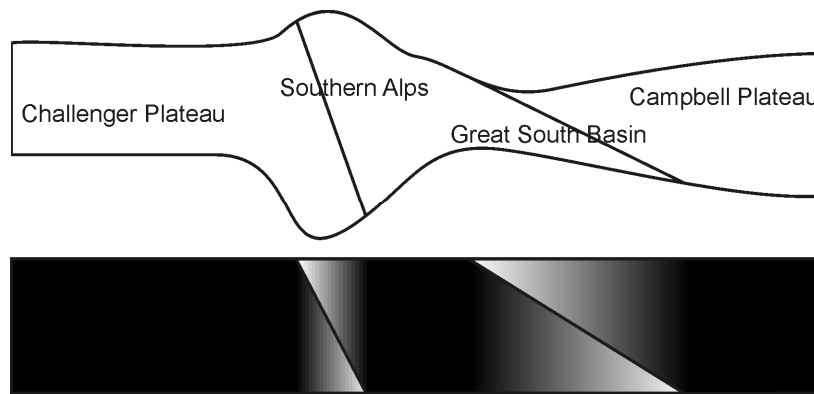


**Figure 9-4: Schematic cross-section through the crust:** This simplified schematic cross section from the Challenger Plateau to the Campbell Plateau illustrates the idea of detachment faults cutting through the crust. The Alpine Fault, which is a transpressional plate boundary, is modelled as a steeply dipping thrust fault. The extensional zone in the Great South Basin is modelled by a gently-dipping detachment fault. Lower sketch illustrates the factors of the masks to be multiplied with the crustal thickness grid. White colour represents a factor of 0, black a factor of 1. The sum of all masks in overlapping areas is always 1.

If, for a plate-kinematic reconstruction, the plate boundaries are considered the outer boundaries of the unaffected continental crust, a “tight fit” reconstruction leads to an overlap whose width can be calculated as  $o = w * (\beta - 1) / \beta$ , where  $w$  is the total width of the continent-ocean transitions and  $\beta$  is the stretching factor. For the Bounty Trough, where  $\beta = 2.7$  and  $w = 350$  km, the overlap caused by a reconstruction of rigid plates would be ca. 220 km. The overlap in such a reconstruction could be removed if the outer boundary of the plates were  $0.5 * o$  larger than the outer boundary of the unaffected continental crust. This would require the knowledge of  $\beta$ -factors, which can be gleaned from the stretched and unstretched crustal thicknesses. These considerations are harder to make at corners and strong bends along plate boundaries because of the possibility of oblique extension, and the results are therefore more error-prone.

In order to gain insight into a region’s early plate kinematic history, and into the likely errors of a plate tectonic reconstruction showing such a history, a reconstruction has to take continental crustal stretching explicitly into account. For this, we rotate the

crustal thickness grid using finite plate rotation parameters. To account for the overlapping plates assuming a crustal extension model (Figure 9-4), we picked overlapping masks for each of the plates to be rotated. The mask outlines were derived on the basis of the crustal thickness grid (Figure 9-5a) and the bathymetry (Figure 9-1). The masked grid nodes are assigned a value of 1 in the area of the unstretched continental crust, a value between 1 and 0 in the continent-ocean transition zone (COTZ) or extended crust of a basin and a value of 0 outside the COT of a plate (Figure 9-5b), in such a way that sum of all the masked nodes at each position in the grid is 1. In extensional areas such as the Great South Basin, the overlapping areas are wide (i.e. the hypothetical detachment fault has a gentle slope) and at transform plate margins the separation between the plates has a steep slope (Figure 9-4). The masks (Figure 9-5b) were multiplied with the crustal thickness grid (Figure 9-5a) to obtain a representation of a plate with a reduced crustal thickness (Figure 9-5c).

The reduced crustal thickness plates were rotated around a finite rotation pole by varying the pole coordinates and the rotation angle systematically within set intervals (Figure 9-5d). After each rotation interval, the crustal thicknesses of each grid cell of all overlapping plates were summed to obtain a new crustal thickness grid (Figure 9-5e) representing the crustal thickness of the area before the plate movement. Rotations producing an overlap in a former basin will result in reconstructions with crustal thicknesses that are too large. Rotations that produce an underlap will lead to crustal thicknesses that are too small. A rotation that closes a basin obliquely (local overlap and local underlap) would result in a region of mixed inappropriate crustal thicknesses.

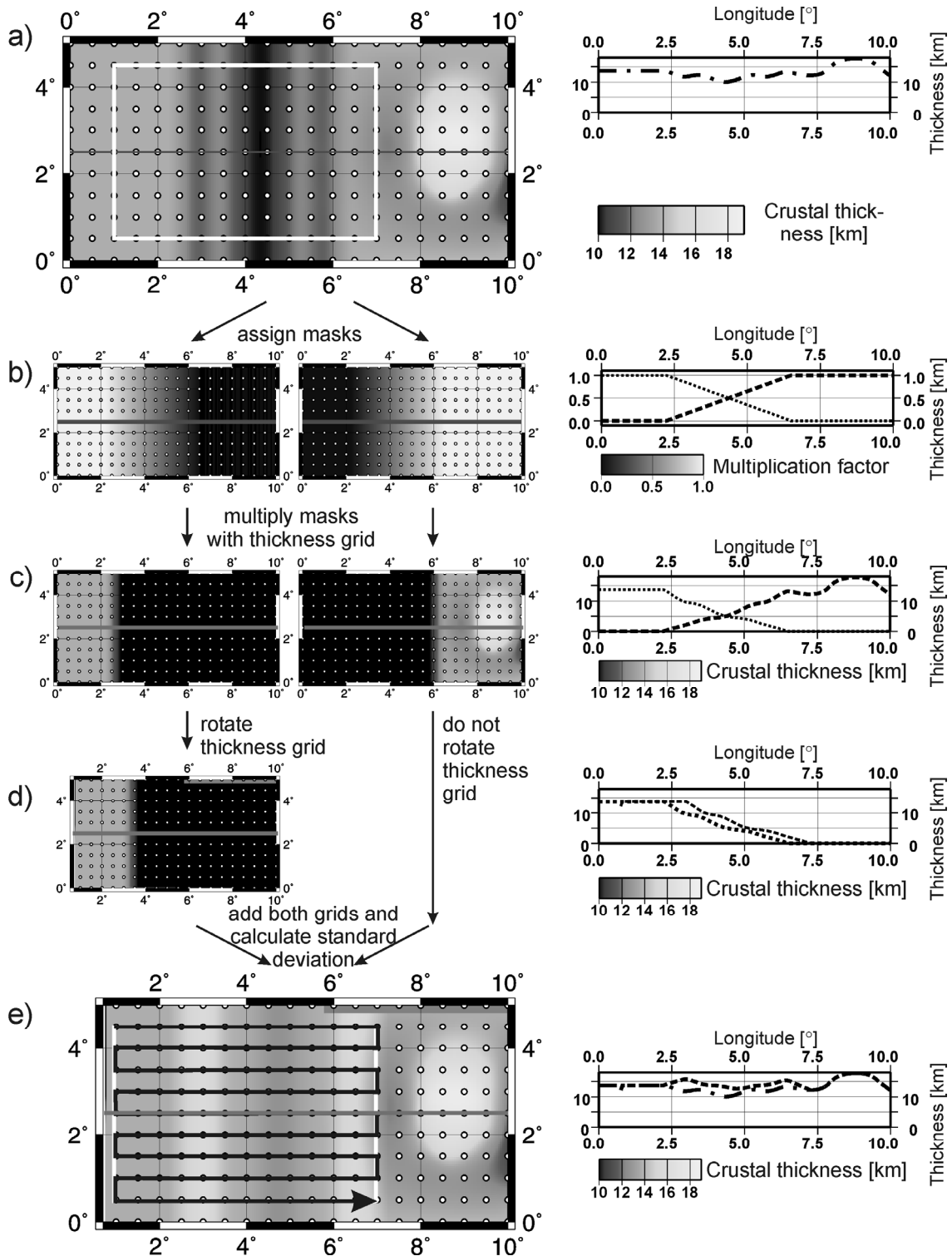


**Figure 9-5: Method of plate-tectonic reconstruction by crustal thickness balancing:** The processing flow illustrates the way in which the standard deviation of a single finite rotation is computed. A crustal thickness grid (a) is multiplied with a mask (b). The masks are assigned on the base of crustal thickness and bathymetric information and have values of between 0 and 1. The multiplication leads to a separation into two grids representing different plates (c). One of the grids is rotated and vertically summed with the second, unrotated grid (d). The standard deviation of the resulting crustal thickness grid is calculated over all grid nodes (e) within a significant window (grey box). Left sides are the grids, right sides are profiles of the grids along the grey lines. White dots with black circles represent the grid nodes.

## 9.6 Assumptions and restrictions

Various crustal extension models have been employed to explain the processes of basin formation. Wernicke and Burchfiel [1982] suggested a lithosphere-scale detachment system as an extensional model. Their simple-shear model can explain the strong structural asymmetry observed across many rift systems. The pure-shear model, proposed by Latin and White [1990], predicts a symmetric rift architecture and crustal thinning when applied to a homogeneous lithosphere. In their model, extension is distributed through the lithosphere uniformly with depth. Studies of rift systems have found that neither of these end-member extension models can explain all observations, but that a combination of both models is applicable, e.g. for the Labrador Sea margin [Louden and Chian, 1999]. A reconstruction on the basis of a pure-shear model or even on the basis of a combination of simple-shear and pure-shear models would need to employ a finite element modelling technique, as it would have to consider particle motion. Simple-shear models, on the other hand, can still explain many features of extensional systems, especially where magmatic intrusions are absent. A method based on an assumption of simple-shear should also reconstruct, but of course not model, of pure-shear in the central areas of extension, but not in the bordering areas of crustal extension. Here, the reconstruction could lead to a slight overthickening after the reconstruction. Both extensional reconstruction models, however, neglect intrusions. Intrusions add to the total crustal thickness, which means that in their presence a rotation angle calculated as described above might be too small. In our case, this is likely in the Middle Bounty Trough, where intrusions are observed. In regions where many intrusions occur, e.g. the Kenya Rift [Mehie, *et al.*, 1997], crustal thickness has to be corrected for. An estimate of the extent of intrusion can be calculated on the basis of p-wave velocity contrasts in seismic profiles [Grobys, *et al.*, 2007]. Small intrusions should not lead to large errors because they do not greatly influence the standard deviation of the reconstructed crustal thickness.

It is important to have a best-fit criterion for a reconstruction technique. In our case, we chose that this criterion should be one of least variability in crustal thickness in the reconstructed grid. Away from their margins, the present crustal thickness of the plateaus surrounding New Zealand is widely uniform. Grobys *et al.* [submitted] suggested that a general thinning of these plateaus occurred in a period prior to the extension of basins such as Bounty Trough, Great South Basin or New Caledonia Basin. For this reason, it seems reasonable to assume that the best-fit reconstruction leads to a most uniform crustal thickness in the entire region. However, as this reconstruction technique calculates rotation parameters on a regional scale, the method requires only the assumption, that the crustal thickness is uniform on both sides of a basin. To assess our best-fit criterion, we calculated the standard deviation of the ‘unperturbed crustal thickness’ within a window (Figure 9-5a and e) covering an area of crust far away from possible overlaps, existing or old basins, and their margins. We assumed that the best-fit reconstruction was the one with the most uniform crustal thickness as expressed by the lowest standard deviation of unperturbed crustal thickness.

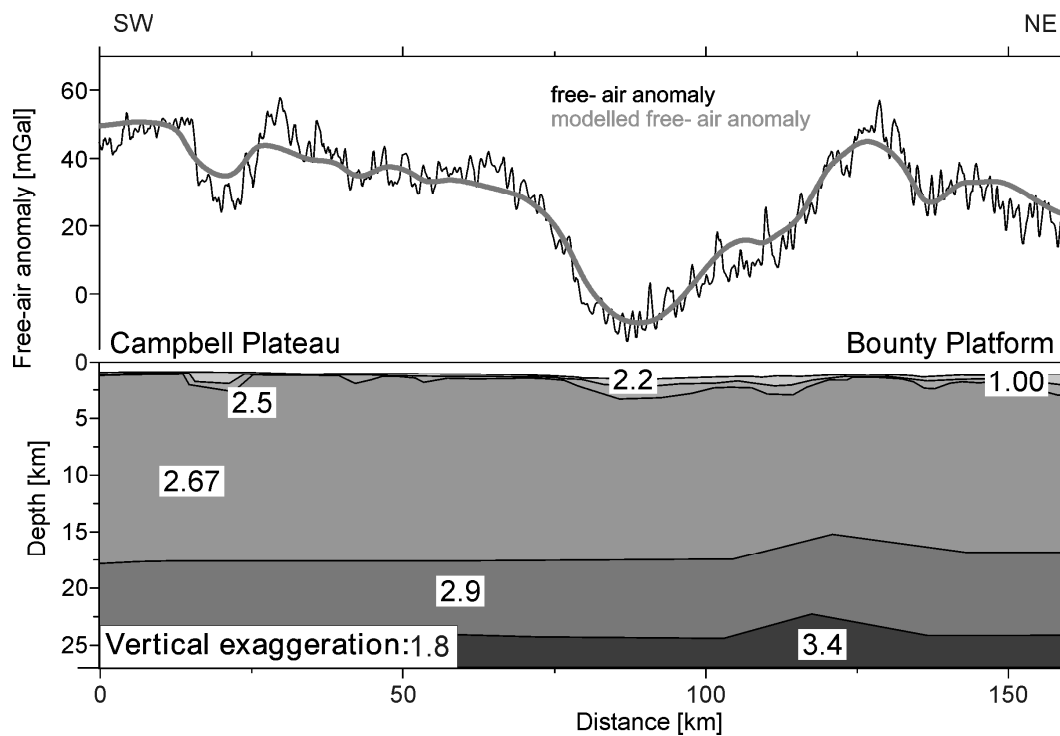


**Figure 9-6: Gravity model across the transition from Campbell Plateau to Bounty Platform:** Minimum structure gravity model, with bodies striking orthogonal to the plane of the section and extending uniformly from each end of the section. Gravity anomalies were obtained from a shipboard gravimeter. Black numbers are densities in  $\text{g/cm}^3$ .

Given some of its restrictions, our type of plate-fitting reconstruction should be most successful as a refinement to an existing conventional plate-kinematic reconstruction. The number of independent plates, the form and size of the masks and the dimensions and spacing of the grid itself can influence the result. We treated Campbell Plateau and Bounty Platform as a single plate, despite the presence of an intervening bathymetric depression of ca. 500 m depth. Gravity modeling (Figure 9-6) shows clearly that little extension has occurred across this depression, and suggests instead a shear zone origin. In support of this view, the Campbell Plateau and Bounty Platform fit the shelf break of Marie Byrd Land very well in their present form [Larter, *et al.*, 2002]. Existing reconstructions of the Zealandia – Antarctic sector of Gondwana did not suggest any great extension of the plateaus themselves (Campbell Plateau, Chatham Rise or Lord Howe Rise) during final break-up [Eagles, *et al.*, 2004; Larter, *et al.*, 2002], so we did not take into account the possibility of extension of the plateaus during the separation of Chatham Rise and Campbell Plateau from Marie Byrd Land between 95 and 85 Ma.

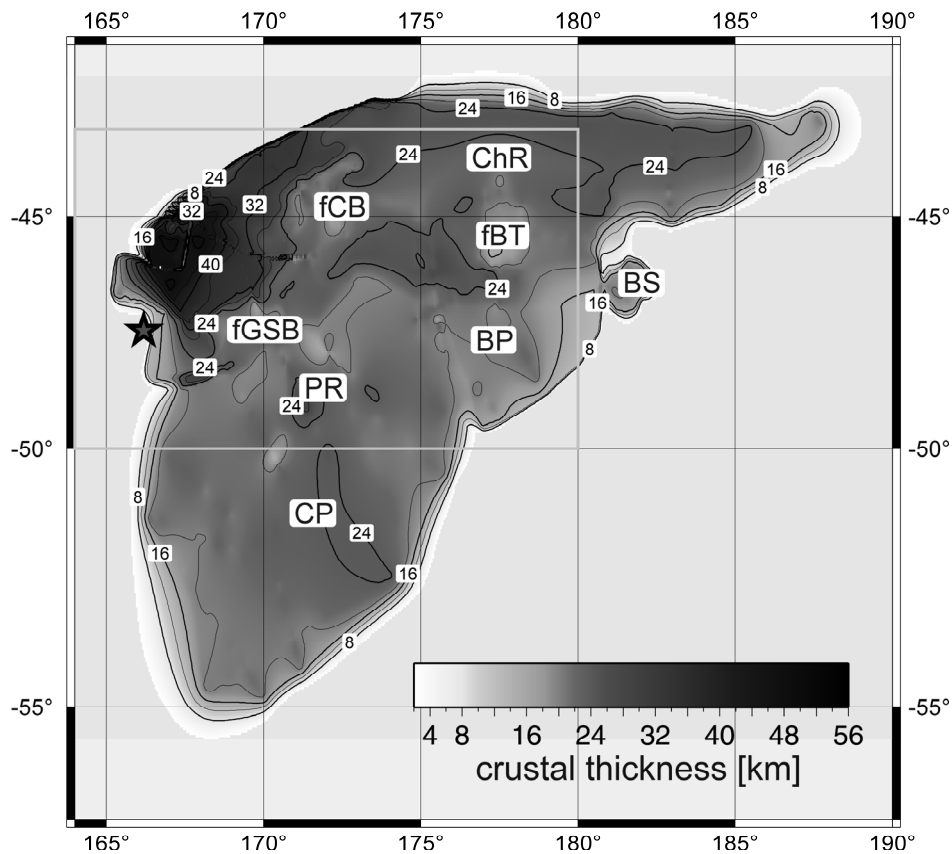


**Figure 9-7: Result of the finite rotation for Campbell Plateau:** This crustal thickness map shows the result of the finite rotation. The light grey box indicates the region in which the standard deviations were calculated; the red star marks the rotation pole. Contour interval is 4 km. Abbreviations are: BP – Bounty Platform, BS – Bollons Seamounts, CP – Campbell Plateau, ChR – Chatham Rise, fGSB – former Great South Basin, fBT – former Bounty Trough, fCB – former Canterbury Basin.

The accuracy of the best-fit reconstruction result responds to two major influences. The first of these is the crustal thickness grid, which influences the calculated standard deviation. The crustal thickness grid southeast of New Zealand depicts all tectonic units that can be seen in the bathymetry or are known by previous surveys, northwest of the New Zealand the grid has a distinctly lower resolution due to being less surveyed, and yet covers far more tectonic complexity. Small-scale variability in the grid should not affect the standard deviation in unperturbed crustal thickness, as this is calculated in a large window. The second influence is that of the window itself (Figures 9-5a, 9-7 and 9-8). On one hand, the window should cover a region that is as large as possible; but on the other hand it is limited to areas affected by the rotation being tested. As long as this window comprises the main tectonic features affected by the extension, the values of the standard deviation seem to be robust and the position of the rotation pole producing its minimum did not vary by more than ca. 2 – 3 degrees. The standard deviation rises by 3 percent within an area of 3 – 4 degrees in longitude and 3 – 5 degrees in latitude (Figure 9-9). Finally, this type of best-fit plate reconstruction cannot provide any age control. For this reason, it is useful to complement the results of such a reconstruction with the results of reconstructions that constrain ages.

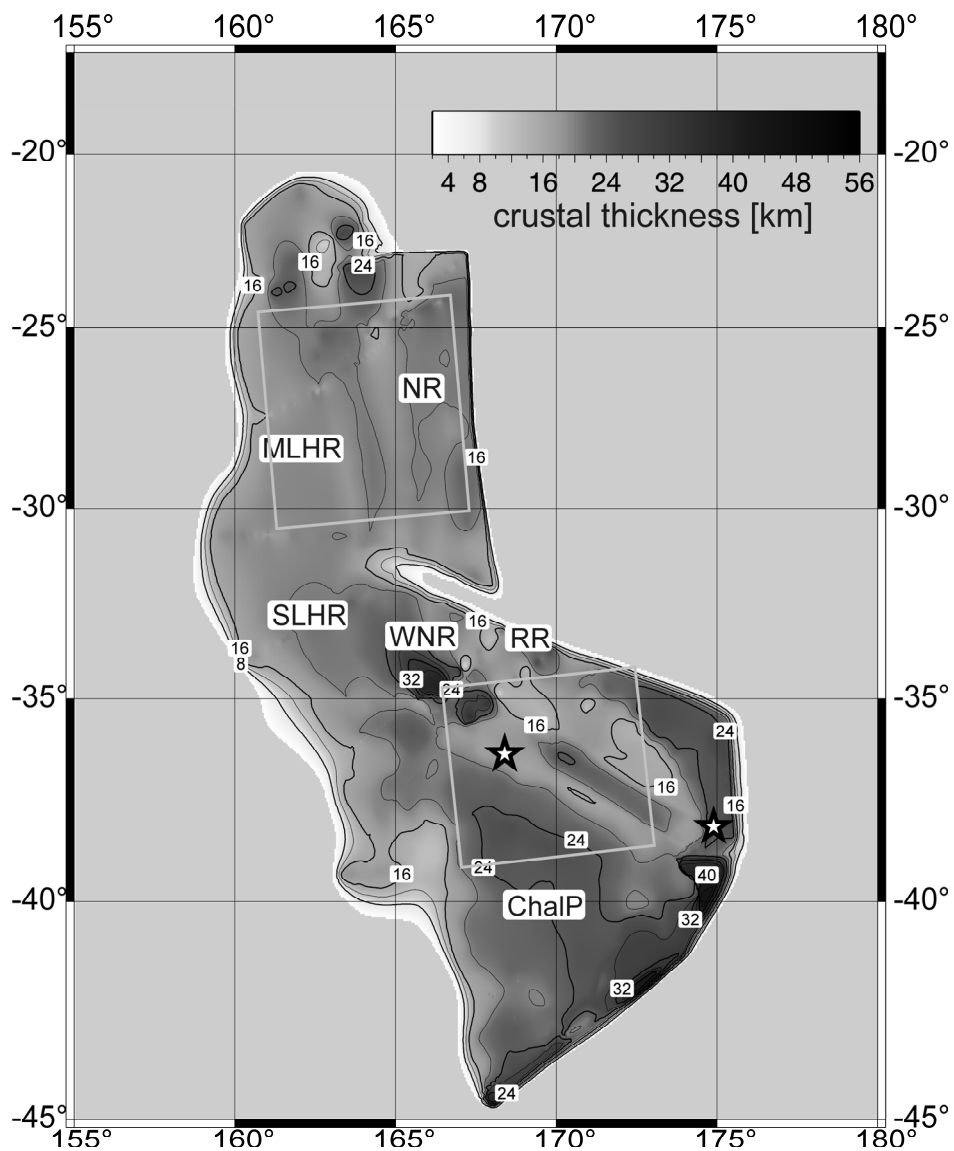


**Figure 9-8: Result of the finite rotation for Lord Howe Rise, Norfolk Ridge and Reinga Ridge:** This crustal thickness map shows the result of the finite rotation with the final rotation poles. The light grey boxes indicate the regions in which the standard deviations were calculated, the red stars mark the rotation poles. Contour interval is 4 km. Abbreviations are: ChalP – Challenger Plateau, SLHR – Southern Lord Howe Rise, MLHR – Middle Lord Howe Rise, NLHR – Northern Lord Howe Rise, NR – Norfolk Ridge, WNR – West Norfolk Ridge, RR – Reinga Ridge

## 9.7 Application to Zealandia

We varied the position of the rotation pole systematically in intervals of  $5^\circ$  in longitude and/or latitude, grazing all nodes between  $80^\circ\text{N}$  and  $80^\circ\text{S}$ , and the rotation angle in steps of  $2.5^\circ$  in order to find the rotations that yield the lowest standard deviations within a certain window (Figures 9-7, 9-8). In a second and third iteration, the search region was divided more finely into cells of  $1^\circ$  and  $0.1^\circ$  in longitude and latitude and  $1^\circ$  and  $0.05^\circ$  (for the Campbell Plateau) or  $0.1^\circ$  (for Norfolk and Reinga ridges) in rotation angle. The lowest standard deviation for the Campbell Plateau reconstruction reached 6.1588 km (compared to 6.5745 km before the rotation), for the Norfolk Ridge the lowest standard deviation was 0.9963 km (3.1462 km before rotation) and for the Reinga Ridge it was 3.4336 km (4.1301 km before rotation; Figure 9-9).

The right-handed rotation of the Campbell Plateau about a pole at  $166^\circ\text{E}$ ,  $47.5^\circ\text{S}$  and an angle of  $6.25^\circ$  leads to a minimum standard deviation in the window (Figure 9-7). The rotation pole lies at the margin of Campbell Plateau, near the Solander Trough. As the pole is close to the rotated plate, relative motion in the plate boundary region has a small translational and a large rotational part. Sample trajectories of points near the edges of the Campbell Plateau and Bounty Platform (Figure 9-11) indicate that points at the Campbell Plateau margins covered a distance of 57 km in the Great South Basin area, 87 km near the Inner Bounty Trough, 100 km near the Middle Bounty Trough and 112 km near the Outer Bounty Trough.

The crustal thickness of Campbell Plateau prior to the rotation was about 20 – 24 km. As Campbell Plateau was rotated and changes of the crustal thickness should only occur at the margins, the plateau is supposed to have the same thickness after the rotation. A small area south of Stewart Island, however, is 24 km thick and suggests a slight overlap (Figure 9-7). In the regions of the former Bounty Trough, the rotation implies that crustal thickness changed from 17 – 24 km before extension to 10 – 18 km afterwards. A similar change in crustal thickness can be observed for the Great South Basin and the Challenger Plateau, where the reconstructed thickness is in general 20 – 22 km compared to ca. 16 km prior to the reconstruction. Small areas in both basins have a thickness of only 18 km and a few patches reach 24 km. In general, the crustal thickness in southeastern Zealandia is well balanced within the range 18 – 24 km. Bollons Seamounts does not fit well to the Bounty Platform, whose margin is only known from sparse data coverage. With its narrow COTZ, the rotation poles for relative motions of Bollons Seamount are well constrained by conventional plate tectonic reconstructions [*Eagles, et al., 2004*].

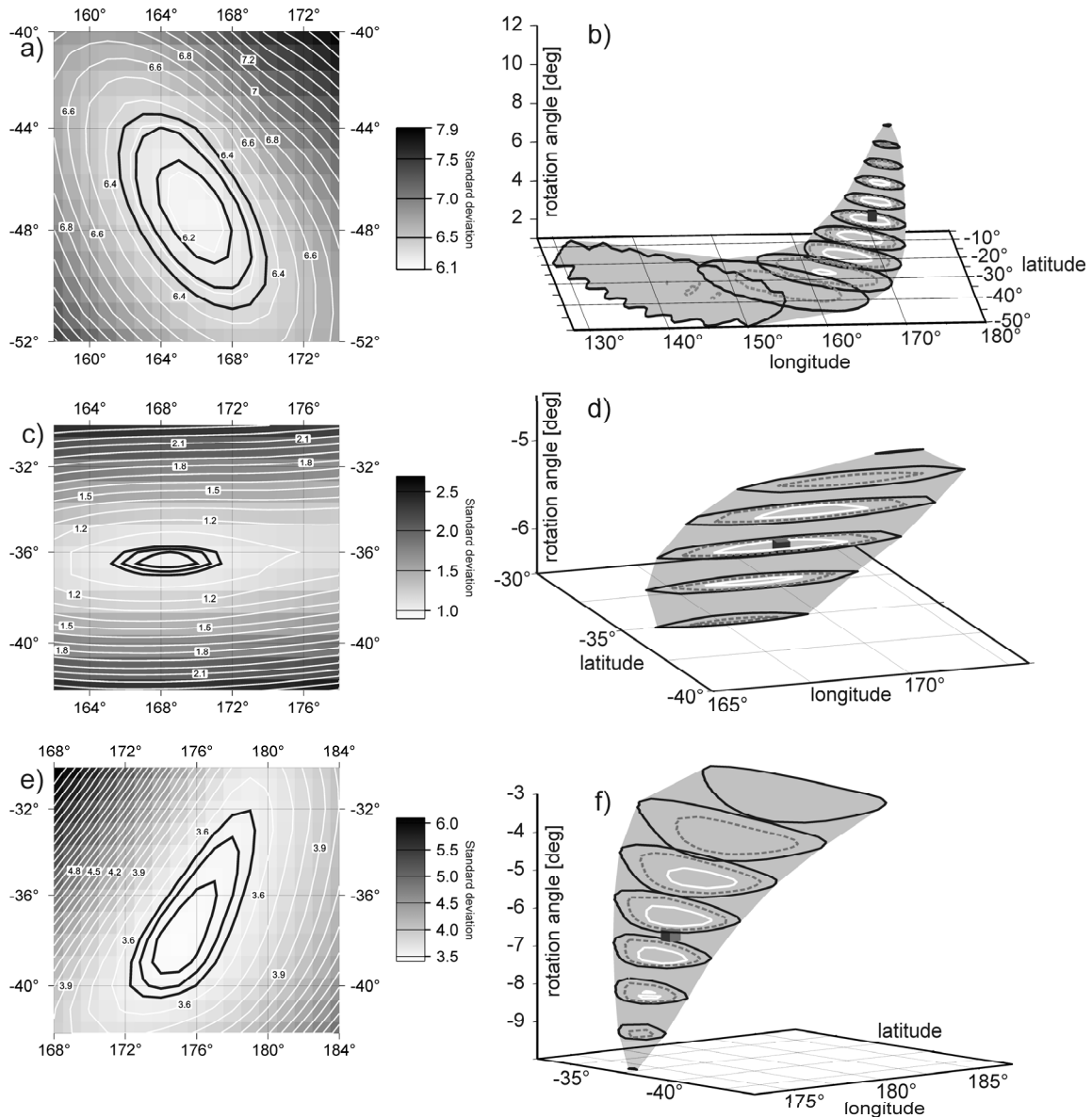


**Figure 9-9: Plots of standard deviation and 3 percent error regions.** a) Left: Standard deviations of crustal thickness for the Campbell Plateau rotation. The pole was varied in 1° steps in latitude and longitude; the rotation angle was 6.25°. Contour interval is 0.1. Right: Three percent error region. The grey hull and the black rings enclose all rotation poles that differ less than 3% in standard deviation from the best-fit pole, grey dashed rings enclose the 2% region, and white rings the 1% region. Mauve cube marks the best-fit pole. b) Same as a) but for the Norfolk Ridge rotation. Rotation angle is 5.5° c) Same as a) but for the Reinga Ridge. Rotation angle is 6.4°.

The rotation of the Norfolk Ridge closes the New Caledonia Basin entirely and leads to a uniform reconstructed crustal thickness with little variation. The Norfolk Ridge and the Middle Lord Howe Rise between 25°S and 31°S keep their thicknesses of 18 – 20 km, which are the same as that of the closed New Caledonia Basin. The result for the southern New Caledonia Basin and the Challenger Plateau is less convincing. The southern New Caledonia Basin can be closed to a large extent, but not entirely, although the minimum thickness increased from a minimum of 11 km before reconstruction to at least ca. 14 – 15 km with a mean thickness of ca. 20 km afterwards.

The rotation of the West Norfolk Ridge has resulted in one small region's thickness increasing to 36 km from 26 km, showing that this solution is not the optimum for this area. The results might be further improved if the West Norfolk Ridge were to be considered as part of an independently rotating plate. As the data coverage is too sparse, however, it was impossible to divide the grid into smaller regions that would allow such an analysis for the West Norfolk and Reinga ridges.

## 9.8 Discussion

The motion of the Campbell Plateau presented in this paper has a larger rotational and a smaller translational component compared to the reconstruction presented by Larter et al. [2002], because our rotation pole lies at the margin of the Campbell Plateau, while previous poles were located within Australia (Tab. 2). The distances (80 – 110 km) covered by points at the Campbell Plateau margin are only one third (Bounty Trough) of the distances (300 – 330 km) proposed by Larter et al. [2002] or suggested by Kamp [1986] (Figure 9-10). In both cases, the assumption was made that Bounty Trough and the Great South Basin were underlain by oceanic crust and had a narrow continent-ocean transition zone. Larter et al. [2002] interpreted the COTZs of Campbell Plateau and Chatham Rise as sharply defined in Sandwell and Smith's [1997] satellite-derived free-air gravity data.

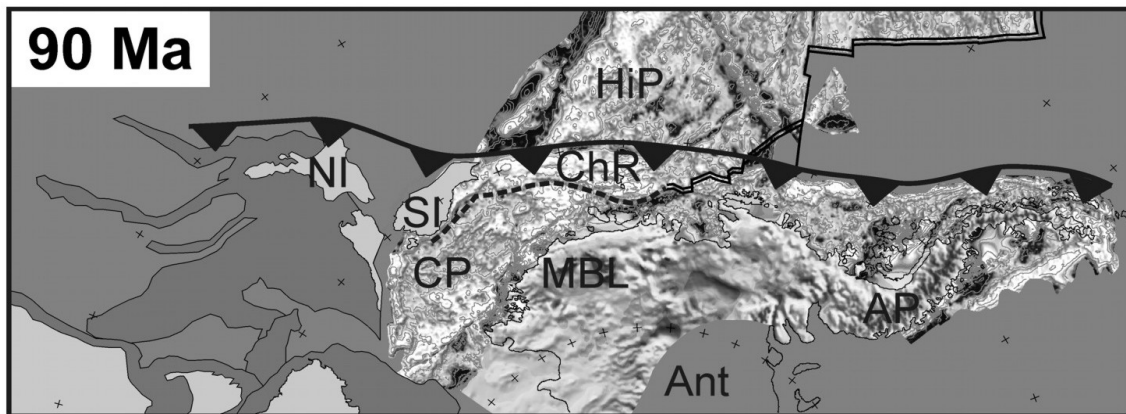


**Figure 9-10: Plate tectonic setting of the southwest Pacific prior to break-up.** Reconstruction of the plate-tectonic setting of the southwest Pacific prior to the break-up in the late Cretaceous, after Eagles et al. [2004]. Campbell Plateau and Chatham Rise are still parts of the same submarine plateau prior to 90 Ma. The black line marks the fossil subduction zone of the Phoenix Plate beneath the Chatham Rise; double lines indicate active extension or seafloor spreading. Dashed black line is the future Bounty Trough axis. The reconstruction includes offshore free-air gravity anomaly data [McAdoo and Laxon, 1997; Sandwell and Smith, 1997] and data from the BEDMAP compilation for onshore Antarctica [Lythe, et al., 2000]. Blue and green colours indicate negative free-air gravity values; orange, red and white colours indicate positive free-air gravity anomalies. Areas not included in the modelling process, or subducted areas, are shaded in solid grey. Abbreviations are: Ant – future Antarctic plate, AP – Antarctic Peninsula, BT – Bounty Trough, CP – Campbell Plateau, ChR – Chatham Rise, HiP – Hikurangi Plateau, MBL – Marie Byrd Land, NI – North Island of New Zealand, SI – South Island of New Zealand.

Larter et al. [2002] presented two solutions for the best fit of Chatham Rise to Marie Byrd Land. The rotation pole in their first, rejected, model differs only by a few degrees in latitude and longitude to our pole, but has a larger rotation angle (11.3° instead of 6.25°). Larter et al.'s [2002] preferred pole differs by tens of degrees in latitude and longitude. It is possible that our rotation angle is slightly too large because it neglects intrusions in the Bounty Trough, while the angle of Larter et al. [2002] is

likely to be too large due to their assumption of narrow COBs off Marie Byrd Land and Chatham Rise.

Area	Lon	Lat	Angle
Campbell Plateau (this work) w/ respect to Chatham Rise	166.0	-47.5	6.25
Campbell Plateau preferred pole [Larter, <i>et al.</i> , 2002] w/ respect to Chatham Rise	129.68	-42.79	5.31
Campbell Plateau rejected pole [Larter, <i>et al.</i> , 2002] w/ respect to Chatham Rise	167.32	-53.23	11.31
Bollons Seamount w/ respect to Chatham Rise	152.96	-50.48	10.74
Reinga Ridge w/ respect to Lord Howe Rise (this work)	174.9	-38.2	6.4
Norfolk Ridge w/ respect to Lord Howe Rise (This work)	168.4	-36.4	5.5
Norfolk Ridge w/respect to Reinga Ridge	33.02	39.18	-1.06

**Table 9-2: Rotation poles.** The finite rotation poles of this work are calculated with the standard deviation of the crustal thickness after the reconstruction. Positive angles indicate anticlockwise rotations when viewed from above the surface of the Earth and going back in time.

Our plate-kinematic reconstruction has many implications for geophysical observations in Zealandia itself. It has been suggested that the two major magnetic anomaly systems of southeast Zealandia, the Stokes Magnetic Anomaly System (SMAS) and the Campbell Magnetic Anomaly System (CMAS) are parts of an originally continuous system offset by ca. 300 km of dextral shear [Davey and Christoffel, 1978; Kamp, 1986; Sutherland, 1999], that has been related to the opening of the Bounty Trough. Sutherland [1999] suggested instead that the dextral offset may have occurred prior to 90 Ma, possibly in Permian times. It is possible, however, that the sources of SMAS and CMAS are not identical, because the styles of the magnetic anomalies differ and the CMAS could be related to underplating beneath the Campbell Plateau [Grobys, *et al.*, submitted]. Our reconstruction limits the dextral offset of the CMAS relative to SMAS to just a few kilometers in the time between 90 Ma and 83 Ma. This observation rules out the idea that CMAS and SMAS were a single connected magnetic anomaly system at the time of the onset of Bounty Trough opening. With these data, we cannot conclude whether or not both anomaly systems had a common origin and displacement from one another that occurred at much earlier times.

In the Middle Bounty Trough, synthetic flowlines describing our rotation strike sub-perpendicular to the gravity anomalies seen there (Figure 9-10). Our reconstruction explains the gravity patterns in the Middle Bounty Trough representing extensional structures [Grobys, *et al.*, 2007] caused by incipient seafloor spreading. They interpreted the Middle Bounty Trough as the locus of incipient seafloor spreading, while the Outer Bounty Trough was underlain by oceanic crust [Davy, 1993] and the Inner Bounty Trough was not enough extended to produce oceanic crust. Our reconstruction postulates a rotational motion of the Campbell Plateau that is consistent with this progression. This motion leads to an extension of ca. 87 km in the Inner Bounty Trough, ca. 100 – 110 km in the Middle Bounty Trough and ca. 115 – 125 km in the Outer Bounty Trough. With the crustal properties of the crust in the Campbell Plateau-Chatham Rise area, the amount of extension necessary to start seafloor spreading can be determined as ca. 110 km, and the  $\beta$ -factor as ca. 2.7 [Grobys, *et al.*, 2007].

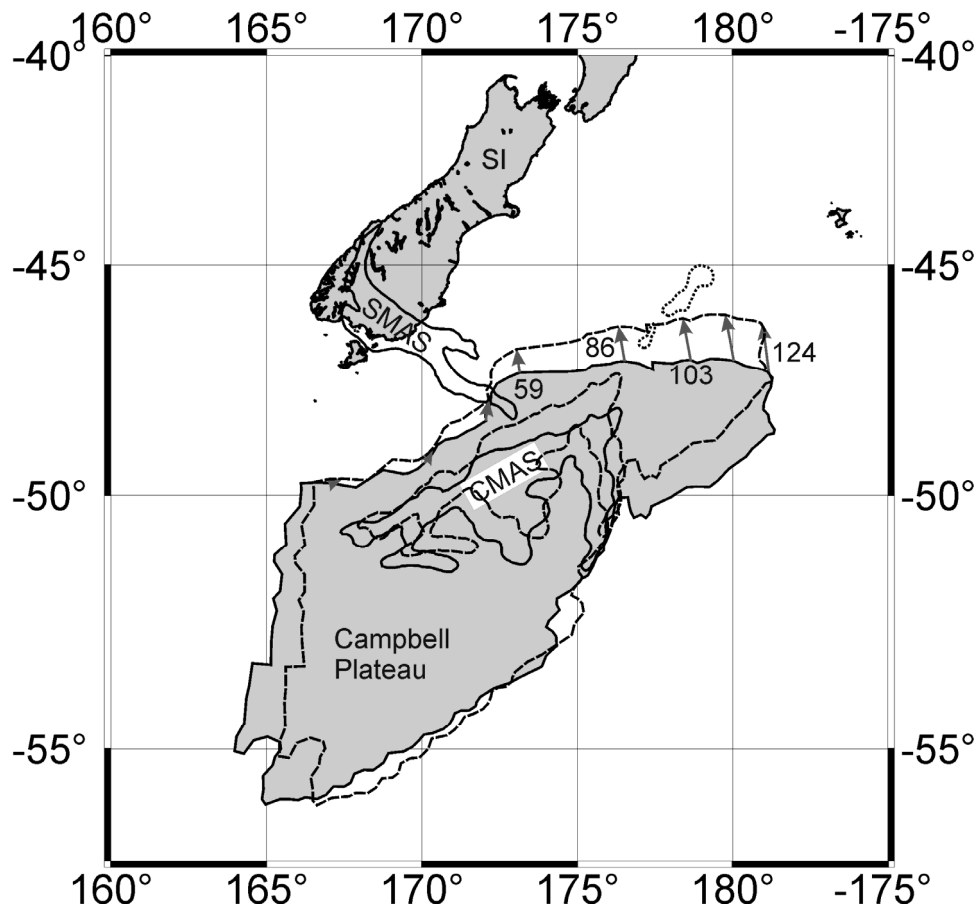


**Figure 9-11: Main magnetic anomaly systems of the Campbell Plateau before and after the rotation.** Bold black lines outline the Campbell Plateau and Campbell Magnetic Anomaly System (CMAS) in its present position; dashed lines outline both after the rotation. Dotted lines are magnetic anomalies of the Bounty Trough interpreted as extensional features. Bold black line at the South Island of New Zealand (SI) is the Stokes Magnetic Anomaly System (SMAS).

We calculated extension of 85 – 121 km in the segment of the New Caledonia Basin between 29°S and 25° S, increasing northwards, and a maximum extension of ca. 105 km for the rotation of the Reinga Ridge decreasing to almost 0 km near the coastline of the North Island. Extension rates in the middle New Caledonia Basin were higher than those that formed oceanic crust in the Bounty Trough, and in view of the fact that the initial crustal thickness is ca. 4 km lower, oceanic crust ought to have appeared earlier in the New Caledonia Basin, presumably after about 80 - 85 km of extension. This means that at 29° S, (present-day coordinates) seafloor spreading could have started and, at 25° S, ca. 35 km of oceanic crust could have formed. Lafoy [2005b] postulated ca. 120 km of oceanic crust beneath the New Caledonia Basin at 24° - 25° S, which is equal to the total amount of extension we calculate for the central New Caledonia Basin. It is possible that the crust interpreted as oceanic crust is highly thinned and intruded continental crust similar to the crust of the Inner Bounty Trough and only parts of this consist of oceanic crust.

The calculated rotation between the Norfolk and Reinga ridges shows extension backwards in time as the Norfolk Ridge is rotated away from the Reinga Ridge. In our reconstruction we separated the two microplates along the Vening Meinesz Fracture Zone [Herzer and Masche, 1996], but we considered Lord Howe Rise as a single block. It has been shown that the Lord Howe Rise consists of at least two blocks and must be treated separately from the Challenger Plateau [Gaina, *et al.*, 1998a]. To do this, Lafoy *et al.* [2005a] continued the Vening Meinesz Fracture Zone into Lord Howe Rise. These observations imply that the underlap between Reinga Ridge and Norfolk Ridge could be reduced if a segmentation of the Lord Howe Rise was introduced into our reconstruction. Another further reduction of the underlap could be yield by a separation of the Reinga Ridge microplate into West Norfolk Ridge and Reinga Ridge microplates, as our reconstruction shows an overlap of the West Norfolk Ridge and the northern tip of the Challenger Plateau.

## 9.9 Conclusions

With this work, we presented the first crustal thickness map of Zealandia based on seismic and gravity data. This map shows well the main features of the microcontinent and outlines the region's basins and plateaus. It indicates a rather uniform crustal thickness of the plateaus of ca. 20 – 24 km and of 10 – 14 km in the basins. We developed a crustal thickness balancing method to constrain finite rotations for describing the extension of continental crust. In regions of two or more neighboring plates the crust was divided in overlapping parts. The plates were rotated, crustal thickness was added up and the standard deviation of the new crustal thickness grid was calculated within a significant window. We defined the best-fit reconstruction as the one with a minimum standard deviation. Reconstructions on the basis of crustal thickness balancing are a powerful tool to produce paleotectonic maps in areas of crustal thinning where magnetic spreading anomalies are absent. The derivation of the rotation parameters is confined by the accuracy of the crustal thickness map and the assumption that the crustal thickness in this region was uniform before the break-up.

In Zealandia, the motion of the Campbell Plateau opens the Bounty Trough, the Canterbury Basin and the Great South Basin simultaneously. The gravity anomalies in the Middle Bounty Trough are confirmed as the expressions of an echelon extensional features formed at the locus of nascent seafloor spreading. The rotational motion of the Campbell Plateau also rules out the possibility that the Stokes Magnetic Anomaly System and the Campbell Magnetic Anomaly System were a single anomaly system until the separation of Zealandia and Antarctica at 90 – 83 Ma. It rather confirms the hypothesis that an earlier event, maybe in Permian times, offset the two anomaly systems or that the anomaly systems have different origins.

Our reconstruction of the New Caledonia Basin region shows an extension of 120 km at most. A comparison with the Bounty Trough extension suggests that a maximum of 35 km, if any, of oceanic crust could have been built in the New Caledonia Basin. It seems possible that the New Caledonia Basin is underlain by highly extended and intruded continental crust similar to that beneath the Bounty Trough. The reconstruction of the southernmost New Caledonia Basin supported the necessity of a Lord Howe Rise that consists of several independently-rotated pieces. Treating the West Norfolk Ridge as a single microplate is necessary to reduce the misfit of plate reconstructions in the southernmost New Caledonia Basin. However, this needs to be verified by a significant improvement in crustal thickness measurements.

## Acknowledgements

We are grateful to the captain and crew of RV *Sonne* during cruise SO-169 for their support and assistance. This project is primarily funded by the German Federal Ministry of Education and Research (BMBF) under contract no. 03G0169A as well as through contributions from AWI and GNS. The German Academic Exchange Service (DAAD) funded a visit of J.G. to GNS for two months. Bryan Davy contributed gravity models and good ideas. We thank him, Rob Larter, Claus-Dieter Hillenbrand and Tara

Deen for fruitful discussions. Most of the figures were generated with Generic Mapping Tools [*Wessel and Smith, 1998*].

# 10 Conclusions and Outlook

## 10.1 Conclusions

In my thesis I investigated the break-up process between Zealandia and Antarctica by means of seismic refraction and gravity modeling, multichannel seismic interpretation and application of a novel method for plate tectonic reconstructions of thinned continental crust. I have shown that the basins and troughs in the region of Campbell Plateau consist of thinned continental crust intruded and underplated by mafic material. The plate-kinematic reconstruction has suggested that the offset of Campbell Plateau relative to Chatham Rise is only one third of the value assumed previously. This finding also influences reconstructions of Zealandia relative to Antarctica. The facts that two different reconstructions are presented in Larter et al. [2002] and their rejected rotation parameters agree well with the new ones presented in this work confirm on the one hand my results and shown on the other hand that reconstructions of this region are still under debate.

Until now, the widespread occurrence of magmatism at the Campbell Plateau and its small crustal thickness raised the question of its crustal composition. Also, it has remained unclear whether the Bounty Trough and the Great South Basin are underlain by oceanic or thinned continental crust (Question 1). The deep crustal seismic refraction profiles acquired across Bounty Trough, Great South Basin and central Campbell Plateau indicated that the Moho lies at depths between 11 – 17 km beneath the basins and troughs and at depths between 23 – 28 km underneath Chatham Rise, Bounty Platform, and central Campbell Plateau. The distribution of the P-wave velocity in all areas mentioned above indicates a felsic composition with local mafic influence. In the lower crust beneath Bounty Trough and central Campbell Plateau, a significant increase in velocities implies mafic intrusions into thinned continental crust and underplating. Assuming that the plateaux had their present crustal thickness prior to the extension in the Bounty Trough and the Great South Basin, I calculated stretching factors of ca. 2 for the Great South Basin and ca. 2.7 for the Bounty Trough. These observations, described in Chapters 7 and 8, indicate that most parts of the region are composed of thinned continental crust which is intruded and underplated with mafic material. Although the crustal composition could not be revealed for the entire Campbell Plateau, it seems reasonable to assume a similar lateral extent.

Sediment layers in the Bounty Trough suggest at least one compressional and two extensional phases. The sediments are divided into a lower, seismically opaque layer with a rugged top and stratified layers above. This observation indicates that a first extensional phase occurred in a proto-Bounty Trough whose opening was caused by the subduction of the Phoenix Plate beneath the Chatham Rise. The opacity of the lower sediments and their rugged top strongly imply that they underwent compressional deformation prior to the last known extension in the Late Cretaceous, when Zealandia separated from Gondwana. The event that could have caused compression in the Bounty Trough was most likely the collision of the Hikurangi Plateau with the Chatham Rise (Question 2).

## CONCLUSIONS AND OUTLOOK

The Great South Basin does not show this interplay of compression and extension that occurred in the Bounty Trough, which complies well with the idea that a first deposition of sediments in a proto-Bounty Trough was caused by back-arc extension related to the Phoenix Plate subduction. However, the extensional processes in Late Cretaceous time were the same, except for the degree of extension. The most striking observations in the Great South Basin are two magnetic anomaly systems. The SMAS can be traced from the North Island to the South Island and continues into the Great South Basin where it terminates. The CMAS strikes in a southwestern – northeastern direction along the Campbell Plateau. The fact that the anomaly systems differ in style and wavelength and correlate with different lower crustal properties suggest that the anomaly systems are not parts of the same anomaly systems that were separated during the late Gondwana break-up as was previously thought. It is more probable that they have different origins. Alternatively, the CMAS was overprinted by ongoing magmatic activity in Cenozoic times but the anomaly systems had a common origin (Questions 3). An answer to the question of the difference between the opening of the Bounty Trough and the break-up between Zealandia and Marie Byrd Land could not be given, as there were too few data from Marie Byrd Land.

The interpretation that CMAS and SMAS have a different history is also confirmed by the plate-tectonic reconstruction presented in Chapter 12. Zealandia has been problematic for plate-kinematic reconstructions. It was uncertain whether Bounty Trough and Great South Basin are underlain by thinned continental or oceanic crust. For some reconstructions of the opening of the southwest Pacific, it was assumed from satellite gravity data that Bounty Trough and Great South Basin were underlain by oceanic crust. In this case, a classical plate-kinematic reconstruction would have produced a good result. But as has been shown in this thesis, the basins of Zealandia are mainly underlain by thinned continental crust, so that standard reconstruction methods must have failed. Previous reconstructions used the fit of shelf breaks of the conjugate margins as a control on the quality of the reconstruction, or rotation poles were calculated with trajectories conserved by fracture zones and spreading anomalies. In this case, there are neither shelf breaks within the microcontinent or, since extension stopped when seafloor spreading started, fracture zones and magnetic seafloor anomalies.

In order to solve this problem, I developed a novel method to be applied to plate-kinematic reconstructions. I used crustal balancing for the reconstruction of Zealandia. Crustal blocks of the microcontinent separated by thinned continental crust were not divided by first order discontinuities but the plate boundary was modeled as two (or more) overlapping plates similar to the simple-shear crustal extension model, so that the crust within the basins was assigned to both plates in varying parts. As a best-fit criterion I assumed that the crust in this region had a uniform thickness prior to the separation of Zealandia from Gondwana (Question 4).

The reconstruction of the late Gondwana break-up in this region confirmed what has been suggested in chapters 7 and 8. The new reconstruction of the Bounty Trough and Great South Basin opening showed that the two processes happened simultaneously. The thinning of the continental crust in both regions can be modelled by a single rotation of Campbell Plateau relative to Chatham Rise/South Island, or

alternatively a single rotation of Chatham Rise/South Island relative to Antarctica. The pole of this rotation lies at the western edge of Campbell Plateau. Therefore, the relative motion of Campbell Plateau relative to Chatham Rise opened Bounty Trough further than the Great South Basin. Crustal extension becomes less relevant approaching the rotation pole.

This result clearly shows that the motion between CMAS and SMAS is a third of the previously assumed motion at most, confirming the different origin of these anomaly systems. It also explains the different stretching factors in Great South Basin and Bounty Trough with a simple model. Such a plate-kinematic reconstruction has also been calculated for the northwestern parts of Zealandia. As I had less data on the crustal thickness of this area than for the Campbell Plateau region, the results are not as significant as the results for southeastern Zealandia. However, the reconstruction also shows that extension in the New Caledonia Basin was less than previously suggested. Previous investigations estimated the amount of oceanic crust built in the New Caledonia Basin at ca. 120 km, while in this thesis the amount is estimated to be a maximum of 30 km (Questions 2 and 4).

Many of the questions of Chapter 1 are answered. Not really surprisingly, most of the questions asked are related tightly to one another, but, surprisingly, they are related even more closely than previously thought. The question of a common origin of the magnetic anomaly systems (Question 3) is consistently answered by the plate-kinematic reconstruction (Question 4) and the investigations designed to answer the question of the crustal composition of the Campbell Plateau (Question 1). Unfortunately, this very important question could not be fully answered by this thesis. However, I showed that the central Campbell Plateau consists of thinned and underplated continental crust.

The most important result of this thesis, however, has global importance (Questions 4). The reconstruction technique introduced in Chapter 12 was invented because the plateaux of Zealandia consist of thinned continental crust. With its large submarine plateaux, Zealandia may be a type location of extended continental crust, and may therefore be a good region to test this innovative reconstruction technique. But most oceans begin their life cycle as a rift system in continental crust. At this stage, seafloor spreading with magnetic anomalies cannot be observed. Thus, plate-kinematic reconstructions have to employ the fit of shelf-breaks as a best-fit criterion and neglect the extension that preceded seafloor-spreading. As a consequence, the size of reconstructed continents and the amount of extension will be over-estimated in most reconstructions. The application of my new reconstruction technique will lead to new rotation poles and better fits of reconstructions in regions affected by crustal extension globally.

## 10.2 Outlook

This work provides innovations in reconstruction techniques for plate tectonic reconstructions which can be applied in all regions affected by crustal extension. As this method does not base on the interpretation of a sharp continent-ocean-boundary but

## CONCLUSIONS AND OUTLOOK

exclusively on crustal thickness information it will lead to improved fits of reconstructions and better rotation poles worldwide. Standard reconstruction techniques based on fracture zone traces, magnetic anomalies and COBs work reliably back to the time where the first magnetic anomaly is found. This new method allows to refine the reconstruction from the time before the occurrence of the first magnetic seafloor anomaly back to the beginning of the first crustal extension. As has been shown in Chapter 12, the amount of extension before the first seafloor spreading is significant but has to be neglected in classic reconstructions. My new technique offers improvement of reconstructions especially in regions with highly extended crust, e.g. in the early stages of the North Atlantic opening and the East African Rift System.

Secondly, the reconstruction of Zealandia leaves open questions for the reconstruction of the opening of the Southwest Pacific. The choice between two reconstructions presented in Larter et al. [2002] has been made on the basis of the amount of extension in the Great South Basin and Bounty Trough. The results presented here would lead to the preference of the model rejected by Larter et al. [2002], but raise new questions such as asymmetry of the seafloor spreading in the Bellingshausen Sea. Together with results from the Polarstern Cruise ANT XXIII/4 where new surprising results, such as abnormally thick crust at the shelf of the Amundsen Sea Embayment, have been found, a reinterpretation of the break-up processes between Marie Byrd Land and Zealandia, especially of the processes of crustal extension, have to be made in the future.

## 11 References

- Adams, C. J., et al. (2005), Nd and Sr isotopic signatures of metasedimentary rocks around the South Pacific margin and implications for their provenance, in *Terrane Processes at the margin of Gondwana*, edited by A. P. M. Vaughan and R. J. Pankhurst, pp. 113 -141, Geological Society of London, London.
- Adams, C. J., and P. Robinson (1977), Potassium-argon age of schists from Chatham Island, New Zealand Plateau, Southwest Pacific, *N.Z. Journal of Geology and Geophysics*, 20, 287-302.
- Aki, K., and P. G. Richards (1980), *Quantitative seismology: Theory and Methods*, W.H. Freeman & Company.
- Allen, P. A., and J. R. Allen (1990), *Basin Analysis, Principles & Applications*, Reprinted 1992 ed., 53 - 91 pp., Blackwell Scientific Publications, Oxford.
- Artemieva, I. M., and W. D. Mooney (2002), On the relationship between cratonic lithosphere thickness, plate motions, and basal drag, *Tectonophysics*, 358, 187 - 207.
- Auzende, J.-M., et al. (2000), Deep See diapirs and bottom simulating reflector in Fairway Basin (SW Pacific), *Marine Geophysical Researches*, 21, 579-587.
- Barley, M. E., et al. (1988), Strontium isotope composition and geochronology of intermediate-silicic volcanics, Mt Somers and Banks peninsula, New Zealand, *N.Z. Journal of Geology and Geophysics*, 31, 197-206.
- Bassin, C., et al. (2000), The current Limits of Resolution for Surface Wave Tomography in North America, *EOS*, 81, F897.
- Beanland, S., and J. Haines (1998), The Kinematics of Active Deformation in the North Island, New Zealand, determined from geological strain rates, *N.Z. Journal of Geology and Geophysics*, 41, 311-323.
- Beggs, J. M. (1993), Depositional and Tectonic History of the Great South Basin, in *South Pacific Sedimentary Basins*, edited by P. F. Ballance, pp. 365-373, Elsevier Science Publishers B.V., Amsterdam.
- Beggs, J. M., et al. (1990), Basement Geology of the Campbell Plateau: implications for correlation of the Campbell Magnetic Anomaly System, *N.Z. Journal of Geology and Geophysics*, 33, 401-404.
- Berndt, C., et al. (2001), Controls on the tectono-magmatic evolution of a volcanic transform margin: the Vøring Transform Margin, NE Atlantic, *Marine Geophysical Researches*, 22, 133-152.
- Birch, F. (1960), The velocity of compressional waves in rocks to 10 kilobars,1, *Journal of Geophysical Research*, 65, 1083 - 1102.

## REFERENCES

- Birch, F. (1961), The velocity of compressional waves in rocks to 10 kilobars, *Journal of Geophysical Research*, *66*, 2199 - 2224.
- Bott, M. H. P. (1992), Modelling of the loading stresses associated with continental rift systems, *Tectonophysics*, *182*, 193 - 209.
- Bott, M. H. P. (1993), Modelling of plate driving mechanisms, *Journal of the Geological Society*, *149*, 941 - 951.
- Bradshaw, J. D. (1989), Cretaceous geotectonic patterns in the New Zealand region, *Tectonics*, *8*, 803 - 820.
- Bradshaw, J. D. (1991), Cretaceous dispersion of Gondwana: continental and oceanic spreading in the south-west Pacific-Antarctic sector, in *Geological Evolution of Antarctica*, edited by M. R. A. C. Thomson, J.A. and Thomson, J.W., pp. 581-585, Cambridge University Press, Cambridge.
- Bradshaw, J. D., et al. (1981), Carboniferous to Cretaceous on the Pacific margin of Gondwana: The Rangitata phase of New Zealand, in *Gondwana Five*, edited by M. M. Creswell, and P. Vella, pp. 217-212, Balkema, Rotterdam.
- Bradshaw, J. D., et al. (1997), New Zealand Superterrane Recognized in Marie Byrd Land and Thurston Island, in *The Antarctic Region: geological evolution and processes; proceedings of the VII International Symposium on Antarctic Earth Sciences*, edited by C. A. Ricci, pp. 429-436, Terra Antarctica Publ., Siena.
- Bradshaw, J. D., et al. (1996), Mid-Cretaceous oroclinal bending of New Zealand terranes, *N.Z. Journal of Geology and Geophysics*, *39*, 461-468.
- Briggs, I. C. (1974), Machine contouring using minimum curvature, *Geophysics*, *39*.
- Burke, K. (1977), Aulacogens and continental breakup, *Ann. Rev. Earth planet Sci.*, *5*, 371-396.
- Cande, S. C., and J. Stock (2004a), Cenozoic Reconstructions of the Australia-New Zealand-South Pacific Sector of Antarctica, in *The Cenozoic Southern Ocean: tectonics, sedimentation, and climate change between Australia and Antarctica*, edited by N. F. Exon, et al., pp. 5 - 18, American Geophysical Union, Washington, DC.
- Cande, S. C., and J. Stock (2004b), Pacific-Antarctic-Australia motion and the formation of the Macquarie Plate, *Geophysical Journal International*, doi:10.1111/j.1365-246X.2004.02224.x.
- Carter, L., and R. M. Carter (1987), The Bounty Channel System: a 55-million-year-old sediment conduit to the deep sea, Southwest Pacific Ocean, *Geo-Marine Letters*, *7*, 183 - 190.
- Carter, L., and R. M. Carter (1993), Sedimentary Evolution of the Bounty Trough: A Cretaceous Rift Basin, Southwestern Pacific Ocean, in *South Pacific sedimentary*

## REFERENCES

- basins*, edited by P. F. Ballance, pp. 51 - 67, Elsevier Science Publishers B.V., Amsterdam.
- Carter, R. M. (1988a), Plate boundary tectonics, global sea-level changes and the development of the eastern South Island continental margin, New Zealand, Southwest Pacific, *Marine and Petroleum Geology*, 5, 90 - 107.
- Carter, R. M. (1988b), Post breakup stratigraphy (Kaikoura Synthem: Cretaceous - Cenozoic) of the continental margin of southeastern New Zealand, *N.Z. Journal of Geology and Geophysics*, 31, 405 - 429.
- Carter, R. M., et al. (1994), Seismic Stratigraphy of the Bounty Trough, south-west Pacific Ocean, *Marine and Petroleum Geology*, 11, 79 - 93.
- Červený, V., et al. (1977), *Ray Method in seismology*, Charles University Press.
- Christensen, N. I. (1996), Poisson's ratio and crustal seismology, *Journal of Geophysical Research*, 101, 3139-3156.
- Christeson, G. L., et al. (2003), Deep crustal structure of Bransfield Strait: Initiation of a back arc basin by rift reactivation and propagation, *Journal of Geophysical Research B: Solid Earth*, 108, doi:10.1029/2003JB002468.
- Collins, C. D. N. (1991), The nature of the crust-mantle boundary under Australia from seismic evidence, in *The Australian Lithosphere*, edited by B. J. Drummond, pp. 67 - 80, Geological Society of Australia special publication.
- Conrad, C. P., and C. Lithgow-Bertelloni (2004), The temporal evolution of plate driving forces: Importance of "slab suction" versus "slab pull" during the Cenozoic, *Journal of Geophysical Research*, 109, doi:10.1029/2004JB002991.
- Cook, R. A., et al. (1999), *Cretaceous-Cenozoic geology and petroleum systems of the Great South Basin, New Zealand*, 188 pp., Institute of Geological and Nuclear Sciences Limited, Lower Hutt, New Zealand.
- Cooper, A. K. C. (2004), *New Zealand Geological Timescale 2004/2 wallchart*.
- Dauteuil, A., et al. (2001), Propagation of an oblique spreading centre: The western Gulf of Aden, *Tectonophysics*, 332, 423-442.
- Davey, F. J. (1977), Marine seismic measurements in the New Zealand Region, *N.Z. Journal of Geology and Geophysics*, 20, 719 - 777.
- Davey, F. J., and D. A. Christoffel (1978), Magnetic Anomalies across Campbell Plateau, New Zealand, *Earth and Planetary Science Letters*, 41, 14 - 20.
- Davy, B. (1993), The Bounty Trough - basement structure influences on sedimentary basin evolution, in *South Pacific sedimentary basins of the World*, edited by P. F. Ballance, pp. 69 - 92, Elsevier Science Publishers B.V., Amsterdam.

## REFERENCES

- Davy, B. (2006), Bollons Seamount and early New Zealand-Antarctic Spreading, *Geochem. Geophys. Geosyst.*, doi:10.1029/2005GC001191.
- Davy, B., and R. Wood (1994), Gravity and magnetic modelling of the Hikurangi Plateau, *Marine Geology*, *118*, 139 - 151.
- Digranes, P., et al. (1998), A regional shear-wave velocity model in the central Vøring Basin, N. Norway, using three-component Ocean Bottom Seismographs, *Tectonophysics*, *293*, 157-174, doi:10.1016/S0040-1951(98)00093-6.
- Digranes, P., et al. (1996), Modelling shear waves in OBS data from the Vøring Basin (northern Norway) by 2-D ray-tracing, *Pure and Applied Geophysics*, *148*, 611 - 629.
- DiVinere, et al. (1995), Early cretaceous paleomagnetic results from Marie Byrd Land, West Antarctica: Implications for the Wedellia collage of crustal blocks, *Journal of Geophysical Research*, *100*, 8133-8152.
- Dugda, M. T., et al. (2005), Crustal structure in Ethiopia and Kenya from receiver function analysis: Implications for rift development in eastern Africa, *Journal of Geophysical Research*, doi:10.1029/2004JB003065.
- Eagles, G., et al. (2004), High-resolution animated tectonic reconstruction of the South Pacific and West Antarctic Margin, *Geochem. Geophys. Geosyst.*, doi:10.1029/2003GC000657.
- Ebinger, C. J., and M. Casey (2001), Continental breakup in magmatic provinces: An Ethiopian example, *Geology*, *29*, 527-530.
- Farrar, E., and J. M. Dixon (1984), Overriding of the Indian-Antarctic Ridge: Origin of Emerald Basin and migration of the late Cenozoic Volcanism in southern New Zealand and Campbell Plateau, *Tectonophysics*, *104*, 243-256.
- Fitzgerald, P. (2002), Tectonics and landscape evolution of the Antarctic plate since the breakup of Gondwana, with an emphasis on the West Antarctic Rift System and the Transantarctic Mountains, *Royal Society of New Zealand Bulletin*, *35*, 453-469.
- Forster, M. A., and G. S. Lister (2003), Cretaceous metamorphic core complexes in the Otago Schist, New Zealand, *Australian Journal of Earth Sciences*, doi:10.1046/j.1440-0952.2003.00986.x.
- Foulger, G. R., and D. L. Anderson (2005), A cool model for the Iceland hotspot, *Journal of Volcanology and Geothermal Research*, *141*, 1 - 22.
- Foulger, G. R., and J. H. Natland (2003), Is "Hotspot" Volcanism a Consequence of Plate Tectonics? *Science*, *300*, 921, 922, doi:10.1126/science.1083376.
- Gaina, C., et al. (1998a), The tectonic history of the Tasman Sea: A puzzle with 13 pieces, *Journal of Geophysical Research*, *103*, 12413 - 12433.

## REFERENCES

- Gaina, C., et al. (1998b), The opening of the Tasman Sea: A gravity anomaly animation, *Earth Interactions*, 2, 1-23.
- Godfrey, N. J., et al. (2002), The effect of crustal anisotropy on reflector depth and velocity determination from wide-angle seismic data: a synthetic example based on South Island, New Zealand, *Tectonophysics*, 355, 145-161, doi:10.1016/S0040-1951(02)00138-5.
- Godfrey, N. J., et al. (2001), Crustal structure and thermal anomalies of the Dunedin Region, South Island, New Zealand, *Journal of Geophysical Research*, 106, 30835-30848.
- Gohl, K. (Ed.) (2003), Structure and dynamics of a submarine continent: Tectonic-magmatic evolution of the Campbell Plateau (New Zealand), *Report of RV "SONNE" cruise SO-169, Project CAMP 17 January to 24 February 2003*, Alfred-Wegener-Institut für Polar- und Meeresforschung, Bremerhaven, Germany.
- Gray, G. G., and I. O. Norton (1988), A palinspastic Mesozoic plate reconstruction, *Tectonophysics*, 155, 391 - 399.
- Grevemeyer, I., et al. (2001), Crustal and upper mantle seismic structure and lithospheric flexure along the Society Island hotspot chain, *Geophysical Journal International*, 147, 123 - 140.
- Grobys, J. W. G., et al. (2007), Is the Bounty Trough, off southeastern New Zealand, an aborted rift? *Journal of Geophysical Research*, doi.:10.1029/2005JB004229.
- Grobys, J. W. G., et al. (submitted), Extensional and magmatic nature of the Campbell Plateau and Great South Basin from deep crustal studies.
- Harrison, A. J., and R. S. White (2004), Crustal structure of the Taupo Volcanic Zone, New Zealand: Stretching and igneous intrusion, *Geophysical Research Letters*, doi:10.1029/2004GL019885.
- Herzer, R. (1995), Seismic stratigraphy of a buried volcanic arc, Northland, New Zealand and implications for Neogene subduction, *Marine and Petroleum Geology*, 12, 511 - 531.
- Herzer, R., et al. (1997), Seismic Stratigraphy and Structural History of the Reinga Basin and its Margins, Southern Norfolk Ridge System, *N.Z. Journal of Geology and Geophysics*, 40, 425-451.
- Herzer, R., and J. Mascle (1996), Anatomy of a Continental-Backarc Transform - the Vening Meinesz Fracture Zone Northwest of New Zealand, *Marine Geophysical Researches*, 18, 401-427.
- Heuret, A., and S. Lallemand (2005), Plate motions, slab dynamics and back-arc deformation, *Physics of the Earth and Planetary Interiors*, 149, 31-51.

## REFERENCES

- Hoernle, K., et al. (2006), Cenozoic intraplate volcanism on New Zealand: Upwelling induced by lithospheric removal, *Earth and Planetary Science Letters*, doi:10.1016/j.epsl.2006.06.001.
- Holbrook, W. S., et al. (1994), Deep Structure of the U.S. Atlantic continental margin, offshore South Carolina, from coincident ocean bottom and multichannel seismic data, *Journal of Geophysical Research*, 99, 9155 - 9178.
- Hunt, T. (1978), Stokes Magnetic Anomaly System, *N.Z. Journal of Geology and Geophysics*, 21, 595 - 606.
- Ilchenko, T. (1996), Dniepr-Donets Rift: deep structure and evolution from DSS profiling, *Tectonophysics*, 286, 83-98, doi:10.1016/S0040-1951(96)00221-1.
- Jongsma, D., and J. C. Mutter (1978), Non-Axial Breaching of a Rift Valley: Evidence from the Lord Howe Rise and the Southeastern Australian Margin, *Earth and Planetary Science Letters*, 39, 226-234.
- Kamp, P., J.J. (1986), Late Cretaceous-Cenozoic Tectonic Development of the Southwest Pacific Region, *Tectonophysics*, 121, 225 - 251.
- Keranen, K., et al. (2004), Three-dimensional seismic imaging of a protoridge axis in the Main Ethiopian Rift, *Geology*, 32, 949-952, doi:10.1130/G20737.1.
- Kimbrough, D. L., et al. (1994), Uranium-lead zircon ages from the Median Tectonic Zone, New Zealand, *N.Z. Journal of Geology and Geophysics*, 37, 393 - 419.
- King, P. R. (2000), Tectonic reconstructions of New Zealand: 40 Ma to the Present, *N.Z. Journal of Geology and Geophysics*, 43, 611-638.
- Klingelhöfer, F., et al. (2005), Crustal Structure of the NE Rockall Trough from wide-angle seismic data modeling, *Journal of Geophysical Research*, doi:10.1029/2005JB003763.
- Kohler, M., and D. Eberhart-Phillips (2002), Three-dimensional lithospheric structure below the New Zealand Southern Alps, *Journal of Geophysical Research*, doi:10.1029/2001JB000182.
- Krause, D. C. (1966), Geology and Geomagnetism of the Bounty Trough, east of the South Island, New Zealand, *N.Z. Oceanogr. Inst. Mem.*, 30, 34 pp.
- Lafoy, Y., et al. (2005a), Structure of the Basin and Ridge System West of New Caledonia (Southwest Pacific): A Synthesis, *Marine Geophysical Researches*, doi:10.1007/s11001-005-5184-5.
- Lafoy, Y., et al. (2005b), Discovery of Continental Stretching and Oceanic Spreading in the Tasman Sea, *EOS, Transactions AGU*, 86, 101.
- Laird, M. G. (1993), *Cretaceous Continental Rifts: New Zealand Region*, 37 - 49 pp., Elsevier Science Publishers B.V.

## REFERENCES

- Laird, M. G., and J. D. Bradshaw (2004), The Break-up of a Long-term Relationship: the Cretaceous Separation of New Zealand from Gondwana, *Gondwana Research*, 7, 273-286.
- Lancaster, P., and K. Salkauskas (1986), *Curve and surface fitting*, Academic Press, Orlando.
- Larter, R. D., et al. (2002), Tectonic evolution of the Pacific margin of Antarctica 1. Late Cretaceous tectonic reconstructions, *Journal of Geophysical Research*, doi:10.1029/2000JB000052.
- Latin, D., and N. White (1990), Generating melt during lithospheric extension: Pure shear vs. simple shear, *Geology*, 18, 327 - 331.
- LeMasurier, W. E., and C. A. Landis (1996), Mantle-plume activity recorded by low-relief erosion surfaces in West Antarctica and New Zealand, *GSA Bulletin*, 108, 1450 - 1466.
- Lister, G. A., et al. (1986), Detachment faulting and the evolution of passive continental margins, *Geology*, 14, 246-250.
- Lithgow-Bertelloni, C., and M. A. Richards (1998), The dynamics of cenozoic and mesozoic plate motions, *Reviews of Geophysics*, 36, 27-78.
- Lizarralde, D., et al. (2002), Crustal construction of a volcanic arc, wide-angle seismic results from the western Alaska Peninsula, *Journal of Geophysical Research B: Solid Earth*, 107, doi.:10.1029/2001JB000230.
- Louden, K. E., and D. Chian (1999), The deep structure of non-volcanic rifted continental margins, *Phil. Trans. R. Soc. Lond. A.*, 357, 767-805.
- Luyendyk, B. P. (1995), Hypothesis for Cretaceous rifting of east Gondwana caused by subducted slab capture, *Geology*, 23, 373-376.
- Luyendyk, B. P., et al. (1996), Paleomagnetic Study of the northern Ford Ranges, western Marie Byrd Land, West Antarctica: Motion between West and East Antarctica, *Tectonics*, 15, 122-141.
- Luyendyk, B. P., et al. (2003), Eastern margin of the Ross Sea Rift in western Marie Byrd Land, Antarctica: Crustal structure and tectonic development, *Geochem. Geophys. Geosyst.*, doi:10.1029/2002GC000462.
- Lythe, M. B., et al. (2000), BEDMAP - Bed topography of the Antarctic, British Antarctic Survey, Cambridge, U.K.
- Mantovani, E., et al. (2001), Back arc extension: which driving mechanism? *Journal of the Virtual Explorer*, 3, 17 - 45.
- McAdoo, D. C., and S. Laxon (1997), Antarctic tectonics: Constraints from an ERS-1 satellite marine gravity field, *Science*, 276, 556-560.

## REFERENCES

- Mechie, J., et al. (1997), A model for the structure, composition and evolution of the Kenya rift, *Tectonophysics*, 278, 95-119.
- Menke, W. (1984), *Geophysical Data Analysis: Discrete Inversion Theory*, Academic Press, Orlando.
- Mjelde, R., et al. (1997), Crustal structure of the central part of the Vøring Basin, mid-Norway margin, from ocean bottom seismographs, *Tectonophysics*, 277, 235-257, doi:10.1016/S0040-1951(97)00028-0.
- Molnar, P., and T. Atwater (1978), Interarc spreading and Cordilleran tectonics as alternates related to the age of subducted oceanic lithosphere, *Earth and Planetary Science Letters*, 41, 330-340.
- Mortimer, N., et al. (2002), Geological interpretation of a deep seismic reflection profile across the Eastern Province and Median Batholith, New Zealand: crustal architecture of an extended Phanerozoic convergent orogen, *N.Z. Journal of Geology and Geophysics*, 45, 349-363.
- Mortimer, N., et al. (2006), New Constraints on the age and evolution of the Wishbone Ridge, southwest Pacific Cretaceous microplates, and Zealandia-West Antarctic break-up, *Geology*, doi:10.1030/G22168.1.
- Mukasa, S. B., and I. W. D. Dalziel (2000), Marie Byrd Land, West Antarctica: Evolution of Gondwana's Pacific margin constrained by zircon U-Pb geochronology and feldspar common-Pb isotopic compositions, *GSA Bulletin*, 112, 611-627.
- Müller, R. D., et al. (2000), Seafloor Spreading around Australia, in *Billion-Year Earth history of Australia and Neighbours in Gondwanaland*, edited by J. J. Veevers, pp. 18-25, Department of Earth and Planetary Sciences, Macquarie University, GEMOC Press, Sydney.
- Musacchio, G., et al. (1997), Composition of the crust in the Grenville and Appalachian Provinces of North America inferred from  $v_p/v_s$  ratios, *Journal of Geophysical Research*, 102, 15225 - 15241.
- Parson, L. M., and I. C. Wright (1996), The Lau-Havre-Taupo back-arc basin: A southward-propagating, multi-stage evolution from rifting to spreading, *Tectonophysics*, 263, 1-22.
- Pedersen, T., and P. van der Beek (1994), Extension and magmatism in the Oslo Rift, southeast Norway: No sign of a mantle plume, *Earth and Planetary Science Letters*, 123, 317 - 329.
- Reyners, M., and H. Cowan (1993), The Transition from subduction to continental collision: crustal structure in the North Canterbury region, New Zealand, *Geophysical Journal International*, 115, 1124 - 1136.

## REFERENCES

- Ritzwoller, M. H., et al. (2001), Crustal and upper mantle structure beneath Antarctica and surrounding oceans, *Journal of Geophysical Research*, doi:10.1029/2001JB000179.
- Ro, H. E., and J. I. Faleide (1992), A stretching model for the Oslo Rift, *Tectonophysics*, 208, 19 - 36.
- Sandwell, D. T., and W. H. F. Smith (1997), Global seafloor topography from satellite altimetry and ship depth soundings, *Science*, 277, 1956 - 1962.
- Sato, T., et al. (2006), P-wave velocity structure of the margin of the southeastern Tsushima Basin in the Japan Sea using ocean bottom seismometers and airguns, *Tectonophysics*, 412, 159-171.
- Schellart, W. P., et al. (2006), A late Cretaceous and Cenozoic reconstruction of the Southwest Pacific region: Tectonics controlled by subduction and slab rollback processes, *Earth-Science Reviews*, 76, 191-233, doi:10.1016/j.earthscirev.2006.01.002.
- Scherwath, M., et al. (2003), Lithospheric structure across oblique continental collision in New Zealand from wide-angle P wave modeling, *Journal of Geophysical Research*, doi:10.1029/2002JB002286.
- Scholz, C. H., and J. Campos (1995), On the mechanism of seismic decoupling and back arc spreading at subduction zones, *Journal of Geophysical Research*, 100, 22103 - 22115.
- Shor, G. G. J., et al. (1971), Crustal Structure of the Melanesian Area, *Journal of Geophysical Research*, 76, 2562-2586.
- Smith, C. H. (1997), Mid-crustal Processes during Cretaceous Rifting, Fosdick Mountains, Marie Byrd Land, in *The Antarctic Region: geological evolution and processes; proceedings of the VII International Symposium on Antarctic Earth Sciences*, edited by C. A. Ricci, pp. 313 - 320, Terra Antarctica Publ., Siena.
- Smith, E. G. C., et al. (1995), A seismic velocity profile across the central South Island, New Zealand, from explosion data, *N.Z. Journal of Geology and Geophysics*, 38, 565 - 570.
- Smith, W., H. F., and P. Wessel (1990), Gridding with continuous curvature splines in tension, *Geophysics*, 55, 29 - 305.
- Smith, W. H. F., and D. T. Sandwell (1997), Marine gravity anomaly from Geosat and ERS 1 satellite altimetry, *Journal of Geophysical Research*, 102, 10039 - 10054.
- Spell, T. L., et al. (2000), Thermochronologic constraints on the breakup of the Pacific Gondwana margin: the Paparoa core complex, South Island, New Zealand, *Tectonics*, 19, 433-451.
- Spörl, K. B., and P. F. Ballance (1989), Mesozoic-Cenozoic ocean floor/continent interaction and terrane configuration, southwest Pacific area around New Zealand, in

## REFERENCES

*The Evolution of the Pacific Ocean Margins*, edited by Z. Ben-Avraham, pp. 176-190, Oxford Monogr. Geol. Geophys.

Sundaralingham, K., and D. Denham (1987), Structure of the upper mantle beneath the Coral and Tasman Seas, as obtained from group and phase velocities of Rayleigh waves, *N.Z. Journal of Geology and Geophysics*, *30*, 329-341.

Sutherland, R. (1995), The Australia-Pacific boundary and Cenozoic plate motions in the SW Pacific: Some constraints from Geosat data, *Tectonics*, *14*, 819-831.

Sutherland, R. (1999), Basement geology and tectonic development of the greater New Zealand region: an interpretation from regional magnetic data, *Tectonophysics*, doi:10.1016/S0040-1951(99)00108-0.

Tamaki, K. (1985), Two modes of back-arc spreading, *Geology*, *13*, 475-478.

Tapponnier, P., et al. (1986), On the mechanics of the collision between India and Asia, in *Collision Tectonics*, edited by M. P. Coward and A. C. Ries, pp. 115 - 157, Geological Society of London, London.

Tarantola, A. (1987), *Inverse Problem Theory*, Elsevier Science Publishers B.V., Amsterdam.

The DOBREFraction'99 Working Group, et al. (2003), "DOBREFraction '99" - velocity model of the crust and upper mantle beneath the Donbas Foldbelt (East Ukraine), *Tectonophysics*, *371*, 81 - 110, doi:10.1016/S0040-1951(03)00211-7.

Trey, H., et al. (1999), Transect across the West Antarctic rift system in the Ross Sea, Antarctica, *Tectonophysics*, *301*, 61-74, doi:10.1016/S0040-1951(98)00155-3.

Uenzelmann-Neben, G., et al. (in review), Neogene magmatic activity in Bounty Trough, eastern New Zealand, *Marine Geology*, in review.

Uruski, C. (2003), Cretaceous paleogeography of the Taranaki Basin, paper presented at Geological Society of New Zealand Inc 2003 annual conference, Geological Society of New Zealand miscellaneous publication, University of Otago, Dunedin.

Uruski, C., and R. Wood (1991), A new look at the New Caledonia Basin, an extension of the Taranaki Basin, offshore North Island, New Zealand, *Marine and Petroleum Geology*, *8*, 379 - 391.

Uyeda, S., and H. Kanamori (1979), Back-arc opening and the mode of subduction, *Journal of Geophysical Research*, *84*, 1049-1062.

Van Avendonk, H. J. A., et al. (2004a), Continental crust under compression: A seismic refraction study of South Island Geophysical Transect I, South Island, New Zealand, *Journal of Geophysical Research*, doi:10.1029/2003JB002790.

## REFERENCES

Van Avendonk, H. J. A., et al. (2004b), Inferring crustal structure in the Aleutian island arc from a sparse wide-angle seismic data set, *Geochem. Geophys. Geosyst.*, 5, doi:10.1029/2003GC000664.

Van de Beuque, S., et al. (1998), Transect sismique continu entre l'arc des Nouvelle-Hébrides et la marge orientale de l'Australie: programme FAUST (French Australian Seismic Transect), *C.R. Acad. Sci. Paris, Sciences de la terre et des plànetes*, 327, 761-768.

Vially, R., et al. (2003), Petroleum Potential of New Caledonia and its Offshore Basins, in *AAPG Int. Conf.*, edited, Barcelona, Spain, Sept. 21-24, 2003.

Voss, M., and W. Jokat (2007), Continent-ocean transition and voluminous magmatic underplating derived from P-wave velocity modelling of the East Greenland continental margin, *Geophysical Journal International*, 170, 580-604, doi: 10.1111/j.1365-246X.2007.03438.x.

Wandres, A. M., and J. D. Bradshaw (2005), New Zealand tectonostratigraphy and implications from conglomeratic rocks for the configuration of the SW Pacific margin of Gondwana, *Geological Society Special Publication*, 179 - 216.

Wandres, A. M., et al. (2004), Provenance analysis using conglomerate clast lithologies: a case study from the Pahau terrane of New Zealand, *Sedimentary Geology*, 167, 57 - 89, doi.:10.1016/j.sedgeo.2004.02.002.

Weaver, S. D., et al. (1994), Antarctica-New Zealand rifting and Marie Byrd Land lithospheric magmatism linked to ridge subduction and mantle plume activity, *Geology*, 22, 811-814.

Werner, R., et al. (in prep.), Origin of Late Cretaceous to Pleistocene submarine intraplate volcanism on the New Zealand micro-continent, *Journal of Petrology*.

Wernicke, B., and B. C. Burchfiel (1982), Modes of extensional tectonics, *Journal of Structural Geology*, 4, 105 - 115.

Wessel, P., and W. Smith, H. F. (1998), New, improved version of Generic Mapping Tools released, *EOS Transactions of the American Geophysical Union*, 79, pp. 579.

White, R. S., and D. H. Matthews (1980), Variations in oceanic upper crustal structure in a small area of the northeastern Atlantic, *Geophys. J. R. Astron. Soc.*, 61, 401 - 431.

Whitmarsh, R. B., et al. (2001), Evolution of magma-poor continental margins from rifting to seafloor spreading, *Nature*, 413, 150-154, doi:10.1038/35093085.

Wilson, M. (1992), Magmatism and continental rifting during the opening of the Atlantic Ocean: A consequence of Lower Cretaceous super plume activity? in *Magmatism and the Causes of Continental Break-up*, edited by B. C. Storey, et al., pp. 241 - 255, Geological Society of London, London.

## REFERENCES

Winberry, J. P., and S. Anandkrishnan (2004), Crustal structure of the West Antarctic rift system and Marie Byrd Land hotspot, *Geology*, 32, 977-980, doi:10.1130/G207768.1.

Wood, R. (1993), The Challenger Plateau, in *South Pacific Sedimentary Basins. Sedimentary Basins of the World, 2*, edited by P. F. Ballance, pp. 351 - 364, Elsevier Science Publishers B.V., Amsterdam.

Wood, R., and R. Herzer (1993), The Chatham Rise, New Zealand, in *South Pacific Sedimentary Basins. Sedimentary Basins of the World, 2*, edited by P. F. Ballance, pp. 329-349, Elsevier Science Publishers, Amsterdam.

Wood, R., and D. J. Woodward (2002), Sediment thickness and crustal structure of offshore western New Zealand from 3-D gravity modelling, *N.Z. Journal of Geology and Geophysics*, 45, 243-255.

Woodcock, N. H. (2004), Life span and fate of basins, *Geology*, 32, 685-688, doi:10.1130/G20598.1.

Woodward, D. J., and T. Hunt (1971), Crustal Structure across the Tasman Sea, *N.Z. Journal of Geology and Geophysics*, 14, 39 -45.

Worthington, T. J., et al. (2006), Osbourn Trough: Structure, geochemistry and implications of a mid-Cretaceous paleosspreading ridge in the South Pacific, *Earth and Planetary Science Letters*, doi:10.1016/j.epsl.2006.03.018.

Yegorova, T. P., et al. (1999), 3-D gravity analysis of the Dniepr-Donets Basin and Donbas Foldbelt, Ukraine, *Tectonophysics*, 313, 41 - 58.

Zelt, C. A. (1999), Modelling strategies and model assessment for wide-angle seismic travelttime data, *Geophysical Journal International*, 139, 183-204, doi:10.1111/j.1365-246x.1999.00934.x.pdf.

Zelt, C. A., and R. M. Ellis (1988), Practical and Efficient Ray Tracing in Two-Dimensional Media for Rapid Travelttime and Amplitude Forward Modeling, *Canadian Journal of Exploration Geophysics*, 24, 16-31.

Zelt, C. A., and D. A. Forsyth (1994), Modelling wide-angle seismic data for crustal structure: Grenville Province, *Journal of Geophysical Research*, 99, 11687 - 11704.

Zelt, C. A., and R. B. Smith (1992), Seismic Travelttime inversion for 2-D crustal velocity structure, *Geophysical Journal International*, 108, 16-34.

Ziegler, P., A., and S. Cloetingh (2004), Dynamic processes controlling evolution of rifted basins, *Earth-Science Reviews*, 64, 1-50, doi:10.1016/S0012-8252(03)00041-2.

## 12 Acknowledgements

Writing a PhD thesis always means dependence from others, mainly in form of help, and interpersonal contact. Many of the people around me made my life easier. Thanks to all of them. Special thanks to:

Prof. Dr. Heinz Miller (AWI) for the opportunity to write this thesis, discussions and encouragement and his helping hand in the case of large administrative problems.

Prof. Dr. Katrin Huhn (MARUM) for co-reviewing my thesis, for discussions and good ideas.

Dr. Karsten Gohl (AWI) for taking me on the best cruises ever, for his participation in Meteor cruise M52/2 and especially for encouraging me to apply for external funds and supervising my work and the CAMP project.

Dr. Gabriele Uenzelmann-Neben (AWI) for co-supervising me, for providing really good reviews as a co-author and the perfect balance of caring and provoking.

Dr. Wilfried Jokat (AWI) for being a loud-and-friendly source of mocking, earthing me from time to time.

Dr. Gesa Netzeband (GEOMAR), my (former) scientific twin for conquering the same field with me. It was a broad field, from science to finally ending up in the same flat – from Monday to Friday.

Dr. Graeme Eagles (AWI) for fighting through my manuscripts. He greatly improved them. Also many thanks for being so British. His departure to Royal Holloway is a great loss for the AWI!

Dr. Daniel Barker, Dr. Bryan Davy, Dr. Rupert Sutherland (GNS Science), and Dr. Tim Allan (Crown Minerals) for the good collaboration and for making my stay in New Zealand so pleasant. This was a time I enjoyed a lot.

Max Voß (AWI) for sharing half of my life as a PhD student. After years of sharing the same food, the same office, the same problems and the same joys, we were sometimes like an old couple.

Dr. Mechita Schmidt-Aursch, Philip Schlüter, Daniela Berger, Dr. Wolfram Geißler and Tom Schmitz (AWI) for making me feel at home in Bremerhaven and at the AWI. I will miss the good discussions and occasional evening beers.

Dr. Claus-Dieter Hillenbrand (BAS) for a good connection to England and his shoe bin.

Dr. Jill Nicola Schwarz (AWI) for reviewing parts of my thesis and good conversations which were unfortunately too few.

## ACKNOWLEDGEMENTS

The AWI, the DAAD and the DFG for financial support and the opportunity for great experience at conferences and research visits and expeditions.

The Forschungsanstalt der Bundeswehr für Wasserschall und Geophysik for providing me with prospects for the future.

My parents for continuous support and love and for a good starting position.

Nicole Parsiegl, for grabbing our luck with both hands. Thank you even more for all the following.

Without all of you, I would not be where I am now. Thanks a lot!

Die "**Berichte zur Polar- und Meeresforschung**" (ISSN 1866-3192) werden beginnend mit dem Heft Nr. 569 (2008) ausschließlich elektronisch als Open-Access-Publikation herausgegeben. Ein Verzeichnis aller Hefte einschließlich der Druckausgaben (Heft 377-568) sowie der früheren "**Berichte zur Polarforschung**" (Heft 1-376, von 1982 bis 2000) befindet sich im Internet in der Ablage des electronic Information Center des AWI (**ePIC**) unter der URL <http://epic.awi.de>. Durch Auswahl "Reports on Polar- and Marine Research" auf der rechten Seite des Fensters wird eine Liste der Publikationen in alphabetischer Reihenfolge (nach Autoren) innerhalb der absteigenden chronologischen Reihenfolge der Jahrgänge erzeugt.

*To generate a list of all Reports past issues, use the following URL: <http://epic.awi.de> and select the right frame to browse "Reports on Polar and Marine Research". A chronological list in declining order, author names alphabetical, will be produced, and pdf-icons shown for open access download.*

#### **Verzeichnis der zuletzt erschienenen Hefte:**

**Heft-Nr. 583/2008** — "The Expedition of the Research Vessel 'Polarstern' to the Antarctic in 2007 (ANT-XXIII/9)", edited by Hans-Wolfgang Hubberten

**Heft-Nr. 584/2008** — "Russian-German Cooperation SYSTEM LAPTEV SEA: The Expedition Lena - New Siberian Islands 2007 during the International Polar Year 2007/2008", edited by Julia Boike, Dmitry Yu. Bolshiyarov, Lutz Schirrmeyer and Sebastian Wetterich

**Heft-Nr. 585/2009** — "Population dynamics of the surf clams *Donax hanleyanus* and *Mesodesma mactroides* from open-Atlantic beaches off Argentina", by Marko Herrmann

**Heft-Nr. 586/2009** — "The Expedition of the Research Vessel 'Polarstern' to the Antarctic in 2006 (ANT-XXIII/7)", edited by Peter Lemke

**Heft-Nr. 587/2009** — "The Expedition of the Research Vessel 'Maria S. Merian' to the Davis Strait and Baffin Bay in 2008 (MSM09/3), edited by Karsten Gohl, Bernd Schreckenberger, and Thomas Funck

**Heft-Nr. 588/2009** — "Selected Contributions on Results of Climate Research in East Germany (the former GDR)", edited by Peter Hupfer and Klaus Dethloff

**Heft-Nr. 589/2009** — "The Expedition of the Research Vessel 'Polarstern' to the Arctic in 2008 (ARK-XXIII/1)", edited by Gereon Budéus

**Heft-Nr. 590/2009** — "The Expedition of the Research Vessel 'Polarstern' to the Arctic in 2008 (ARK-XXIII/2)", edited by Gerhard Kattner

**Heft-Nr. 591/2009** — "The Expedition of the Research Vessel 'Polarstern' to the Antarctic in 2008 (ANT-XXIV/4)", edited by Andreas Macke

**Heft-Nr. 592/2009** — "The Expedition of the Research Vessel 'Polarstern' to the Antarctic in 2007 (ANT-XXIV/1)", edited by Sigrid Schiel

**Heft-Nr. 593/2009** — "The Campaign MELTEX with Research Aircraft 'POLAR 5' in the Arctic in 2008", edited by Gerit Birnbaum, Wolfgang Dierking, Jörg Hartmann, Christof Lüpkes, André Ehrlich, Thomas Garbrecht, and Manuel Sellmann

**Heft-Nr. 594/2009** — "The Expedition of the Research Vessel 'Polarstern' to the Antarctic in 2008 (ANT-XXV/1)", edited by Gerhard Kattner and Boris Koch

**Heft-Nr. 595/2009** — "The Expedition of the Research Vessel 'Polarstern' to the Antarctic in 2008/2009 (ANT-XXV/2)", edited by Olaf Boebel

**Heft-Nr. 596/2009** — "Crustal evolution of the submarine plateaux of New Zealand and their tectonic reconstruction based on crustal balancing", by Jan Werner Gerhard Grobys